

**Analysis of Natural Forest and Plantation Forest Changes in  
Vietnam Using Remote Sensing Data**

January 2021

HOANG THANH TUNG

**Analysis of Natural Forest and Plantation Forest Changes in  
Vietnam Using Remote Sensing Data**

A Dissertation Submitted to  
the Graduate School of Life and Environmental Sciences,  
the University of Tsukuba  
in Partial Fulfillment of the Requirements  
for the Degree of Doctor of Philosophy in Environmental Studies  
(Doctoral Program in Sustainable Environmental Studies)

HOANG THANH TUNG

## Abstract

Forest in Vietnam consists of 10.3 million ha of natural forests and 4.3 million ha of plantation forests (as of 2019), according to national statistics of the Vietnamese government. Since the 1990s, Vietnam has experienced a forest transition, in which net forest loss has been shifted to net forest gain. The main contribution of the reforestation in Vietnam was from the increase of plantation forest area which increased by more than 3.6 million ha from 1990 to 2020. However, deforestation in natural forests has been occurred, especially in Central Highlands of Vietnam with about 51,000 ha forest loss per year during 2010–2019, reported by the statistical data of Vietnamese government. The loss of natural forests has led to tremendous impacts, i.e., habitat fragmentation, changing water cycle, increasing carbon emission via conversion from forest to non-forest land-uses. To alleviate these issues, management and policies have been proposed and implemented from local to national scales. In such frameworks, the importance of highly detailed and accurate monitoring of the two forest types have been emphasized. To this end, this study provides a comprehensive solution comprising of mapping, change analysis, and investigating the causes of the changes of natural forests and plantation forests based on remote sensing data.

This study demonstrates a comprehensive and geographically transferable approach to produce a 12-category high-resolution land use/land cover (LULC) map over mainland Vietnam in 2016 by remote sensing data. The map included several natural forest categories (evergreen broadleaf, deciduous (mostly deciduous broadleaf), and coniferous (mostly evergreen coniferous)) and one category representing all popular plantation forests in Vietnam such as acacia (*Acacia mangium*, *Acacia auriculiformis*, *Acacia* hybrid), eucalyptus (*Eucalyptus globulus*), rubber (*Hevea brasiliensis*), and others. The approach combined the advantages of various sensor data by integrating their posterior probabilities resulting from applying a probabilistic classifier (comprised of kernel density estimation and Bayesian inference) to each datum individually. By using different synthetic aperture radar (SAR) images (PALSAR-2/ScanSAR, PALSAR-2 mosaic, Sentinel-1), optical images (Sentinel-2, Landsat-8) and topography data (AW3D30), the resultant map achieved 85.6% for the overall accuracy. The major

forest classes including evergreen broadleaf forests and plantation forests had a user's accuracy and producer's accuracy ranging from 86.0% to 95.3%. This study's map identified  $9.55 \times 10^6$  ha ( $\pm 0.16 \times 10^6$  ha) of natural forests and  $3.89 \times 10^6$  ha ( $\pm 0.11 \times 10^6$  ha) of plantation forests over mainland Vietnam, which were close to the Vietnamese government's statistics (with differences of less than 8%). This result provides a reliable input/reference to support forestry policy and land sciences in Vietnam.

Understanding deforestation is critically important for effective forest management, climate change mitigation, and biodiversity conservation. However, deforestation information from currently available forest data has limitations that reduce reliability and application. This study demonstrates an approach to deriving more accurate deforestation mapping based on high-resolution land use/land cover (LULC) maps. These LULC maps provide a means of distinguishing between natural forests and plantation forests over large spatial scales. Importantly, through this approach, deforestation of natural forests and the temporary loss of plantation forests can be effectively distinguished. In the deforestation hotspot in the Vietnam Central Highlands, the result show that the deforested area is closer to that reported in national statistics compared to other satellite-based datasets. In addition, I hypothesize a link between deforestation mean patch size (MPS) and the direct drivers of deforestation, including shifting agriculture and commodity-driven deforestation. That is, shifting agriculture-driven deforestation is likely to have smaller MPSs than commodity-driven deforestation across the entire country. Temporally, the regional mean deforestation MPS in Northern and Central Vietnam showed a steady increase during the period 2001–2019. In the Central Highlands, the regional mean deforestation MPS sharply increased between 2001 and 2010, and then decreased until 2019. Overall, the findings provide valuable reference information for developing and evaluating appropriate policy responses to deforestation.

**Keywords:** *natural forest, plantation forest, remote sensing, Vietnam, acacia, eucalyptus, rubber, land use/land cover change, PALSAR-2, Sentinel, forestry policy, sustainable forest management, forest transition.*



## Table of Contents

Chapter 1. Introduction.....	1
1.1. Background.....	2
1.2. Research questions.....	6
1.3. Objectives .....	6
1.4. Structure of this dissertation .....	7
Chapter 2. Study Area and Field Surveys .....	9
2.1. Study area .....	10
2.2. Field surveys.....	13
2.2.1. Field survey in northern Vietnam .....	13
2.2.2. Field survey in Central Highlands, Mekong Delta, and Ha Noi.....	20
Chapter 3. Mapping Plantation Forest and Natural Forest for entire Mainland Vietnam .....	38
3.1. Background.....	39
3.2. Materials and methods.....	42
3.2.1. Method.....	42
3.2.2. Satellite data and preprocessing.....	45
3.2.3. Reference data and classification scheme.....	51
3.3. Results.....	54
3.3.1. Evaluation of the classification performance of satellite data .....	54
3.3.2. The resultant Vietnam LULC map 2016 and its comparison to other LULC map products .....	58
3.3.3. Comparison of forest areas between this study’s map in 2016 and Vietnam national statistical data.....	61
3.3.4. Comparison between this study’s map and the Vietnam Forest Resource (VFR) Map 2016.....	62
3.4. Discussion.....	65
3.4.1. Advantages and potential applications of the resultant LULC map .....	65
3.4.2. Limitations and challenges of this study’s map.....	66

3.4.3. Future research directions.....	67
3.5. Summary.....	68
Chapter 4. A spatiotemporal Analysis of Deforestation in Vietnam over the Last Two Decades.....	70
4.1. Background.....	71
4.2. Materials and method .....	73
4.2.1. Satellite data and preprocessing.....	73
4.2.2. Methods .....	77
4.2.3. Reference Data.....	83
4.3. Results and Discussion .....	84
4.3.1. High-resolution 2007 LULC map and LULC changes between 2007 and 2016 .....	84
4.3.2. 2007–2016 deforestation map and comparison with other data .....	87
4.3.3. Spatial variations in deforestation MPS .....	90
4.3.4. Temporal variations in deforestation MPS .....	93
4.4. Summary.....	98
Chapter 5. Discussion.....	100
Chapter 6. Conclusion .....	103
Acknowledgement.....	106
Reference .....	107

## List of Tables

Table 3.1. Spectral bands of Sentinel-2A (ESA, 2015b) and Landsat 8 (USGS, 2020b) used in this study .....	49
Table 3.2. Organization of datasets, the number of images for each $1^{\circ} \times 1^{\circ}$ tiles .....	51
Table 3.3. Description of the land cover categories of the Vietnam LULC map in 2016 .....	52
Table 4.1. Spectral bands of ALOS/AVNIR-2 ORI (JAXA, 2020b), Landsat-5, and Landsat-7 (USGS, 2020b) used in this study .....	76
Table 4.2. Accuracies and errors of deforestation map for Vietnam between 2007 and 2016 corresponding with various fractional cover difference thresholds .....	79
Table 4.3. Comparison of deforestation MPS in Northern Vietnam, Central Vietnam, the Central Highlands of Vietnam, and Southern Vietnam. Statistical significance of differences was estimated using the Wilcoxon rank-sum test. ....	92
Table 4.4. Differences in 5-year means (2001–2005, 2006–2010, 2011–2015, and 2016–2019) of deforestation mean patch size (MPS) for the main regions in Vietnam. The statistical significance of the differences was estimated using the Wilcoxon rank-sum test. ....	97

## List of Figures

Figure 2.1. Study area and forest types in mainland Vietnam through ground-truth photos and high-resolution Google Earth (GE) images. ....	12
Figure 2.2. Field photo locations of two field surveys (in 2019 and 2020) of this study in Vietnam.....	15
Figure 2.3. (a) The primary forest in Cuc Phuong national park; (b) the secondary forest in Hoang Lien national park.....	16
Figure 2.4. (a) Shifting cultivation in northern Vietnam; (b) barren hills in northern Vietnam.....	17
Figure 2.5. (a) Interview local people in the Bao Yen district, Lao Cai province, Vietnam; (b) wood production in a local factory in the Bao Yen district.....	18
Figure 2.6. (a) Eucalyptus in field photo; (b) Acacia in field photo .....	19
Figure 2.7. Plantation forest survey in Phat Tich hill, Bac Ninh province.....	21
Figure 2.8. Acacia plantation forest survey in Dong Mo, Ba Vi district.....	22
Figure 2.9. Plantation forest survey at Den Giong, Soc Son district.....	23
Figure 2.10. Rubber plantation in Buon Ma Thuot, Dak Lak province .....	26
Figure 2.11. Agricultural plantation trees and deciduous broadleaf forests in Dak Lak and Dak Nong provinces.....	27
Figure 2.12. Acacia plantation in M’Drak, Dak Lak and shrubland, sand dunes in Mui Doi, Khanh Hoa .....	29
Figure 2.13. Evergreen needle-leaf forests and deciduous broadleaf forests in Lam Dong .....	30
Figure 2.14. Field survey in Binh Thuan province.....	32
Figure 2.15. Field surveys in Dong Thap and Long An provinces .....	33
Figure 2.16. Field surveys in Tra Vinh and Ca Mau provinces.....	35
Figure 3.1. The overall workflow of establishing the high-resolution LULC map for Vietnam in 2016.....	45
Figure 3.2. Distribution and quantity of reference data for 2016 mapping. ....	53

Figure 3.3. Receiver operating characteristic (ROC) curves of the 12 land cover categories for each input data model in 2016 mapping. ....	57
Figure 3.4. Comparison of the area under the curve (AUC) value of input data in forest classes in 2016 mapping. ....	58
Figure 3.5. The resultant Vietnam LULC map 2016 and its comparison to other LULC products.....	60
Figure 3.6. Comparison of forest areas between this study’s LULC map in 2016 with Vietnam national statistical data. ....	61
Figure 3.7. Comparison of the 10-km resolution forest fraction maps between this study and the Vietnam Forest Resource (VFR) Map in 2016 and their forest fraction differences.....	63
Figure 3.8. The three zoom-in sites in the VFR Map 2016 and in this study’s map 2016. ....	64
Figure 4.1. (a) Coverage of 626 ALOS/PALSAR RTC scenes and (b) 177 ALOS/AVNIR-2 ORI scenes.....	75
Figure 4.2. Four main regions of Vietnam .....	81
Figure 4.3. The overall workflow of chapter 4.....	83
Figure 4.4. High-resolution LULC maps for (a) 2007 and (b) 2016 (Chapter 3) (Hoang et al., 2020).....	86
Figure 4.5. Overall LULC net changes in Vietnam between 2007 and 2016 estimated from LULC maps for 2007 and 2016 (Chapter 3) (Hoang et al., 2020). ....	87
Figure 4.6. (a) 2001–2016 deforestation map derived in this study; (b) a comparison of the estimated total deforestation area for mainland Vietnam (2007–2016) with national statistics (net change in natural forest area), GFC* (year of gross forest cover loss event data with a natural forest mask from the 2007 LULC map 2007 created in this study), and CCI-LC; (c) a comparison of estimated the deforestation area in the Central Highlands of Vietnam (2007–2016). ...	90
Figure 4.7. (a) Deforestation mean patch size (MPS) map for Vietnam for the period 2007–2016; (b) histogram of deforestation MPS in Northern Vietnam; (c) histogram of deforestation MPS in Central Vietnam; (d) histogram of	

deforestation MPS in the Central Highlands region of Vietnam; (e) histogram of deforestation MPS in Southern Vietnam .....	92
Figure 4.8. (a) Percentages of deforestation areas caused by corresponding drivers (Curtis et al., 2018) in different regions and (b) regional deforestation mean patch size (MPS) between 2007 and 2016 in the ascending order.....	93
Figure 4.9. Annual maps of deforestation mean patch size (MPS) during the period 2001–2019 created from GFC year of gross forest cover loss event data with natural forest masks from the 2007 LULC map created in this study and the 2016 LULC map created by Hoang et al., (2020) .....	96
Figure 4.10. Trajectories of regional deforestation MPS means for the main regions of Vietnam during the last two decades. ....	98

## List of Abbreviation and Acronyms

AFOLU	Agriculture, Forestry and Other Land Use
AFVI	Aerosol Free Vegetation Index
ALOS	Advanced Land Observing Satellite
ARVI	Atmospherically Resistant Vegetation Index
ASF	Alaska Satellite Facility
AVNIR-2	Advanced Visible and Near Infrared Radiometer type 2
AW3D30	ALOS World 3D - 30m
CCI	Climate Change Initiative
DBH	Diameter at Breast Height
DMSP-OLS	Defense Meteorological Satellite Program - Operational Line-Scan System
DSM	Digital Surface Model
EBF	Evergreen Broadleaf Forest
EORC	Earth Observation Research Center
ESA	European Space Agency
EVI	Enhanced Vegetation Index
FAO	Food and Agriculture Organization
FBD	Fine Beam Dual
FRA	Global Forest Resources Assessments
FROM-GLC	Finer Resolution Observation and Monitoring - Global Land Cover
GEE	Google Earth Engine
GFC	Global Forest Changes
GPS	Global Positioning System

GRVI	Green-Red Vegetation Index
GSO	General Statistics Office of Vietnam
IBI	Index-based Built-up Index
IPCC	Intergovernmental Panel on Climate Change
JAXA	Japan Aerospace Exploration Agency
JDS	The Project for Human Resource Development Scholarship by Japanese Grant Aid
JICA	Japan International Cooperation Agency
JJ-FAST	JICA-JAXA Forest Early Warning System in the Tropics
LSWI	Land Surface Water Index
LULC	Land use/land cover
LULUCF	Land Use, Land-Use Change, and Forestry
MARD	Ministry of Agriculture and Rural Development
MCD12Q1	MODIS land cover data product
MODIS	Moderate Resolution Imaging Spectroradiometer
MONRE	Ministry of Natural Resources and Environment
MPS	Mean Patch Size
MSAVI	Modified Soil-adjusted Vegetation Index
MSI	Moisture Stress Index
NASA	National Aeronautics and Space Administration
NDI	Normalized Difference Index
NDTI	Normalized Difference Tillage Index
NDVI	Normalized Difference Vegetation Index
NDWI	Normalized Difference Water Index



OA	Overall Accuracy
ORI	Ortho Rectified Image
OSM	OpenStreetMap
PA	Producer Accuracy
PALSAR	Phased Array type L-band Synthetic Aperture Radar
PRISM	Panchromatic Remote-Sensing Instrument for Stereo Mapping
REDD+	Reducing Emissions from Deforestation and Forest Degradation
RTC	Radiometric Terrain Corrected
SAR	Synthetic Aperture Radar
SARVI	Soil and Atmosphere Resistant Vegetation Index
SATVI	Soil-Adjusted Total Vegetation Index
UA	User Accuracy
UMD	University of Maryland
USGS	United States Geological Survey
VFR	Vietnam Forest Resource
VNFOREST	Vietnam Administration of Forestry

## List of Publications

### Papers

1. **Hoang T.T.**, Phan C.D., Tadono T., Nasahara K.N. (2021) A spatiotemporal analysis of deforestation in Vietnam over the last two decades, *Remote Sensing*, (Under review in *Remote Sensing*)
2. **Hoang T.T.**, Truong V.T., Hayashi M., Tadono T., Nasahara K.N. (2020) New JAXA High-resolution Land Use/Land Cover Map for Vietnam aiming for Natural Forest and Plantation Forest Monitoring. *Remote Sensing*, 12, 2707. <https://doi.org/10.3390/rs12172707>
3. **Hoang T.T.**, Nasahara K.N., Katagi J. (2018) Analysis of Land Cover Changes in Northern Vietnam Using High Resolution Remote Sensing Data. In: Tien Bui D., Ngoc Do A., Bui HB., Hoang ND. (eds) *Advances and Applications in Geospatial Technology and Earth Resources*, pp 134-151. GTER 2017. Springer, Cham. <https://doi.org/10.1007/978-3-319-68240-2>
4. Truong V.T., **Hoang T.T.**, Phan C.D., Hayashi M., Tadono T., Nasahara K.N. (2019) JAXA Annual Forest Cover Maps for Vietnam during 2015-2018 Using ALOS-2/PALSAR-2 and Auxiliary Data. *Remote Sensing*, 11, 2412. <https://doi.org/10.3390/rs11202412>
5. Van T.T., Wilson N., **Hoang T.T.**, Quisthoudt K., Vo Q.M., Le X.T., Dahdouh-Guebas F., Koedam N. (2015) Changes in Mangrove Vegetation Area and Character in a War and Land Use Change Affected Region of Vietnam (Mui Ca Mau) over Six Decades. *Acta Oecologica*, 63(71). <https://doi.org/10.1016/j.actao.2014.11.007>

### Data publications

1. JAXA High-Resolution Land Use and Land Cover Map of the Northern Region of Vietnam (Released in September 2016 / Version 16.09). [https://www.eorc.jaxa.jp/ALOS/en/lulc/lulc\\_vnm.htm](https://www.eorc.jaxa.jp/ALOS/en/lulc/lulc_vnm.htm)
2. JAXA High-Resolution Land Use and Land Cover Map of Mainland Vietnam (Released in June 2020 / Version 20.06). [https://www.eorc.jaxa.jp/ALOS/en/lulc/lulc\\_vnm\\_v2006.htm](https://www.eorc.jaxa.jp/ALOS/en/lulc/lulc_vnm_v2006.htm)

## **Chapter 1. Introduction**

## 1.1. Background

Forest in Vietnam consists of 10.3 million ha of natural forests and 4.3 million ha of plantation forests (as of 2019), according to national statistics of the Vietnamese government (GSO, 2020). In the documents of the national statistics, a natural forest is defined as a forest that is naturally generated or regenerated (GSO, 2019), including both primary and secondary forests in line with the “naturally regenerating forest” definition of the FAO (2020) (FAO, 2018). In this study, I adopted the definition from the national statistics for natural forests. For plantation forests, according to FAO, a plantation forest is defined as a forest “that is intensively managed and meet all the following criteria at planting and stand maturity: one or two species, even age class, and regular spacing” (FAO, 2018).

Since the 1990s, Vietnam has experienced a forest transition, in which net forest loss has been shifted to net forest gain (Mather, 2007). According to the Forest Resource Assessment Vietnam report 2020 provided by FAO, the forest area in Vietnam increased by more than 5 million ha from 9.375 million ha in 1990 to 14.643 million ha in 2020 (FAO, 2020a). The main contribution of the reforestation in Vietnam was from the increase of plantation forest area. The plantation forests increased by more than 3.6 million ha from 0.745 million ha in 1990 to 4.349 million ha in 2020 (FAO, 2020a). Natural forests experienced an increase of 1.674 million ha during 1990–2010, from 8.630 million ha to 10.304 million ha, and stay remain after that. The data of the report show that plantation forests have kept the steadily increasing trend, whereas the natural forest area shows mostly no change since 2010 until now.

Although the plantation forest area increased, deforestation in natural forests has been occurred, especially in Central Highlands of Vietnam. 1.77 million ha of natural forest was lost throughout entire Vietnam between 2000–2010 based on national forest maps of the Vietnamese government (Khuc et al., 2018). Central Highlands has been considered the most severe deforestation region with about 51,000 ha forest loss per year during 2010–2019, reported by statistical data of the Vietnamese government (VNFOREST, 2020a).

Deforestation in Vietnam is mainly caused by direct anthropogenic drivers such as shifting agriculture, commodity-driven deforestation, and urbanization. Shifting agriculture is a practice of subsistence food production, which causes the conversion of forests to cultivated lands, after several years of which the soil degrades and the land is abandoned. Shifting agriculture in Vietnam is mostly practiced in mountainous areas by ethnic minority households (P. Li et al., 2014). Commodity-driven deforestation is caused by the conversion of forests to market-based agriculture, mining, and energy infrastructure. For example, the expansion of cash crops (e.g., coffee and pepper) and plantation forests (e.g., acacia, eucalyptus, and rubber) are considered to be the main causes of deforestation since the 2000s (Kissinger, 2020; Meyfroidt et al., 2013; Nghiem et al., 2020; M. P. Nguyen et al., 2018). In addition, the construction of new small- and medium-scale hydropower plants has become a widespread driver of deforestation; Pham et al. (2019) noted that 19,792 ha of forests in 29 provinces were destroyed as a result of the building of 160 hydropower plants between 2006 and 2012. Finally, urbanization is considered a minor direct driver of deforestation in Vietnam in comparison to these other drivers. Previous studies have also emphasized the underlying drivers of deforestation, such as poverty, local governance, and population growth (Khuc et al., 2018).

The loss of natural forests and the increase of plantation forests in Vietnam have led to tremendous impacts. One of the serious impacts is that deforestation has caused habitat fragmentation. It was observed that in several regions, the reforestation by plantation forests reduced habitat fragmentation, whereas other regions clearing primary forests caused an increase in forest fragmentation (Meyfroidt & Lambin, 2008b). Deforestation has also harbored indirect consequences such as changing the water cycle by altering infiltration characteristics of the ground surface (Ziegler et al., 2004), altering flow regimes due to the loss of forest cover (N. C. Q. Truong et al., 2018), increasing carbon emission via conversion from forest to non-forest land-use types (Avitabile et al., 2016). In terms of plantation forests, although the plantation forests can contribute to economic growth by improving the income of local smallholders, it may reinforce the existing inequalities in landholding, which in turn increases the vulnerability of the landless and ethnic minorities (Sandewall et al., 2010; Thulstrup, 2014; Thulstrup et al., 2013; Van Khuc et al., 2020).

To alleviate these issues, management and policies have been proposed and implemented from local to national scales. In such frameworks, the importance of detailed and accurate measurements of forest types have been emphasized.

In terms of remote sensing-based mapping of natural forests and plantation forests, the synergy of structural information from Synthetic Aperture Radar (SAR) images and biophysical information from optical images has improved the accuracy and map detail. In recent studies, this integration of different data types has been carried out by data fusion at a feature level, where the optical and SAR images are stacked into a single dataset as a classification input (De Alban et al., 2018; Poortinga et al., 2019; Sarzynski, Giam, & Carrasco, 2020; Torbick et al., 2016).

One of the biggest persistent challenges of large-scale forest type mapping is distinguishing between plantation evergreen broadleaf forests (EBFs) and natural EBFs. The spectral characteristics of these two forest types are mostly identical. Several approaches have been attempted to address this challenge. For instance, the detection of acacia has been based on very high-resolution satellite images such as GeoEye (Morales et al., 2011), airborne photos (Isaacson et al., 2017), or complex radiative transfer models (Masemola et al., 2020). These approaches are suitable for a small scale. Additionally, several studies exploited the fluctuation in the spectral indices during short-rotation cycles to detect a short-rotation eucalyptus (Deng et al., 2020; le Maire et al., 2014). This method required inter-annual time-series data for at least 5 to 7 years to sufficiently cover at least one rotation.

In Vietnam plantation forests comprise of various tree types. Acacia is the most popular plantation tree in Vietnam with over 1.1 million ha (as of 2014 (Nambiar et al., 2015)) and it has been showing a substantial expansion in southeast Asia during the last three decades (Griffin et al., 2015). Besides, Vietnam has nearly 1 million ha of rubber and about 500 thousand ha of eucalyptus (Harwood & Nambiar, 2014). Therefore, there is a need for constructing a comprehensive mapping approach that is applicable for (1) different plantation forest types; (2) various ranges of geographic regions; (3) short time coverage (e.g., annual mapping).

Accurate mapping of natural forests and plantation forests can provide accurate input for the detection of deforestation and changes in plantation forests. Precise deforestation monitoring and quantitative understanding of deforestation are, therefore, fundamental for informing sustainable forest management (Geist & Lambin, 2002; Hosonuma et al., 2012; Kissinger et al., 2012). However, current forest data have substantial limitations that reduce the reliability of the information that they provide.

Forest data can be obtained from two main sources—remote sensing-based land use/land cover (LULC) maps and national forest censuses. Both of these sources have limitations, however. The global forest change (GFC) data produced by Hansen et al. (2013), which is the most widely used remote sensing-based forest dataset, has been reported to contain overestimations in forest cover and forest loss areas including Gabon (Sannier et al., 2016) and Guyana (Galiatsatos et al., 2020), indicating that appropriate data calibration is essential to ensure accuracy. Other land-cover datasets such as the Land Cover project of the Climate Change Initiative (CCI-LC) (ESA, 2015a) and the Terra and Aqua combined Moderate Resolution Imaging Spectroradiometer (MODIS) Land Cover Type (MCD12Q1) datasets (M. Friedl & Sulla-Menashe, 2019) are limited by their low spatial resolution (300 m and 500 m, respectively); hence, small deforestation areas (e.g., 1–3 ha) may be missed. Another limitation of remote sensing-based LULC data is the lack of discrimination between natural forests and plantation forests. This may lead to an overestimation of the deforested area due to the inclusion of temporary losses of plantation forests due to harvesting. In the case of Vietnam’s national forest census data, the most noticeable limitation is that “forest” is taken to represent forestlands registered by the government even when no trees are present. This can lead to inaccurate estimates of physical forest cover. Given these limitations, a means of obtaining accurate data is necessary to improve deforestation monitoring and characterization.

In addition, understanding deforestation requires both quantitative and spatially explicit presentations. To meet these demands, spatial attributes, such as landscape pattern metrics and proximity, have been used to characterize deforestation (Austin et al., 2017; G. Chen et al., 2015; Kalamandeen et al., 2018; Senf & Seidl, 2020). Among the pattern metrics, the deforestation patch size has mostly been used as it can reflect the

drivers of deforestation (Austin et al., 2017; Kalamandeen et al., 2018; Senf & Seidl, 2020). For example, Austin et al. (2017) found that increasing trends in the size of tropical deforestation indicated an increasing dominance of industrial-scale drivers, and Kalamandeen et al. (2018) reported a pervasive rise in drivers of small-scale deforestation in Amazonia.

In Vietnam, previous characterizations of deforestation have mostly focused on identifying both direct and indirect drivers (Cochard et al., 2017; Curtis et al., 2018; Khuc et al., 2018; T. T. Pham et al., 2019) and explaining the underlying mechanisms at a local scale (Meyfroidt et al., 2013; Tachibana et al., 2001). However, the spatiotemporal characteristics of deforestation drivers in Vietnam remain unknown. Such information would enrich the understanding of deforestation and provide a valuable reference for the development of appropriate conservation policy and action plans.

## **1.2. Research questions**

This research aims to answer the following questions:

1. Whether plantation forests and natural forests can be mapped by the integration of various remote sensing data?
2. Whether this study's map with discrimination of plantation forests and natural forests can provide a better deforestation detection in comparison to other current remote sensing-based data, and forest statistical data of the government of Vietnam?
3. Whether spatiotemporal variations in deforestation mean patch size (MPS) can indicate spatiotemporal variations in direct drivers of deforestation over the last two decades in Vietnam?

## **1.3. Objectives**

This study focused on three objectives as follows:



1. To establish a comprehensive and geographically transferable approach to produce a 12-category high-resolution land use/land cover (LULC) map which distinguish plantation forests (i.e., acacia, eucalyptus, rubber, and others) and natural forests (i.e., EBFs, deciduous forests, and coniferous forests) for entire mainland Vietnam;
2. To establish an approach to create a deforestation map based on two LULC maps which were created based on the approach in objective 1, and comparing the deforestation area of this study's map with other data.
3. To analyze spatiotemporal variations in the deforestation mean patch size and its link with spatiotemporal variations in drivers of deforestation.

#### **1.4. Structure of this dissertation**

This thesis contains 5 chapters:

Chapter 1 provides the general background, the significance of this study, objectives of this study, research questions, and the structure of the thesis.

Chapter 2 provides the description of the study area and two field surveys conducted in 2019 and 2020 in two different regions of Vietnam.

Chapter 3 illustrates the process of producing a high-resolution LULC map that distinguishes natural forests and plantation forests (acacia, eucalyptus, rubber, and others) across different geographic regions in mainland Vietnam in 2016 using remote sensing data. The resultant map was then compared with other forest/LULC maps, and official data of the Vietnamese government including national statistics (VNFOREST, 2020a) and the Vietnam Forest Resource Map 2016 (VNFOREST, 2020b).

Chapter 4 aimed for objective 2 and objective 3. The main results described in this chapter are: (1) create a high-resolution LULC map in 2007 based on the mapping approach of the JAXA high-resolution LULC map product in 2016 in Vietnam (Hoang et al., 2020); (2) create a deforestation map of 2007–2016 based on the two LULC maps, and compare the deforestation area identified by the resultant map with the GFC data,

CCI-LC data, and the national statistics of the Vietnamese government; (3) analyze spatiotemporal variations in the deforestation mean patch size and its link with spatiotemporal variations in drivers of deforestation over the last two decades.

Chapter 5 shows the discussion for the answers of research questions.

Chapter 6 is the conclusion.

## **Chapter 2. Study Area and Field Surveys**

## 2.1. Study area

Mainland Vietnam is located in the southeast Asia region and extends from 8°37'N to 23°23'N and from 102°11'E to 109°27'E (Figure 2.1a). This paper focused on mainland Vietnam, which excluded isolated and insufficiently observed islands. Mainland Vietnam accounts for about 332,000 km<sup>2</sup> and consists of a diversity of ecological landscapes and climate regions. Northern Vietnam's climate is characterized by monsoonal features with four distinct seasons, whereas, in the south, the climate is tropical monsoon with two seasons (rainy and dry). The topography of Vietnam is featured by mountains and hills (75% of total area), deltas, and coastal areas (25%). Forest in Vietnam has been considered abundant ecosystems (FAO, 2012) and biodiversity-rich areas (The Government of Vietnam, 2014). In terms of foliage characteristics, natural forests in Vietnam can be categorized into three main types: (1) evergreen broadleaf forest (EBF) which is major and widely distributed (occupies more than 88% of total natural forest area); (2) deciduous forest, distributed in Central Highlands and South-Central Coast; (3) coniferous forest, distributed in Central Highlands (Figures 2.1b–d). According to Phuong (2007), the main dominant species of EBFs includes *Hopea spp.*, *Dipterocarpus costatus*, *D. alatus*, *Shorea obtusa*. Deciduous forests are dominated by several species including *Lagerstroemia angustifolia*, *L. macrocarpa*, *L. floribunda*, *L. duperreana*, etc. (Phuong, 2007). The dominant species of coniferous forests includes *Pinus merkusii*, *P. khasya*, *Dacrydium pierrei*, *Fokienia hodginsii*, *Pinus krempfii*, *Glyptostrobus* (Phuong, 2007).

Vietnam has been considered one of a few developing countries that the forest transition, from net forest loss to net forest gain, has been occurring (Keenan et al., 2015; Mather, 2007). After the deforestation period from the Vietnam War to the early 1980s, the forest cover in Vietnam has been increased due to many causes such as decollectivisation in Doi Moi economic reform 1986, allocation of forestry land to households, development of timber market (Meyfroidt & Lambin, 2008a) and national reforestation programs (De Jong et al., 2006; McElwee, 2009). The increase of forest cover in Vietnam mainly comes from the expansion of plantation forests.

The forest cover of Vietnam has reached 42% of the total land area until 2019, in which plantation forests account for 29.5% (4.3 million ha) of the total forest area (14.6 million ha) (VNFOREST, 2020a). Plantation forests in Vietnam are dominated by acacia (*Acacia mangium*, *Acacia auriculiformis*, *Acacia hybrid*), rubber (*Hevea brasiliensis*), and eucalyptus (*Eucalyptus globulus*) (Figures 2.1e and 2.1f). Acacia is the most popular plantation tree in Vietnam with over 1.1 million ha (as of 2014 (Nambiar et al., 2015)). Besides, Vietnam has nearly 1 million ha of rubber and about 500 thousand ha of eucalyptus (Harwood & Nambiar, 2014). Other plantation trees, such as pine (*Pinus*), *Manglietia conifera* Dandy, *Melaleuca cajuputi*, etc., occupy minor areas.

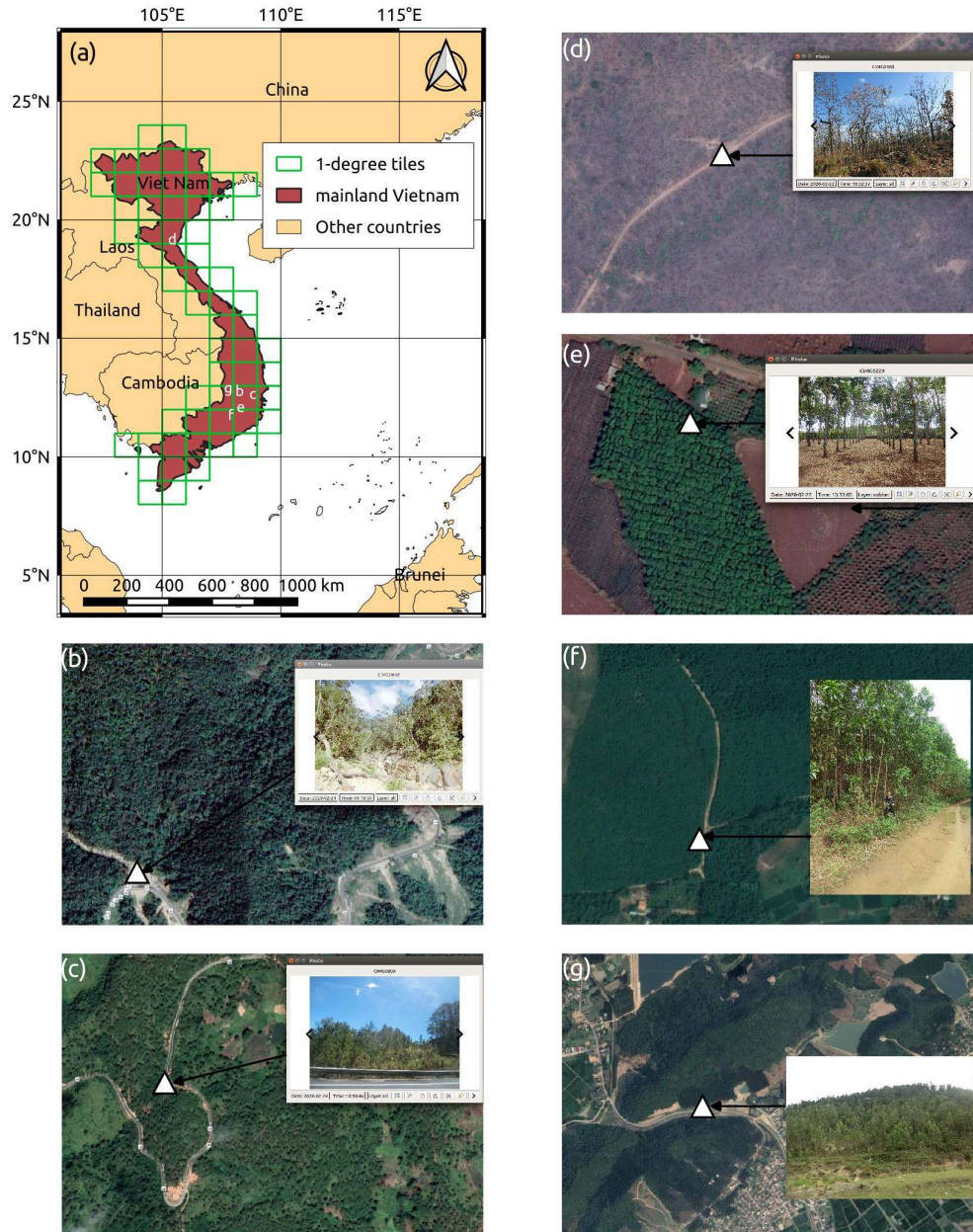


Figure 2.1. Study area and forest types in mainland Vietnam through ground-truth photos and high-resolution Google Earth (GE) images. (a) Location of mainland Vietnam; (b) natural evergreen broadleaf forest at  $12.2209^{\circ}$  N,  $108.7455^{\circ}$  E with a field photo (2020-02-24) and GE image (2019-03-09); (c) natural coniferous forest at  $12.1338^{\circ}$  N,  $108.6196^{\circ}$  E with a field photo (2020-02-24) and GE image (2020-01-19); (d) natural deciduous forest at  $12.8436^{\circ}$  N,  $107.7780^{\circ}$  E with a field photo (2020-02-22) and GE image (2020-03-01); (e) rubber plantation at  $12.6557^{\circ}$  N,  $107.8437^{\circ}$  E with a field photo (2020-02-22) and GE image (2019-03-01); (f) acacia plantation at  $12.7768^{\circ}$  N,  $108.8242^{\circ}$  E with a field photo (2020-02-23) and GE image (2020-03-09); (g) eucalyptus plantation at  $19.1783^{\circ}$  N,  $105.5992^{\circ}$  E with a field photo (2018-03-23) and GE image (2020-03-09).

## **2.2. Field surveys**

### **2.2.1. Field survey in northern Vietnam**

The field survey in northern Vietnam was conducted in March 2019. In this trip, this study collected about 42,000 GPS photos along 1,800 km total length of survey routes (Figure 2.2). Various types of forest in northern Vietnam were observed, i.e., a primary forest in Cuc Phuong national park (Ninh Binh province), a secondary forest in Hoang Lien national park (Lao Cai province), sparse forests on limestone (Cao Bang province), subtropical mountain deciduous needle-leaf forests (Cao Bang province), and plantation forest including mostly acacia and eucalyptus along the routes.

The primary forest in Cuc Phuong national park is the habitat of old-growth trees and tropical flora and fauna. Several large trees with massive biomass in Cuc Phuong may have about a thousand years old (Figure 2.3a). In contrast, the secondary forest in Hoang Lien national park harbors mostly small and medium trees (Figure 2.3b). An interview with a ranger in the Ranger Station Tram Ton, Hoang Lien national park was conducted. According to the interview, the main cause of deforestation in the Hoang Lien area is forest fires. The reason for forest fires can come from hot and dry weather in the dry season or from swidden burning in shifting cultivation practice (Figure 2.4a).

Swidden and barren hills (Figures 2.4a and 2.4b) appeared substantially along the survey routes in northern Vietnam. Shifting cultivation has been sustained widely in ethnic minorities. Many previous studies showed that shifting cultivation is the main driving force of deforestation in this region (Curtis et al., 2018; Tachibana et al., 2001).

Other interview was conducted on the way from Ha Noi to Lao Cai (Figures 2.5a and 2.5b). The interviewee is a manager of a wood production facility in Bao Yen district, Lao Cai province. Some information from the interview was recorded as follows:

- From 1992, the government of Vietnam stopped wood exploitation in protection forests, special-use forests, and sparse forests. The reforestation programs were then deployed for “re-greening bare hills”.

- From 1996, the forestry sector received great support from foreign governments, especially Finland and Germany. Since then, wood production from plantation trees has been continually increased.
- Wood products in this area are mainly exported to China.

According to the Law on Forest Protection and Development (2004) of the Vietnamese government, protection forests were defined as forests to be “used mainly to protect water sources and land, prevent erosion and desertification, restrict natural calamities and regulate climate, thus contributing to environmental protection”. Special-use forests were defined as forests to be “used for mainly conservation of nature, specimens of the national forest ecosystems and forest biological gene sources; for scientific research; protection of historical and cultural relics as well as landscapes; in service of recreation and tourism in combination with protection, contributing to environmental protection”.

The authenticity of the information from the interview was examined with material and documents (Mustalahti, 2011; T. T. H. Phan, 2017). Under the context discussed in the interview, the expansion of plant forests in Vietnam is the result of not only the national reforestation programs but also the wood market with huge demand for timber from China and western countries.

Another task of field survey was recognizing the actual LULC categories and collating it with the corresponding LULC categories in satellite images. Thereby, my ability of satellite image visual interpretation can be improved. For example, the pattern of eucalyptus plantation in a field photo was shown in Figure 2.6a and the pattern of acacia plantation in a field photo was shown in Figure 2.6b.



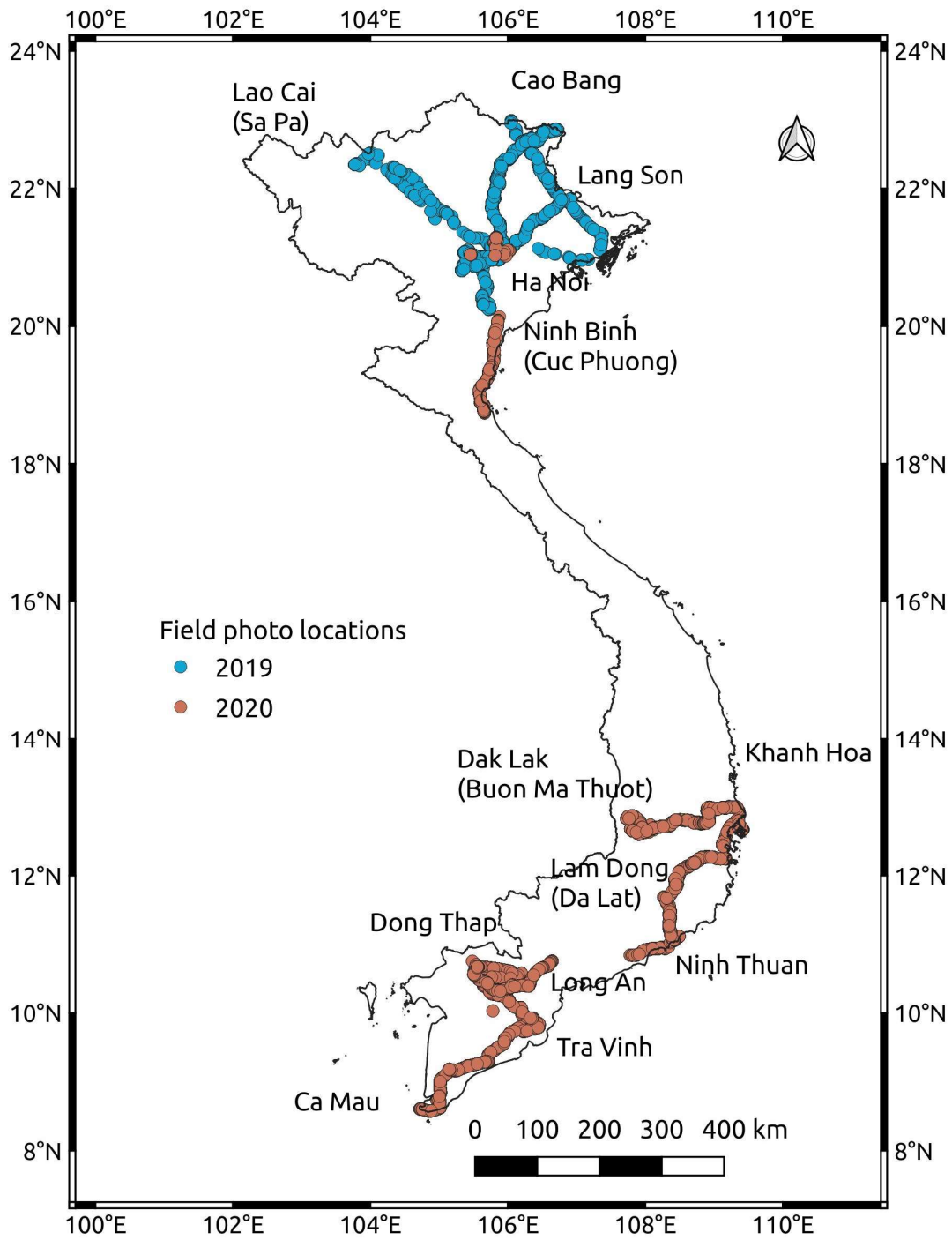


Figure 2.2. Field photo locations of two field surveys (in 2019 and 2020) of this study in Vietnam



2019-03-08, Location: 20°19'0.16"N, 105°38'25.77"E



2019-03-10, Location: 22°21'3.83"N, 103°46'20.66"E

Figure 2.3. (a) The primary forest in Cuc Phuong national park; (b) the secondary forest in Hoang Lien national park





2019-03-10, Location: 22°11'31.73"N, 104°19'23.31"E



2019-03-12, Location: 22°12'43.42"N, 106°31'1.45"E

Figure 2.4. (a) Shifting cultivation in northern Vietnam; (b) barren hills in northern Vietnam



2019-03-09, Location: 22°15'41.98"N, 104°25'46.76"E



2019-03-09, Location: 22°15'41.89"N, 104°25'47.15"E

Figure 2.5. (a) Interview local people in the Bao Yen district, Lao Cai province, Vietnam; (b) wood production in a local factory in the Bao Yen district



a



2019-03-12, Location: 21°8'18.52"N, 106°34'52.16"E

b



2019-03-13, Location: 20°29'33.02"N, 105°40'15.21"E

Figure 2.6. (a) Eucalyptus in field photo; (b) Acacia in field photo

### 2.2.2. Field survey in Central Highlands, Mekong Delta, and Ha Noi

The field survey in Central Highlands, Ha Noi, and Mekong Delta was conducted in February and March 2020. In this trip, this study collected about 34,247 GPS photos along 2,000 km of total length of survey routes (Figure 2.2). Plantation forests in the vicinity of Ha Noi were observed. Various forests were observed such as typical deciduous broadleaf forests in Yok Don national park (Dak Lak province), evergreen needle-leaf forests in Da Lat (Lam Dong province), tropical shrublands in Phan Thiet (Binh Thuan province), desert in Phan Thiet, acacia and rubber plantations, and evergreen broadleaf forests in many places in Central Highlands and South Central of Vietnam. Wetland and mangroves in Mekong delta were investigated lastly. Local people interviews were also conducted to investigate the LULC categories, historical changes of forests, and the relation to socioeconomic contexts.

#### (a) Field surveys in Ha Noi areas

The first place in the field survey in Ha Noi areas was the Phat Tich hill (Bac Ninh province) (Figure 2.7a). Although the majority of land use in the Red River Delta is agriculture, there are several steep lands like hills or low mountains that have been used for growing plantation forests. The plantation forests in Phat Tich hill were dominated by *Pinus* (Thông) and *Acacia auriculiformis* (tràm bông vàng or keo lá tràm) (Figure 2.7b). I measured a diameter at breast height (DBH) of some pine trees (Figure 2.7c) and *Acacia auriculiformis* (Figure 2.7d).

\* Interview with local people in Phat Tich hill:

- The plantation forest in Phat Tich hill includes mostly: *Pinus*, *Acacia auriculiformis*. The purpose of the plantation forest is protection. According to the Law on Forest Protection and Development (2004) of the Vietnamese government, a production forest was defined as a forest which is “mainly used for production and trading of timber, and non-timber forest products, combined with purposes of protection and environmental protection”. The year of planting was about 1996.

- The year of planting trees in Phat Tich hill is compatible with the background of national programs of forestry. In 1992, The government of Vietnam launched program 327 aiming for “re-greening the barren hills”. The salient point of this program is to allocate forest to the private sector such as local people, small cooperative associations.
- Besides, land cover in the Gia Lam district is characterized by mostly paddy, other crops, and orchards. In recent years, agricultural land has been converted to urban and built-up due to enhancing housing supply.



2020-02-18, Location: 21°6'21.24"N,  
105°59'53.87"E

a) Phat Tich Pagoda



2020-02-18, Location: 21°5'42.62"N,  
106°1'32.16"E

b) Leaves of *acacia auriculiformis*



2020-02-18, Location: 21°5'46.41"N,  
106°1'37.41"E

c) Measuring DBH of pine: 20.0 cm



2020-02-18, Location: 21°5'47.07"N,  
106°1'37.65"E

d) Measuring DBH of *acacia auriculiformis*:  
26.7 cm

Figure 2.7. Plantation forest survey in Phat Tich hill, Bac Ninh province

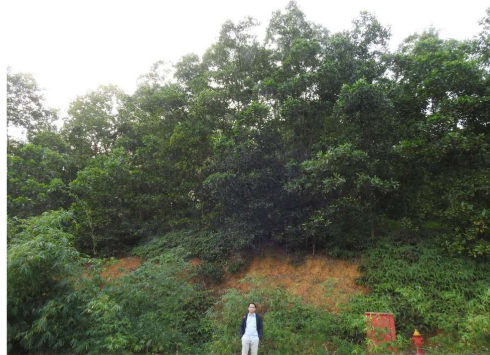


The second place of the survey in Ha Noi locates in the Dong Mo reservoir area (Figures 2.8a–d). The reservoir is surrounded by plantation forests, mostly acacia (Hybrid *acacia* which is *Acacia mangium* × *Acacia auriculiformis*). This area has been planned as a recreation area with golf courses and Vietnam National Village for Ethnic Culture and Tourism. Although several areas of plantation forests have been demolished for building infrastructure, acacia forests are preserved in some places. Old acacia trees and young acacia trees in this location can be compared via Figures 2.8a and 2.8b, respectively.



2020-02-19, Location: 21°2'35.05"N,  
105°28'8.37"E

a) Old acacia, planted in the 1990s



2020-02-19, Location: 21°2'19.98"N,  
105°27'18.10"E

b) Young acacia, planted in the 2010s



2020-02-19, Location: 21°2'24.68"N,  
105°27'30.13"E

c) Measuring DBH of old acacia: 12.7 cm



2020-02-19, Location: 21°2'25.51"N,  
105°27'29.74"E

d) Leaves of acacia (hybrid)

Figure 2.8. Acacia plantation forest survey in Dong Mo, Ba Vi district



The third survey place in Ha Noi areas was Den Giong (Giong Temple), Soc Son district, Ha Noi (Figure 2.9). On the way to Den Giong along the highway AH14, there are many croplands, mostly vegetable which supplies Hanoi and vicinity areas. Plantation forests in Den Giong are protection forests. The dominant trees are *Acacia auriculiformis* (Keo lá tràm) (Figure 2.9a) and *Pinus* (Thông) (Figure 2.9b). *Acacia auriculiformis* is a large body tree type. The mature body of *Acacia auriculiformis* is larger than *Acacia* hybrid. In the mature stage, the height of this tree can reach up to 30 m (Figure 2.9c).



2020-02-20, Location: 21°17'28.74"N,  
105°49'48.62"E

a) A hill of *acacia auriculiformis* at Den Giong



2020-02-20, Location: 21°16'42.35"N,  
105°49'45.81"E

b) *Pinus* plantation at Den Giong



2020-02-20, Location: 21°17'29.45"N,  
105°49'43.29"E

c) Measuring DBH of *acacia auriculiformis*:  
23.5 cm



2020-02-20, Location: 21°17'23.25"N,  
105°49'28.03"E

d) Interview local people at Den Giong about  
forest changes

Figure 2.9. Plantation forest survey at Den Giong, Soc Son district

Interview with local people in Den Giong (Figure 2.9d):

- The dominant trees of these plantation forest areas: *Pinus*, *Acacia auriculiformis*, Hybrid *acacia*.
- Before 1978, the land cover of this area was mostly barren hills and paddy rice in flat land.
- After 1978, the government (Ministry of Agriculture and Rural Development) hired local people to plant pine in the barren hills. The plantation pine forests were under the management of the government at that time.
- From 1993, the government allocated forest land to private sectors: local households and private companies. The government supported seedling trees. The local households were responsible for raising and taking care of the allocated forest land. For productive plantation forests, private households could exploit wood production under regulation of planting duration and maximum exploitation areas.
- *Acacia auriculiformis* and Hybrid *acacia* were planted in 1990s.
- Some of the acacia areas have been cultivated by private farms.
- Recently, some plantation forest in these places has been converted to golf courses.

In summary, observing the plantation forest in the Ha Noi survey route improved the ability of satellite image visual interpretation of plantation. The influence of national policies on reforestation was reflected through informative interviews. Most of the plantation forests in Hanoi were planted around 1993 when the government started to launch the “Greening the barren hills” program (327). Land cover changes in Hanoi such as conversion from agricultural land or forest to built-up were examined through field observation.

## **(b) Field surveys in Central Highlands and South Central of Vietnam**

Rubber has been widely planted in Central Highlands. The first selected location to investigate the rubber plantation was the vicinity of Buon Ma Thuot city, Dak Lak province (Figures 2.10a–d). GPS photos taking and local people interviews were conducted.

Interview with local people in Buon Ma Thuot city:

- The rubber planting year in these places was the 1980s.
- The rubber tree can reach the mature stage after 3 years.
- Rubber leaves fall in around Oct and Nov (dry season).
- DBH of an exploited rubber tree can reach 20 cm to 30 cm (Figures 2.10b and 2.10d).
- The distance between rows is 6m. The distance between 2 trees in a row is 3 – 4 m.
- Rubber latex is collected in the early morning every day, approximately 5:00 am.
- At the mature stage, the height of a rubber tree can reach 10–15 m.
- The latex exploitation duration can last about 50 years.
- However, when the latex amount decreases substantially after 15–20 years, rubber trees might be chopped down for wood production.





2020-02-21, Location: 12°42'45.64"N,  
108°6'8.37"E

a) Exploited rubber plantation in Buon Ma Thuot



2020-02-21, Location: 12°41'31.93"N,  
108°7'5.31"E

b) DBH of an exploited rubber tree: 27.7 cm



2020-02-21, Location: 12°44'7.20"N,  
108°4'29.08"E

c) Young and unexploited rubber trees



2020-02-21, Location: 12°44'7.20"N,  
108°4'29.08"E

d) DBH of an unexploited rubber tree: 20.0 cm

Figure 2.10. Rubber plantation in Buon Ma Thuot, Dak Lak province

The main driving forces of deforestation in Central Highlands of Vietnam has been attributed to conversion from forests to agriculture lands, in which rubber (Figure 2.10), coffee and pepper (Figures 2.11a and 2.11b) are main agriculture plantations (Curtis et al., 2018; Ha & Shively, 2008; Meyfroidt et al., 2013).



2020-02-22, Location: 12°39'18.02"N,  
107°50'40.95"E

a) Coffee and pepper in Cu Jut, Dak Lak



2020-02-22, Location: 12°42'10.83"N,  
108°7'13.97"E

b) Coffee



2020-02-22, Location: 12°51'0.36"N,  
107°47'15.85"E

c) Local people interview



2020-02-22, Location: 12°51'0.19"N,  
107°47'15.94"E

d) Deciduous broadleaf forests at Yok Don

Figure 2.11. Agricultural plantation trees and deciduous broadleaf forests in Dak Lak and Dak Nong provinces

\* Interview with local people (the driver) in Cu Jut, Dak Lak province (Figure 2.11c) about other croplands and rubber plantation:

- The combination of coffee and pepper is very popular in Central Highlands. Coffee is also mix-planted with orchards such as durian or avocado
- There are 3 main types of coffee:



- *Coffea robusta* (Cà phê vối): 2 m height at the mature stage. This is the most popular coffee tree in Dak Lak and entire Vietnam. This coffee has the highest productivity in comparison to others.
- *Coffea arabica* (Cà phê chè): 1 m height at the mature stage. It looks similar to tea (chè). This coffee has higher quality than the robusta coffee but lower productivity.
- *Coffea liberica* (Cà phê mít): 2–5 m height at the mature stage. It looks similar to jackfruit (mít).
- The harvesting time of coffee is around December.
- The pepper is a climbing plant. The platform for pepper might be concrete pillars, woody pillars, or living woody trees. The platforms are normally 3–4 m in height. The harvesting time of pepper is around October.

The recognition of pepper in satellite images is also important since its vertical structure is similar to plantation forests.

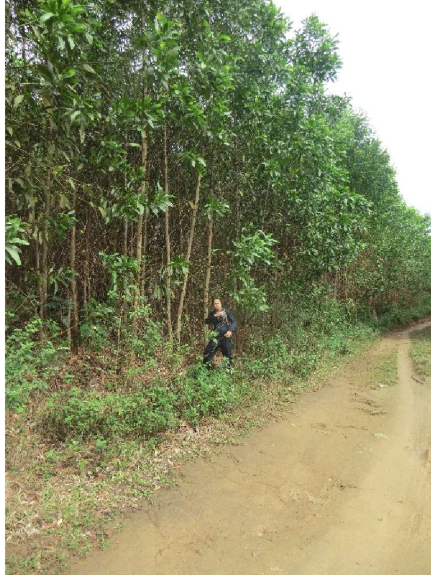
The pattern of typical deciduous broadleaf forests in Yok Don national park, Dak Lak province was observed and recorded (Figure 2.11d).

Acacia was also observed in M' Drak District, Dak Lak province (Figure 2.12a). In the local people interview in M' Drak, I focused on the economic value of acacia in comparison to other agricultural plantations. From the interview, the crop structure of this area varies depending on the variation of the price of the products.

\* Interview with local people in M' Drak, Dak Lak province (Figure 2.12b):

- The acacia forest in this area was planted around 2005.
- Before the acacia plantations, this area is mostly barren.
- The acacia plantations were conducted by a company, namely Tan Mai from 2005 – 2010.
- After 2010, the acacia plantations were conducted by some local households.
- The rotation of the acacia is normally 5 years.
- The economic value of the acacia: 1 ha in 5 years ~ 60–80 million Vietnam Dong (\$3000– \$4000)
- In his household, he is planting some orchards, peppers, and coffee.

- Investment for pepper: 200 million Vietnam Dong (~\$10000). Rural households can apply for preferential loans from banks for agriculture production.
- 1 ha pepper can contain 1200 pillars.
- Pepper can be harvested after 2 years. One pillar can give 10 kg pepper/year.
- Climate is a big factor affecting agriculture productivity, especially coffee. Excessive rainfall in this region decreases the effectiveness of coffee.



2020-02-23, Location: 12°46'33.96"N,  
108°49'25.10"E

a) Acacia plantation at M'Drak. DBH: 20 cm



2020-02-23, Location: 12°46'25.70"N,  
108°49'23.49"E

b) Interview local people at M'Drak



2020-02-23, Location: 12°40'13.76"N,  
109°24'50.62"E

c) Sand dunes in Mui Doi, Khanh Hoa province



2020-02-23, Location: 12°40'5.09"N,  
109°25'21.23"E

d) Tropical shrubland at Mui Doi

Figure 2.12. Acacia plantation in M'Drak, Dak Lak and shrubland, sand dunes in Mui Doi, Khanh Hoa

Subtropical shrubland and coastal sand dune near Mui Doi - the easternmost point of Vietnam, in Khanh Hoa province were observed (Figures 2.12c and 2.12d). High temperatures and strong wind in this area have formed an arid area with barren sand dunes and shrubland.

In Lam Dong province, evergreen needle-leaf forests (Figures 2.13a and 2.13b), deciduous broadleaf forests (Figure 2.13c) were observed. Vegetation cover in the Da Lat area is characterized by homogeneous evergreen needle-leaf forests (pine) forests. This is a unique regional-scale forest in Vietnam. The canopy cover of the pine forests is sparser than that of natural forests and other plantation forests (e.g., acacia or rubber).



2020-02-24, Location: 12°7'10.11"N,  
108°35'7.64"E

a) Evergreen needleleaf forests (pine) in Lam Dong province



2020-02-24, Location: 11°53'46.91"N,  
108°26'25.21"E

b) Pine forest in Da Lat



2020-02-24, Location: 11°40'50.60"N,  
108°16'28.23"E

c) Deciduous broadleaf forests in Duc Trong, Lam Dong



2020-02-24, Location: 11°37'13.64"N,  
108°18'15.03"E

d) Interview local people at Duc Trong, Lam Dong

Figure 2.13. Evergreen needle-leaf forests and deciduous broadleaf forests in Lam Dong



\* Interview with local people near Dai Ninh hydroelectric plant, Duc Trong district, Lam Dong (Figure 2.13d):

- The Dai Ninh hydroelectric plant started into operation in 2008.
- Before the Dai Ninh dam and reservoir were built, the croplands in this area were mainly sugar cane.
- After Dai Ninh hydroelectric plant appeared, sugar cane was replaced by coffee. It was mainly due to the economic effectiveness of coffee was higher at that time.
- His household has 3 ha coffee.
- In this area, every farming household has 3–5 ha on average for cultivation.
- Recently, since the price of coffee has decreased, there is a trend to replaced coffee with higher economic value plantation such as vegetables: carrot, sweet potato...
- Pine forests are natural in Lam Dong, some small areas are plantation pines.
- Coffee is normally mix-planted with other orchards: cacao, macadamia.

The interview revealed the influence of the market price to distribution of crops in Duc Trong, Lam Dong.

In Binh Thuan province, shrubland and sand dunes landscapes were observed (Figure 2.14a).

Notably, local people interview in Bac Binh, Binh Thuan revealed that the cause of forest fires is attributed to both weather and native people activity (Figure 2.14b).



2020-02-25, Location: 11°7'5.90"N,  
108°29'30.35"E

a) Coastal sand dunes and shrub land in Binh Thuan province



2020-02-25, Location: 11°23'16.38"N,  
108°21'43.40"E

b) Interview local people in Bac Binh district, Binh Thuan province

Figure 2.14. Field survey in Binh Thuan province

\* Interview with local people in Bac Binh district, Binh Thuan province (Figure 2.14b):

- Natural forests: extreme dry weather can lead to forest fires. The grass at understory is selectively burned by rangers to avoid forest fire.
- Some small forest areas are burned by local people when they are hunting.
- Acacia has been planted in some places.
- In the rainy season, the deciduous forests in this region turn back to green.
- Crops can be cultivated mainly in the rainy season.
- His household has 2.2 ha cashew.
- The biggest problem in this area is the shortage of water resources.
- At some places in the Bac Binh district, local people exploited underground water. The depth of the groundwater level is about 55 m.
- His household needs to purchase drinking water from other areas.
- A new reservoir, the Luy river reservoir, has been built to supply and harmonize water for the semi-arid Bac Binh district and Tuy Phong district of Binh Thuan province.

In summary, the field survey in Central Highlands and South Central of Vietnam obtained much useful information and experience about biophysical features of forest types and forest changes in history. The information about growth stages and the development of rubber and acacia plantation such as mature year, the period of leaf-falling, installation of rubber fields is very important in the detection of rubber by remote sensing images. Notably, the vertical structure of evergreen needle-leaf forests in Lam Dong is similar to that of plantation forests. This similarity may cause misclassification in the mapping process. The changes between agricultural crops and plantation trees in these regions can be governed by the market price. The expansion of perennial crops is the main cause of deforestation in Central Highlands of Vietnam.

### **(c) Field surveys in the Mekong delta**

Before the 17<sup>th</sup> century, the intact Mekong Delta was characterized by a seasonally inundated wetland. Later on, along with the immigration of Vietnamese from

the north, land and channel networks in the Mekong Delta have been developed for cultivating mainly rice and orchard. Inundated grass is the dominant vegetation cover in the original wetland. Woody trees are mainly plantations and the dominant species is *Melaleuca Cajuputi* (Figure 2.15a). Land resources in this region are mainly used for agriculture. Paddy, orchards (Figure 2.15b), and aquaculture are the most dominant land cover types.



2020-02-27, Location: 10°45'22.01"N,  
105°29'0.76"E

a) *Melaleuca Cajuputi* (Tram Nuoc), an inundated woody plantation tree



2020-02-27, Location: 10°33'3.48"N,  
106°8'37.40"E

b) A pine apple field



2020-02-27, Location: 10°40'30.46"N,  
105°31'56.44"E

c) A mango field and cultivation design for reducing acid sulfate in soil



2020-02-27, Location: 10°40'32.68"N,  
105°32'26.12"E

d) Interview local people in Tam Nong district, Dong Thap province

Figure 2.15. Field surveys in Dong Thap and Long An provinces

\* Interview with local people in Tam Nong district, Dong Thap province:

Man 1 (Figure 2.15c):

- The purpose of the small channels is to reduce acid sulfate in soil (Figure 2.15c).
- Tien river provide water resources to this area
- Recently, there has been a trend of converting rice land to orchard land in this area.
- The popular orchards in this area include mango, coconut, pineapple, and jackfruit.

Man 2, 86 years old (Figure 2.15d):

- He came to Dong Thap province in 1973.
- In the 1970s, the land cover of the Mekong Delta mostly is wetland with inundated grass and rice. There was no woody plantation forest at that time.
- 1982–1984: plantation forests (*Melaleuca Cajuputi*) were planted in the Mekong Delta. In general, the *Melaleuca* can turn to the mature stage after 10 years from the seedling.
- From 1982 to now, the plantation forest area has not changed remarkably.
- During 1970–1980, the channel network system in this area was developed and expanded.

In recent years, drought and water shortage have become one of the biggest environmental issues in the Mekong Delta (Figure 2.16a). Drought always is accompanied by the salt intrusion. For example, the drought in 2016 caused salt intrusion into the central Mekong Delta, which is Can Tho province (Nguyen, 2017; M. N. Nguyen et al., 2020). The reduction of water resources the in lower Mekong Delta has derived from many causes. One of the main causes is the development of large reservoirs and dams upstream Mekong basin, mostly in China and other countries such as Thai Land and Laos (Räsänen et al., 2012). Over-exploitation of groundwater also leads to a decrease in the water level of river networks (Minderhoud et al., 2017). Therefore, a decrease of precipitation can make the water shortage in Mekong Delta more severe. Many paddy areas could not be cultivated under the drought condition.



The surface area of aquaculture in Ca Mau province is characterized by 70% mangrove and 30% aquaculture pond (Figure 2.16b). The mangrove area of Ca Mau has experienced remarkable changes during recent decades. The changes consisted of being destroyed by dioxin in the Vietnam War, regeneration after the war, and then being used as a part of the aquaculture ecosystem.



2020-02-29, Location: 9°47'31.29"N,  
106°26'18.70"E

a) Drought in Tra Vinh province



2020-02-29, Location: 8°43'34.21"N,  
105°0'32.89"E

b) Aquaculture: mangrove (*Rhizophora*) and pond



2020-02-29, Location: 8°39'55.79"N,  
105°0'8.58"E

c) Interview local people in Ca Mau



2020-02-29, Location: 8°43'33.49"N,  
105°0'32.90"E

d) Interview local people in Ca Mau

Figure 2.16. Field surveys in Tra Vinh and Ca Mau provinces

\*) Interview local people in Nam Can district, Ca Mau province

Man 1, 72 years old (Figure 2.16c):

- From 30 years ago until now, mangrove was converted to cropland, then after that cropland was converted to aquaculture: fish, shrimp, and crabs (no information of exact time).
- Water was contaminated by acid sulfate for some years, affecting the productivity of aquaculture.
- The saltwater for agriculture is supplied by river networks. Recently, water quality has reduced because rivers have been polluted by industry areas and discharge of large-scale aquaculture.
- Recently, households in this area restricts taking water from the river to their ponds. They clean the aquaculture ponds with microbiological substances.
- Keeping mangroves above the aquaculture ponds is of the local government policy. The mandatory rate is 70% mangrove, 30 % water in terms of area coverage.

Man 2, 72 years old (Figure 2.16d):

- He has been living here since 1988. At that time, this area was mainly fallow land. The government then allocated land to people for establishing new economic areas.
- From 1988, mangrove was converted to aquaculture ponds with the regulation on surface area of 70% forest and 30% pond, or 60% forest and 40% pond.
- Concern about water pollution.
- The purpose of mangrove above aquaculture ponds:
  - Harmonize the temperature
  - Food for shrimp

In summary, the field surveys in the Mekong delta investigated and explored many forest cover characteristics and environmental issues of this region. Forests in Mekong Delta mostly are plantation forests (*Melaleuca Cajuputi*) and mangrove (mostly *Rhizophora*) near the coastline. The typical characteristic of Mekong Delta soil is the contamination of acid sulfate. Therefore, in cultivation, farmers make small channels (~1 m width) interleaved with embanked soil beds (1–3 m width). This design

can reduce acid sulfate in the embankment. This makes the unique pattern of the agricultural land of the Mekong Delta region in satellite images. Water shortage is a big problem in the Mekong Delta. It is due to the development of large reservoirs and dams upstream of the Mekong basin, mostly in China and other countries such as Thai Land and Laos. Another reason is the over-exploitation of the groundwater. The pollution of water resources due to sewage discharge from industry areas to rivers. The unique characteristics of aquaculture in Ca Mau province is characterized by the surface area consisting of 70% mangrove cover and 30% aquaculture pond beneath. This distinct pattern can be displayed in satellite images.

## **Chapter 3. Mapping Plantation Forest and Natural Forest for entire Mainland Vietnam**

### **Publications:**

- **Paper:** Hoang T.T., Truong V.T., Hayashi M., Tadono T., Nasahara K.N. (2020) New JAXA High-resolution Land Use/Land Cover Map for Vietnam aiming for Natural Forest and Plantation Forest Monitoring. *Remote Sensing*, 12, 2707. <https://doi.org/10.3390/rs12172707>
- **Data publication:** the LULC map has been published on JAXA website as open LULC data of JAXA: [https://www.eorc.jaxa.jp/ALOS/en/lulc/lulc\\_vnm\\_v2006.htm](https://www.eorc.jaxa.jp/ALOS/en/lulc/lulc_vnm_v2006.htm)



### 3.1. Background

Globally, 4.7 million ha/year of net forest loss and a 3 million ha/year increase in planted forests have been reported between 2010 to 2020, according to Food and Agriculture Organization of the United Nations (FAO) (FAO, 2020b). The forest dynamics have been attributed to main drivers such as land use/land cover (LULC) conversion for commodity production, forestry, agriculture shifting, wildfire, and urbanization (Curtis et al., 2018). These land modifications have led to negative environmental impacts including the increase in greenhouse gas emission (Rivera et al., 2020), disruption of the water cycle (Hornung et al., 1987; Salati & Nobre, 1991), increase in soil erosion (Anselmetti et al., 2007), biodiversity loss (Barlow et al., 2016; Carnus et al., 2006), and disruption of local livelihoods (Campbell et al., 2008). To alleviate these issues, managements and policies have been proposed and implemented from local to global scales. In such frameworks, the importance of detailed and accurate measurements of forest types have been emphasized. The mapping of natural forests and plantation forests can provide a more accurate input for actual deforestation detection, carbon assessment, climate change modelling, and biodiversity loss detection.

Previous studies present various approaches to distinguish plantation forests and natural forests using remote sensing data. One approach is to make use of the phenological characteristics of specific plantation types based on time-series imagery. Typical studies using this approach have adopted the difference in spectral characteristics of the defoliation period of deciduous rubber to separate it from natural forests (B. Chen et al., 2016; Dong et al., 2013; H. Fan et al., 2015; Senf et al., 2013; C. Xiao et al., 2019). Another approach is to use image processing techniques for enhancing the separability of plantation forests and natural forests. Specifically, texture analysis (Haralick et al., 1973) has been used to differentiate the unique spatial pattern of the targeted plantation, e.g., oil palm fields, from surrounding land covers (Cheng et al., 2018; Thenkabail et al., 2004). This technique is usually applicable to high-resolution and cloudless images. Another technique is using remote sensing indices to amplify the differences in the spectral information of the two forest types. A number of optical vegetation indices have proved their effectiveness in mapping plantation forests and natural forests (Dong et al., 2013; Dong, Xiao, Sheldon, Biradar, & Xie, 2012; Kou

et al., 2015; Qin et al., 2016; Torbick et al., 2016; X. Xiao et al., 2002) such as the normalized difference vegetation index (NDVI), enhanced vegetation index (EVI), soil-adjusted total vegetation index (SATVI), normalized difference tillage index (NDTI), and land surface water index (LSWI). In addition, the development of new radar satellites has facilitated the increasing involvement of radar data in LULC mapping and forest monitoring (Flores-Anderson et al., 2019). L-band synthetic aperture radar (SAR) images have been widely used in forest mapping at the global scale as well as at the regional scale (Dong et al., 2014; Shimada et al., 2014; V. T. Truong et al., 2019) since it can provide cloud-free structural information sensitive to forest cover. Radar indices such as the polarization ratio, normalized difference index (NDI), and the NL index have also been used in forest type mapping (Almeida-Filho et al., 2009; De Alban et al., 2018; Dong et al., 2014; Dong, Xiao, Sheldon, Biradar, & Xie, 2012; Dong, Xiao, Sheldon, Biradar, Duong, et al., 2012; G. Li et al., 2012; Miettinen & Liew, 2011; Qin et al., 2015; Sarzynski, Giam, & Carrasco, 2020). Another comprehensive approach that recent studies have frequently demonstrated is the combination of optical and SAR imagery (De Alban et al., 2018; Dong et al., 2013; Dong, Xiao, Sheldon, Biradar, & Xie, 2012; Gutiérrez-Vélez & DeFries, 2013; Kou et al., 2015; Poortinga et al., 2019; Sarzynski, Giam, & Carrasco, 2020; Torbick et al., 2016). The synergy of structural information from SAR images and biophysical information from optical images has improved the accuracy and map detail. In recent studies, this integration of different data types has been carried out by data fusion at a feature level, where the optical and SAR images are stacked into a single dataset as a classification input.

One of the biggest challenges of forest type mapping is distinguishing between plantation evergreen broadleaf forest (EBF) and natural EBF since the spectral characteristics of these two forest types are mostly identical as mentioned in section 1.1. It is, therefore, necessary to build a comprehensive mapping approach that is applicable for different plantation forest types, various ranges of geographic regions, short time coverage.

The advantage of forest mapping studies nowadays is the development of data-rich sources. The availability of open satellite data such as Global PALSAR-2/PALSAR (phased array type L-band synthetic aperture radar) mosaic (JAXA, 2020c), Sentinel

constellation (ESA, 2014a), and new Landsat satellites (USGS/NASA, 2020), with advances in their specifications, has offered mapping forest types at a large scale and in high detail. Besides, open cloud-computing platforms for remote sensing, such as Google Earth Engine, have supported data curation in high performance at any spatial scope.

Japan Aerospace Exploration Agency (JAXA) has released several LULC map products for Vietnam using remote sensing data (JAXA/EORC, 2016). The previous high-resolution LULC products of Vietnam (version 16.09, 18.07, 18.09) (Hoang et al., 2018; D. C. Phan et al., 2018) with a 10 or 15 m resolution have presented the changes in land cover over about one decade (2007–2017). The most recent LULC products (version 19.08) showed annual changes in land cover from 2015 to 2018 in a 50 m resolution (V. T. Truong et al., 2019). In terms of forest mapping, these above-mentioned LULC products categorized forests in Vietnam as one class whereas the advantage of this research is to produce a 10 m resolution LULC map with many forest classes. Highly detailed forest maps for Vietnam would be of importance in supporting the REDD+ (reducing emissions from deforestation and forest degradation), in which Vietnam is one of the first countries to have participated.

The goal of this chapter was to produce a high-resolution LULC map that distinguishes natural forests and plantation forests (acacia, eucalyptus, rubber, and others) across different geographic regions in mainland Vietnam in 2016 using remote sensing data. The specific objectives were to: (1) construct a comprehensive mapping approach that classifies various types of natural forests and plantation forests for the entire mainland Vietnam; (2) evaluate the classification performance of satellite data including PALSAR-2/ScanSAR, PALSAR-2 mosaic, Sentinel-2, Sentinel-1 and Landsat 8; (3) compare the resultant map with other land cover products such as the European Space Agency (ESA) CCI land cover map 2016 (ESA, 2015a), FROM-GLC 10 m 2017 (Gong et al., 2019), JAXA Forest/Non-forest map 2016 (JAXA, 2020c), JAXA land use/land cover map of Vietnam 2016 v19.08 (V. T. Truong et al., 2019) and MODIS land cover product MCD12Q1 2016 (Mark a. Friedl et al., 2010); (4) compare the resultant map with official data of the Vietnamese government including national statistics (VNFOREST, 2020a) and the Vietnam Forest Resource Map 2016

(VNFOREST, 2020b). The accurate measurement of natural forest and plantation forest changes would support an investigation about potential telecouplings in plantation forest lands in Vietnam such as the expansion of farm-based plantation of smallholders (Sandewall et al., 2010) or vulnerable households under the plantation forest expansion (Thulstrup, 2014).

## **3.2. Materials and methods**

### **3.2.1. Method**

To distinguish natural forests and plantation forests over many geographic regions in Vietnam, this study's mapping approach was designed based on the differences between the two forest types. These differences were supposed to be independent of foliage characteristics since both plantation and natural forests in Vietnam contain several tree types (EBF, deciduous, coniferous). Here, I formed a hypothesis relating to the differences between natural forests and plantation forests as follows:

- (1) Vertical structure: plantation forests demonstrate uniform structures such as the lattice pattern of rubber in Figure 2.1e or the dense pattern of acacia in Figure 2.1f. Trees of plantation forests have the same height, same diameter at breast height (DBH), and same density. On the contrary, natural forests present nonuniform structures such as a random pattern of canopies as seen in Figure 2.1b. Natural forests are structurally very diverse with a high degree of variation in height classes, DBH and densities. This difference can be recognized by the combinations of L-band SAR polarizations of horizontal transmit–horizontal receive (HH) and horizontal transmit–vertical receive (HV);
- (2) Biophysical features and water content: the chlorophyll concentration, greenness, brightness, moisture, etc. of plantation forest canopies are different from those of natural forest canopies. This difference can be recognized using water and vegetation indices derived from optical images;

- (3) Topography: plantation forests are mostly cultivated in low slope lands while natural forests grow in higher slope lands. This difference can be recognized by topography data.

Based on the hypothesis, this study constructed a comprehensive mapping approach that satisfied the following criteria:

- Integrating information from various sensors to recognize all the differences between the two forest types;
- Making use of time series data for phenology capture, which are essential for the classification of deciduous forest, rice, and other crops;
- Making use of spectral indices and radar indices aside from the original bands and polarizations. As the indices are less sensitive to atmospheric noise and viewing geometry, they can support the geographical transferability.

To integrate various information from multi-temporal images of multiple sensors, this study's approach adopted a non-parametric probabilistic classifier for each of sensor data, then the integration was implemented by multiplying the resultant probability of each sensor data's classification results. The classifier was based on Kernel Density Estimation (KDE) with Bayesian inference (Hashimoto et al., 2014). In previous studies, this method was applied for mapping high-resolution land use and land cover products for entire Japan (Hashimoto et al., 2014; Katagi et al., 2018) and Vietnam (Hoang et al., 2018; D. C. Phan et al., 2018; V. T. Truong et al., 2019). The resulting products were published as open land cover data by JAXA (JAXA, 2020d).

A brief explanation of the classification process is as follows. The classifier simulated the probability density function of each land cover category based on the KDE technique with the training data as the input (Equation (3.1)). The selected kernel type in this study was the Gaussian function (Equation (3.2)). The posterior probability values corresponding to each of the land cover types were then estimated at the pixel-wise level for the entire feature space based on the Bayes theorem (Equation (3.3)). For the integration of multitemporal images of the sensors, the joint posterior probability of each of the land cover categories was estimated by multiplying the component posterior probability values of each single-date image from each sensor's data (Equation (3.4)).

Finally, the predicted land cover type of each pixel was assigned by choosing the one having the highest probability (Equation (3.5)). The engineering of the classification process was conducted using the Saiclass software version 17.06 developed by JAXA and the University of Tsukuba (Hashimoto et al., 2014)).

$$p(x | C_k) = \frac{1}{N_k} \sum_{n=1}^{N_k} \left\{ \prod_{d=1}^D \frac{1}{h_d} K\left(\frac{x_d - x_{n,d}}{h_d}\right) \right\} \quad (3.1)$$

$$K(u) = \frac{1}{\sqrt{2\pi}} \exp\left(-\frac{u^2}{2}\right) \quad (3.2)$$

$$p(C_k | x) = \frac{p(C_k)p(x | C_k)}{p(x)} = \frac{p(C_k)p(x | C_k)}{\sum_{k=1}^M p(C_k)p(x | C_k)} \quad (3.3)$$

$$p'(C_k) = \prod_{i=1}^s p'_i(C_k | x_i) \quad (3.4)$$

$$\hat{C} = \underset{k}{\operatorname{argmax}} p'(C_k) \quad (3.5)$$

$$h_d = N_k^{-1/(D+4)} \cdot \sigma_d \quad (3.6)$$

Where:  $C_k$  is the  $k$ -th category ( $k = 1, 2, \dots, M$ , where  $M$  is the number of categories; here,  $M = 12$ );  $p(C_k)$  is the prior probability of category  $C_k$ ;  $p(x | C_k)$  was estimated based on the training data using the KDE (Equation (1));  $x_d$  is the  $d$ -th component of the feature vector  $x$  ( $1 \leq d \leq D$ );  $D$  is the number of dimensions of the feature space;  $x_{n,d}$  is the  $d$ -th component of vector  $x_n$  (training data), where ( $1 \leq n \leq N^k$ );  $N^k$  is the number of training data in category  $C_k$ ;  $h_d$  is the bandwidth of the KDE, defined by Scott's rule in Equation (3.6);  $\sigma_d$  is the standard deviation of the  $d$ -th component training data of category  $C_k$ ;  $p(C_k | x)$  is the posterior probability;  $p'(C_k)$  is the joint posterior probability;  $\hat{C}$  is the predicted land cover type.

This study conducted mapping for each  $1^\circ \times 1^\circ$  tiles (Figure 2.1a) individually, instead of mapping the Vietnam area as a whole. The overall workflow of establishing the high-resolution LULC map for Vietnam is illustrated in Figure 3.1. The preprocessing step for the input data is discussed in Section 3.2.2.

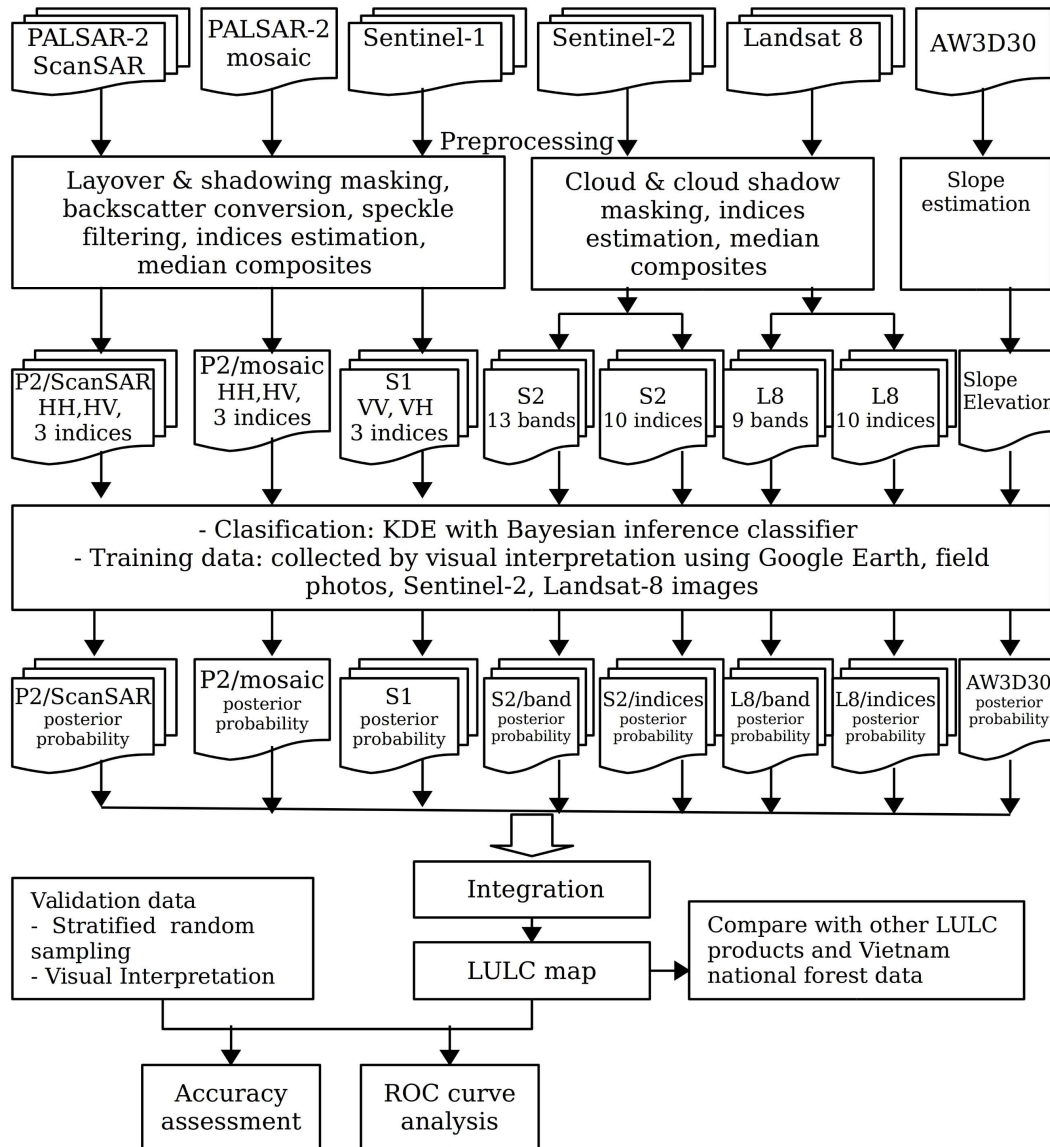


Figure 3.1. The overall workflow of establishing the high-resolution LULC map for Vietnam in 2016

### 3.2.2. Satellite data and preprocessing

#### (a) PALSAR-2/ScanSAR time series data and single-temporal PALSAR-2 mosaic

The PALSAR-2 is a radar imaging sensor onboard the Advanced Land Observing Satellite 2 (ALOS-2) operated by JAXA. ScanSAR is the name of the image product acquired in the ScanSAR observation mode of PALSAR-2. The ScanSAR mode has a

wide swath (350 km) which is suitable for LULC studies and forest monitoring at large scales. The sensitivity of the L-band (1270 MHz) PALSAR/PALSAR-2 images to the forest covers has been exploited in many forest monitoring studies (Flores-Anderson et al., 2019; Shimada et al., 2014; V. T. Truong et al., 2019). The revisit time of the ALOS-2 satellite, which considers one “cycle”, is 14 days. The ScanSAR data are provided in  $1^\circ \times 1^\circ$  tile mosaic images merged by images acquired in one cycle. Therefore, one ScanSAR image can contain the observation data of several days within a 14-day period. These time-mixed images are acceptable for LULC mapping since the phenology would not have a significant discrepancy in such 14-day intervals. The ScanSAR data are a high level-processing product with geometric corrections and terrain corrections including the application of radiometric terrain flattening (Small, 2011). ScanSAR images have a 50 m resolution with a georeference of the geographic latitude/longitude WGS84 coordinate system. Each of the images had two polarization data which are HH (horizontal transmit—horizontal receive) and HV (horizontal transmit—vertical receive). The number of ScanSAR images over the Vietnam area in one year depends on the PALSAR-2 Basic Observation Scenario (JAXA, 2015). For this study, the available ScanSAR images in 2016 for the entire Vietnam were 450  $1^\circ \times 1^\circ$  tile images. The Vietnam area was covered by 60  $1^\circ \times 1^\circ$  tiles (Figure 2.1a). Therefore, the number of images in one coverage tile could be 7 or 8 scenes. The ScanSAR data used in this study were provided by JAXA under the research agreement of “Generation of the Precise Land Cover Map”.

Another PALSAR-2 data used in this study was the single-temporal PALSAR-2 mosaic. This yearly product is open data with global coverage provided by JAXA. Originated from Fine Beam Dual Mode (FBD), the PALSAR-2 mosaic product has a spatial resolution of 25 m (JAXA, 2019). In this study, PALSAR-2 mosaic was used as a complement for ScanSAR data since its resolution is higher than the ScanSAR’s resolution. This product was provided in  $1^\circ \times 1^\circ$  tiles with HH and HV polarizations.

For preprocessing, PALSAR-2/ScanSAR time-series data and single-temporal PALSAR-2 mosaic had the same procedure. First, the gamma-0 radar backscatter (unit in decibel (dB)) was derived from the digital number ( $DN$ ) by Equation (3.7) (JAXA, 2019) ( $CF$  is the calibration factor with a given value of  $-83.0$  dB;  $\langle \rangle$  is an ensemble



averaging operator). The radar shadowing and layover pixels were masked by the enclosed mask files. A Lee filter (Lee, 1980) with a  $5 \times 5$  moving window was applied to suppress the speckle noises in gamma-0 images. The radar indices were estimated and then stacked with the two original gamma-0 HH, HV images. The radar indices included ratio (*RAT*, Equation (3.8)), normalized difference index (*NDI*, Equation (3.9)), and NL index (*NLI*, Equation (3.10)). These indices have been proved to be effective in the classification of natural forests and plantation forests (De Alban et al., 2018; Sarzynski, Giam, & Carrasco, 2020).

$$\gamma^0 = 10 \cdot \log_{10} \langle DN^2 \rangle + CF \quad (3.7)$$

$$RAT = \frac{\gamma_{HH}^0}{\gamma_{HV}^0} \quad (3.8)$$

$$NDI = \frac{\gamma_{HH}^0 - \gamma_{HV}^0}{\gamma_{HH}^0 + \gamma_{HV}^0} \quad (3.9)$$

$$NLI = \frac{\gamma_{HH}^0 \times \gamma_{HV}^0}{\gamma_{HH}^0 + \gamma_{HV}^0} \quad (3.10)$$

Where:  $\gamma^0$  is the gamma-0 radar backscatter; *DN* is the digital number; *CF* is the calibration factor with a given value of -83.0 dB,  $\langle \rangle$  is an ensemble averaging operator;  $\gamma_{HH}^0$  and  $\gamma_{HV}^0$  are the gamma-0 radar backscatters corresponding to polarizations of HH and HV, respectively.

## (b) Sentinel-1 time-series data

Sentinel-1 satellites provide C-band SAR images (at 5.045 GHz) with an incidence angle between 20 and 45°. The revisit time of Sentinel-1 constellation (Sentinel-1A and Sentinel-1B) is 6 days (12 days for each individual Sentinel-1). This study used Sentinel-1 images in interferometric wide swath (IW) mode with a swath width of 250 km, and a resolution of 10 m. All the images were acquired in descending observation, with two polarizations including VV (vertical transmit—vertical receive) and VH (vertical transmit—horizontal receive). The Sentinel-1 data were collected from the Google Earth Engine (GEE) cloud platform. These data were provided in the ground range detected (GRD) level 1 product (ESA, 2014b) with additional preprocessing including thermal noise removal, radiometric calibration, and a terrain correction using SRTM 30 or ASTER DEM (Google Earth Engine, 2020b). Since the radiometric terrain

flattening was not applied, the pixel value of the data presented a sigma-0 value (unit in decibel (dB)). I generated 8 composite images during 2016, and each composite image was created by taking the pixel-wise median values of all images during each 1.5-month interval using a median reducer function of the GEE (Google Earth Engine, 2020a). These data were then trimmed into  $1^\circ \times 1^\circ$  tiles (Figure 2.1a). Similar to the PALSAR-2 data, a Lee filter with a  $5 \times 5$  moving window was applied to remove the speckle noise in sigma-0 Sentinel-1 images. The radar indices of the Sentinel-1 data, which were analogous to those of the PALSAR-2 data, were then estimated (Equations (3.10)–(3.12)). The utilization of these radar indices was based on an assumption that the C-band SAR indices can support and improve the classification of a low biomass plantation and natural vegetation, e.g., crops and natural grass or shrubs (Filgueiras et al., 2019).

$$RAT = \frac{\sigma_{VV}^0}{\sigma_{VH}^0} \quad (3.11)$$

$$NDI = \frac{\sigma_{VV}^0 - \sigma_{VH}^0}{\sigma_{VV}^0 + \sigma_{VH}^0} \quad (3.12)$$

$$NLI = \frac{\sigma_{VV}^0 \times \sigma_{VH}^0}{\sigma_{VV}^0 + \sigma_{VH}^0} \quad (3.13)$$

Where:  $\sigma_{VV}^0$  and  $\sigma_{VH}^0$  are the sigma-0 radar backscatters corresponding to polarizations of VV and VH, respectively.

### (c) Sentinel-2 and Landsat-8 data

The Sentinel-2A MultiSpectral Instrument (MSI) data have been available from June 2015 with a high spatial resolution (10 m, 20 m, 60 m), high temporal resolution (10-day revisit time) and 290 km swath width. The Sentinel-2 data during 2016 used in this study were collected from the GEE. The data archived in the GEE were in level 1C, which included cloud masking flags for dense clouds and cirrus clouds (ESA, 2015c). After applying cloud masking, 8 median composite images were generated with 1.5-month intervals (same as the composite method applied for the Sentinel-1 images). Even after cloud masking by a quality assessment (QA) file and conducting the median composite, non-negligible cloud covers were still present in several images. To remove these cloud covers, I adjusted the too-bright threshold value of visible spectral bands

and masked out bright pixels (Vermote et al., 2014). The images were then trimmed to  $1^\circ \times 1^\circ$  tiles (Figure 2.1a). All 13 multispectral bands of the Sentinel-2 were used in this study (Table 3.1).

Table 3.1. Spectral bands of Sentinel-2A (ESA, 2015b) and Landsat 8 (USGS, 2020b) used in this study

<b>Data</b>	<b>Band</b>	<b>Spectral Range (nm)</b>	<b>Electromagnetic Region</b>
Sentinel-2A	Band 1	432–453	Aerosols
	Band 2	459–525	Blue
	Band 3	542–578	Green
	Band 4	649–680	Red
	Band 5	697–712	Red Edge 1
	Band 6	733–748	Red Edge 2
	Band 7	773–793	Red Edge 3
	Band 8	780–886	NIR (Near Infrared)
	Band 8A	854–875	Red Edge 4
	Band 9	935–955	Water vapor
	Band 10	1358–1389	Cirrus
	Band 11	1568–1659	SWIR1 (Shortwave Infrared 1)
Band 12	2115–2290	SWIR2 (Shortwave Infrared 2)	
Landsat 8	Band 1	430–450	Coastal aerosol
	Band 2	450–510	Blue
	Band 3	530–590	Green
	Band 4	640–670	Red
	Band 5	850–880	NIR (Near Infrared)
	Band 6	1570–1650	SWIR1 (Shortwave Infrared 1)
	Band 7	2110–2290	SWIR2 (Shortwave Infrared 2)
	Band 10	10,600–1,190	TIRS1 (Thermal Infrared 1)
Band 11	11,500–12,510	TIRS2 (Thermal Infrared 2)	

The Landsat 8 surface reflectance product from the Operational Land Imager (OLI) and Thermal Infrared Sensor (TIRS) were collected from the GEE. With a 30 m resolution, 180 km swath width, and 16-day revisit cycle, the Landsat 8 data are the useful complement of the Sentinel-2 data, especially in cloudy areas. The surface reflectance product embedded the atmospheric corrections using LaSRC codes and included cloud and cloud shadow masks using the CFMASK algorithm (USGS, 2019). After applying cloud and cloud shadow masking, 8 median composite Landsat 8 images were generated with 1.5-month intervals, and then they were trimmed to  $1^\circ \times 1^\circ$  tiles

(Figure 2.1a). This study used 7 spectral bands from the OLI and 2 brightness temperature bands from the TIRS (Table 3.1).

Aside from the original bands, the spectral indices estimated from both Sentinel-2 and Landsat 8 were utilized. I selected a set of vegetation indices and water indices that were the most useful for the classification of natural forests and plantation forests based on previous studies (De Alban et al., 2018; Poortinga et al., 2019; Sarzynski, Giam, & Carrasco, 2020; Torbick et al., 2016). The indices included the NDVI (Equation (3.14)) (Rouse et al., 1973; Tucker, 1979), EVI (Equation (3.15)) (A. Huete et al., 2002; A. R. Huete et al., 1997), LSWI (Equation (3.16)) (X. Xiao et al., 2002), aerosol free vegetation index (AFVI; Equation (3.17)) (Karnieli et al., 2001), atmospherically resistant vegetation index (ARVI; Equation (3.18)) (Kaufman & Tanré, 1992), soil and atmosphere resistant vegetation index (SARVI; Equation (3.19)) (A. R. Huete et al., 1997), moisture stress index (MSI; Equation (3.20)) (Hunt & Rock, 1989), SATVI (Equation (3.21)) (Hagen et al., 2012), NDTI (Equation (3.22)) (Daughtry et al., 2005), and index-based built-up index (IBI; Equation (3.23)) (Xu, 2008).

$$NDVI = \frac{NIR - Red}{NIR + Red} \quad (3.14)$$

$$EVI = G \frac{NIR - Red}{NIR + C_1 \times Red - C_2 \times Blue + L} \quad (3.15)$$

$$LSWI = \frac{NIR - SWIR1}{NIR + SWIR1} \quad (3.16)$$

$$AFVI = \frac{NIR - 0.5SWIR2}{NIR + 0.5SWIR2} \quad (3.17)$$

$$ARVI = \frac{NIR - (Red - \beta(Blue - Red))}{NIR + (Red - \beta(Blue - Red))} \quad (3.18)$$

$$SARVI = \frac{(1 + L)(NIR - (Red - \beta(Blue - Red)))}{NIR + (Red - \beta(Blue - Red)) + L} \quad (3.19)$$

$$MSI = SWIR1/NIR \quad (3.20)$$

$$SATVI = \left( \frac{SWIR1 - Red}{SWIR1 + Red + 0.1} \right) \times \left( 1.1 - \frac{SWIR1}{2} \right) \quad (3.21)$$

$$NDTI = \frac{SWIR1 - SWIR2}{SWIR1 + SWIR2} \quad (3.22)$$

$$IBI = \frac{2SWIR1/(SWIR1 + NIR) - (NIR/(NIR + Red) + Green/(Green + SWIR1))}{2SWIR1/(SWIR1 + NIR) + (NIR/(NIR + Red) + Green/(Green + SWIR1))} \quad (3.23)$$

#### (d) AW3D30 topographic data

AW3D30 is a 30 m resolution digital surface model (DSM) product generated from the Panchromatic Remote-sensing Instrument for Stereo Mapping (PRISM), which is an optical sensor onboard the Advanced Land Observing Satellite (ALOS). The purpose of using this auxiliary data was to improve the separability of natural categories from human-impacted landscapes. For example, plantation vegetations are grown mostly in a specific range of altitudes and slopes due to the ecological requirements of plantation species, and to facilitate human accessibility. AW3D30 was provided open and freely by JAXA (JAXA, 2020a). The DSM data were downloaded in  $1^\circ \times 1^\circ$  tiles, and the slope images were then estimated from the DSM images.

All the preprocessing steps were implemented by Python, Shell Script, Geospatial Data Abstraction Library (GDAL; available online: <https://gdal.org/>), and Quantum Geographic Information System 3.4 (QGIS; available online: <https://qgis.org/en/site/>). After preprocessing steps, all the data were organized as in Table 3.2.

Table 3.2. Organization of datasets, the number of images for each  $1^\circ \times 1^\circ$  tiles

Datasets	Year of Acquisition	Features of each data	Number of images/tile
PALSAR-2/ScanSAR	2016	HH, HV, and 3 indices	7 or 8
PALSAR mosaic	2016	HH, HV, and 3 indices	1
Sentinel-1	2016	VV, VH, and 3 indices	8
Sentinel-2 original bands	2016	13 original bands	8
Sentinel-2 indices	2016	10 indices	8
Landsat 8 original bands	2016	9 original bands	8
Landsat 8 indices	2016	10 indices	8
AW3D30	-	Elevation & slope	1

### 3.2.3. Reference data and classification scheme

The land use/land cover category system in this study was established following criteria from the Land Cover Classification System of the FAO (Gregorio, 2016) and

systematically inherited from previous JAXA LULC products (Hoang et al., 2018; D. C. Phan et al., 2018; V. T. Truong et al., 2019) (Table 3.3). All forest classes complied with the following conditions: areas must be at least 0.5 ha, the tree height must be higher than 5 m and the canopy cover must be at least 10% (FAO, 2018).

Table 3.3. Description of the land cover categories of the Vietnam LULC map in 2016

<b>Code</b>	<b>Category</b>	<b>Definition</b>
1	Water	Permanent fresh/salt water bodies such as oceans, lakes, rivers, inundation areas
2	Urban/built-up	Artificial construction structures, impervious surfaces
3	Rice	Paddy fields with inundated planted rice
4	Other crops	Herbaceous crops or shrub crops other than rice
5	Grass/Shrub	Herbaceous or shrub (non-woody) natural vegetation
6	Orchard/Crop mosaic	Tree crops and herbaceous crops mosaic, immature plantation trees
7	Barren	Lands with exposed soil, sand or rocks that always have vegetation cover less than 10%
8	Evergreen broadleaf forest	Mixed natural forests dominated by evergreen broadleaf trees
9	Coniferous forest	Natural forests with coniferous trees.
10	Deciduous forest	Natural forests with deciduous or semi-deciduous trees.
11	Plantation forest	Mature acacia, rubber, eucalyptus and other plantation trees
12	Mangrove	Woody vegetation on waterlogged soil, mostly along the coastline

The training data were collected by visual interpretation using high-resolution Google Earth images, Sentinel-2, and Landsat 8 images, with the support of GPS photos taken from field surveys. The training data were created in point-sample form, with each training data point representing a homogeneous area of the targeted land cover type. I created 179,970 training data points in total for 12 LULC categories (Figure 3.2a). The number of training data points for each category are shown in Figure 3.2a in square brackets.

This study used GPS photos taken from many field surveys in Vietnam in 2015, 2016, 2018, 2019, and 2020 (Figure 3.2b), which were designed to serve not only this study but also the production of previous Vietnam LULC maps (Hoang et al., 2018; D. C. Phan et al., 2018; V. T. Truong et al., 2019). The ground-truth photos supported the visual identification of land cover types from remote sensing imagery. The GPS photos

were taken using GPS cameras or automatic time-lapse GPS cameras (Gopro). The number of GPS photos in each of the field surveys are described in the square brackets of Figure 3.2b.

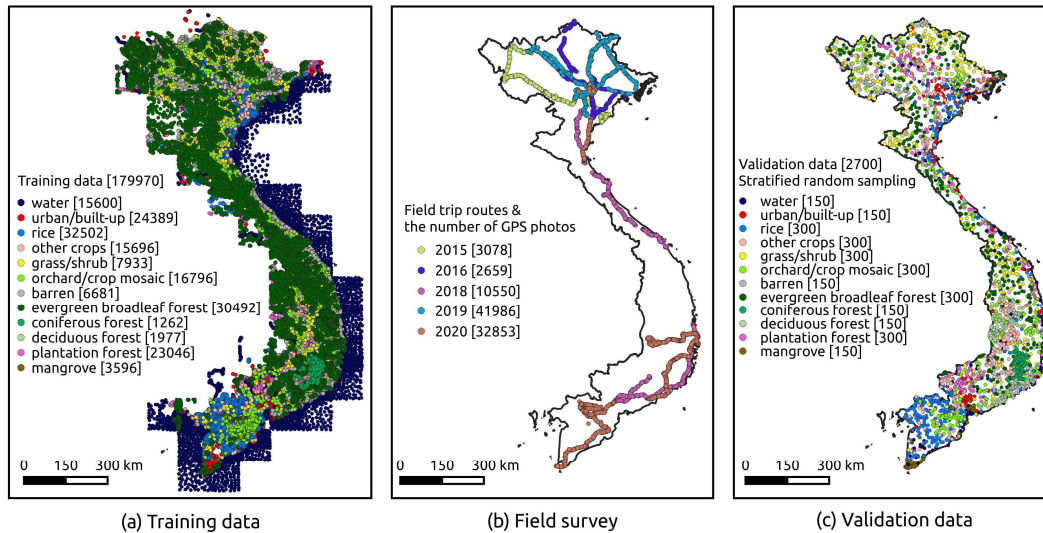


Figure 3.2. Distribution and quantity of reference data for 2016 mapping. (a) Distribution and quantity of training data; (b) Distribution and quantity of field survey data; (c) Distribution and quantity of validation data.

The validation data were designed and created following the method described by Olofsson et al. (2013). First, I used the stratified random sampling method to create sampling points. The land cover types of the resultant map were used as strata. Depending on the area values of each stratum, I allocated different numbers of sampling points (Appendix Table A1). The strata having areas greater than 2 million ha were sampled by 300 points whereas the strata having areas smaller than 2 million ha were sampled by 150 points. The number of samples in each stratum was given in square brackets of Figure 3.2c. The total number of samples was 2700 points. The stratified random sampling process was conducted using the AcATaMa plugin of QGIS software. The sampling points were then labeled with land cover types by visual interpretation using Sentinel-2 and Landsat 8 images in 2016. The labeled points were then used as the validation dataset to create the error matrix of the resultant LULC map (Appendix Table A1). The overall accuracy (OA), user's accuracy (UA), producer's accuracy (PA),

and their standard errors were estimated following the methods of Olofsson et al. (2013, 2014).

As the classification was conducted for each  $1^\circ \times 1^\circ$  tile individually (mentioned in Section 3.2.1), the training data used for the targeting tile was taken from all the training data sampling points located within that tile and its 8 surrounding tiles. This practice could avoid the edge mismatching issue which may occur in the resultant LULC map tiles after classification.

### 3.3. Results

#### 3.3.1. Evaluation of the classification performance of satellite data

The receiver operating characteristic (ROC) (Zweig & Campbell, 1993) was employed to evaluate the classification performance of input data. The ROC curves illustrated the graphs of true positive rates (*TPR*) (Equation (3.24)) versus the false positive rates (*FPR*) (Equation (3.25)) at different classification thresholds. The thresholds were determined by the predicted probabilities of positive classes. Generally, ROC curves indicate the trade-off between the *TPRs* and *FPRs* of a classification model. A model having ROC curves closer to the top-left corner would indicate a better performance. The area under the curve (*AUC*), which is estimated by the two-dimensional area underneath the ROC curve (Equation (3.26)), is the numerical measurement of the ROC curve. A higher value of *AUC* implies a better classification performance.

This study generated ROC curves for all 12 land cover classes for each input data and the model with all the input data integrated (Figure 3.3). A total of 2700 validation data points were used for establishing the ROC curves.

$$TPR = \frac{\text{True Positive}}{\text{True Positive} + \text{False Negative}} \quad (3.24)$$

$$FPR = \frac{\text{False Positive}}{\text{False Positive} + \text{True Negative}} \quad (3.25)$$



$$AUC = \int_0^1 TPR d(FPR) \quad (3.26)$$

Where: In the validation, *True Positive* of a category is the number of data points having the classified value correctly predicted; *False Negative* of a category is the number of data points having the classified value incorrectly predicted that it does not belong to the category; *False Positive* of a category is the number of data points having the classified value incorrectly predicted that it belongs to the category; *True Negative* of a category is the number of data points having the classified value correctly predicted that it does not belong to the category;

The ROC plots in Figure 3.3 showed that the integration of all sensor data gave the best overall classification performance. This can be interpreted from the Figure that the ROC curves of the integration model (Figure 3.3h) were closer to the top-left corner than those of other individual input (Figures 3.3a–g). The grass/shrub class was the most challenging since its AUC showed the lowest values in all models compared to that of other classes. The comparison of ROC plots of PALSAR-2/ScanSAR and PALSAR-2 mosaic showed that ScanSAR time-series data have better classification performance on forest classes than PALSAR-2 mosaic single-temporal data. This was proved in Figures 3.3e and 3.3f, AUC values of EBF, coniferous, deciduous, plantation of ScanSAR data (0.87, 0.93, 0.70, 0.79, respectively) are mostly higher than those of PALSAR mosaic data (0.83, 0.90, 0.71, 0.76, respectively). On the other hand, the C-band Sentinel-1 ROC plot showed lower classification performance in forest classes in comparison to all other sensor data.

AUC values of all the input data for each of the forest classes was shown in Figure 3.4. As can be seen in Figure 3.4, the integration of all the input data showed the best performance, which was reflected by the highest AUC values in all the forest classes. As for the major forest classes, including EBFs and plantation forests (Figures 3.4a and 3.4b), the PALSAR-2 and Sentinel-2 data indicated higher AUC values than the Landsat 8 and Sentinel-1 data. In terms of deciduous forests (Figure 3.4c), the AUC

values of optical data (Sentinel-2, Landsat 8) are higher than those of SAR data (Sentinel-1, PALSAR-2). A possible reason would be the high sensitivity of the time-series optical data to the phenological characteristics of deciduous forests (seasonal leaf drop). The trend of the AUC values of coniferous forests was mostly similar to that of EBFs, with higher AUC values for PALSAR-2 and lower AUC values for other data (Figure 3.4d). Another salient point is that in most of the cases, the time-series PALSAR-2/ScanSAR data have higher AUC values than the single-temporal PALSAR-2 mosaic data, and the Sentinel-2 data have higher AUC values than the Landsat 8 data. This proof emphasizes the advantages of the L-band time-series ScanSAR and high-resolution optical time-series Sentinel-2 data in forest type mapping in Vietnam.

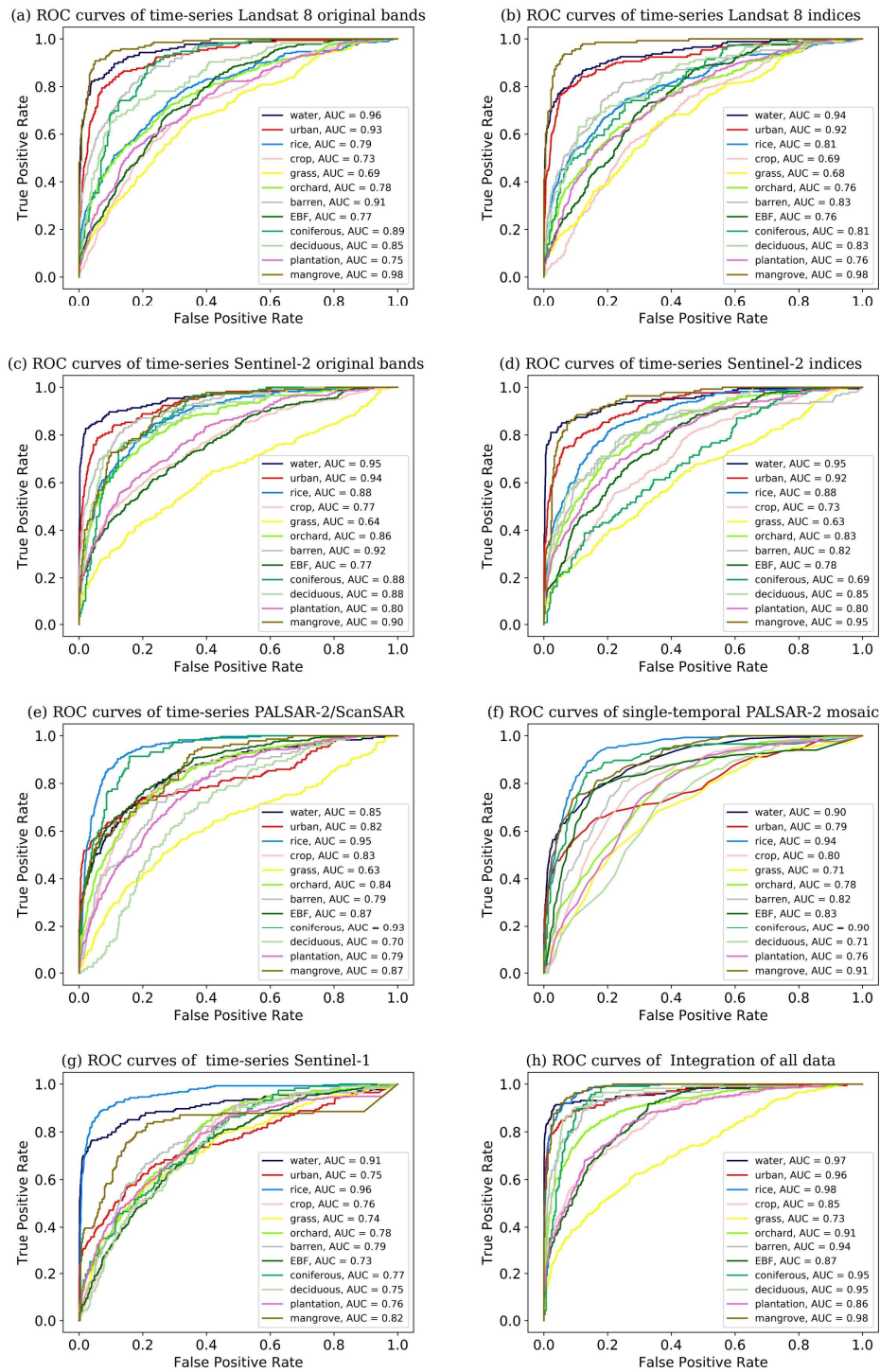


Figure 3.3. Receiver operating characteristic (ROC) curves of the 12 land cover categories for each input data model in 2016 mapping. (a) ROC curves of time-series Landsat 8 original bands; (b) ROC curves of time-series Landsat 8 indices; (c) ROC curves of time-series Sentinel-2 original bands; (d) ROC curves of time-series Sentinel-2 indices; (e) ROC curves of time-series PALSAR-2/ScanSAR; (f) ROC curves of single-temporal PALSAR-2 mosaic; (g) ROC curves of time-series Sentinel-1; (h) ROC curves of integration of all data

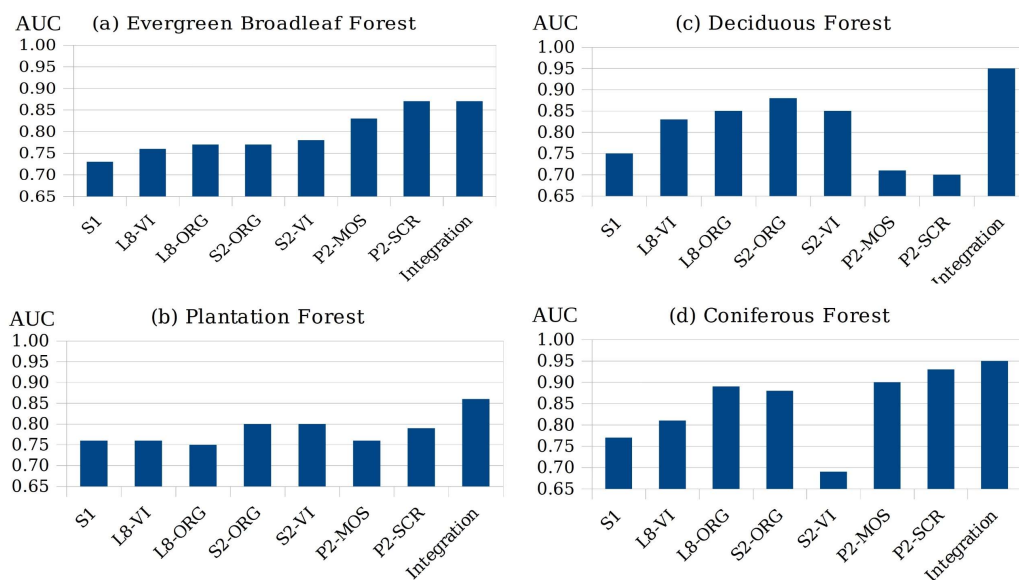


Figure 3.4. Comparison of the area under the curve (AUC) value of input data in forest classes in 2016 mapping. (a) The AUC value of input data in evergreen broadleaf forests; (b) The AUC value of input data in plantation forests; (c) The AUC value of input data in deciduous forests; (d) The AUC value of input data in coniferous forests where: S1 is the Sentinel-1 time-series; L8-VI is the Landsat 8 vegetation indices time-series; L8-ORG is the Landsat 8 original bands time-series; S2-ORG is the Sentinel-2 original bands time-series; S2-VI is the Sentinel-2 vegetation indices time-series; P2-MOS is the PALSAR-2 mosaic; P2-SCR is the PALSAR-2/ScanSAR time-series; integration is the integration of all inputs

### 3.3.2. The resultant Vietnam LULC map 2016 and its comparison to other LULC map products

The resultant 10-m resolution LULC map of Vietnam in 2016 was shown in Figure 3.5a. The overall accuracy of the map was 85.6%. The evergreen broadleaf forest class, which accounts for more than 88% of total natural forest area, showed high UA and PA (95.3% and 89.6%, respectively). The other natural forest classes including deciduous forest and coniferous forest had accuracies lower than 80%. The plantation forest class also had high UA and PA (86.0% and 88.0%, respectively). The errors of forest classes mainly came from misclassification between the forest types. Besides, other confusion came from grass/shrub versus EBF and deciduous forest versus crops.

Mangrove demonstrated high accuracies with both UA and PA reached more than 92%. The detail of the error matrix was provided in Appendix Table A1.

An acacia plantation forest area in this study's map, Google Earth imagery, and several open land cover products was shown in Figures 3.5b–h. The acacia area was a field site that was close to the site described in Figure 2.1f. As can be seen in the Figures, the acacia plantation forest areas were detected in this study's map while in ESA-CCI map, MODIS land cover map (MCD12Q1), JAXA LULC map v19.08, JAXA Forest/Non-Forest map the acacia forest areas mostly presented as cropland or non-forest areas. In the FROM-GLC 2017v1 map (Figure 3.5f), some of the acacia areas were detected as forest. However, the FROM-GLC map does not distinguish natural forests and plantation forests.

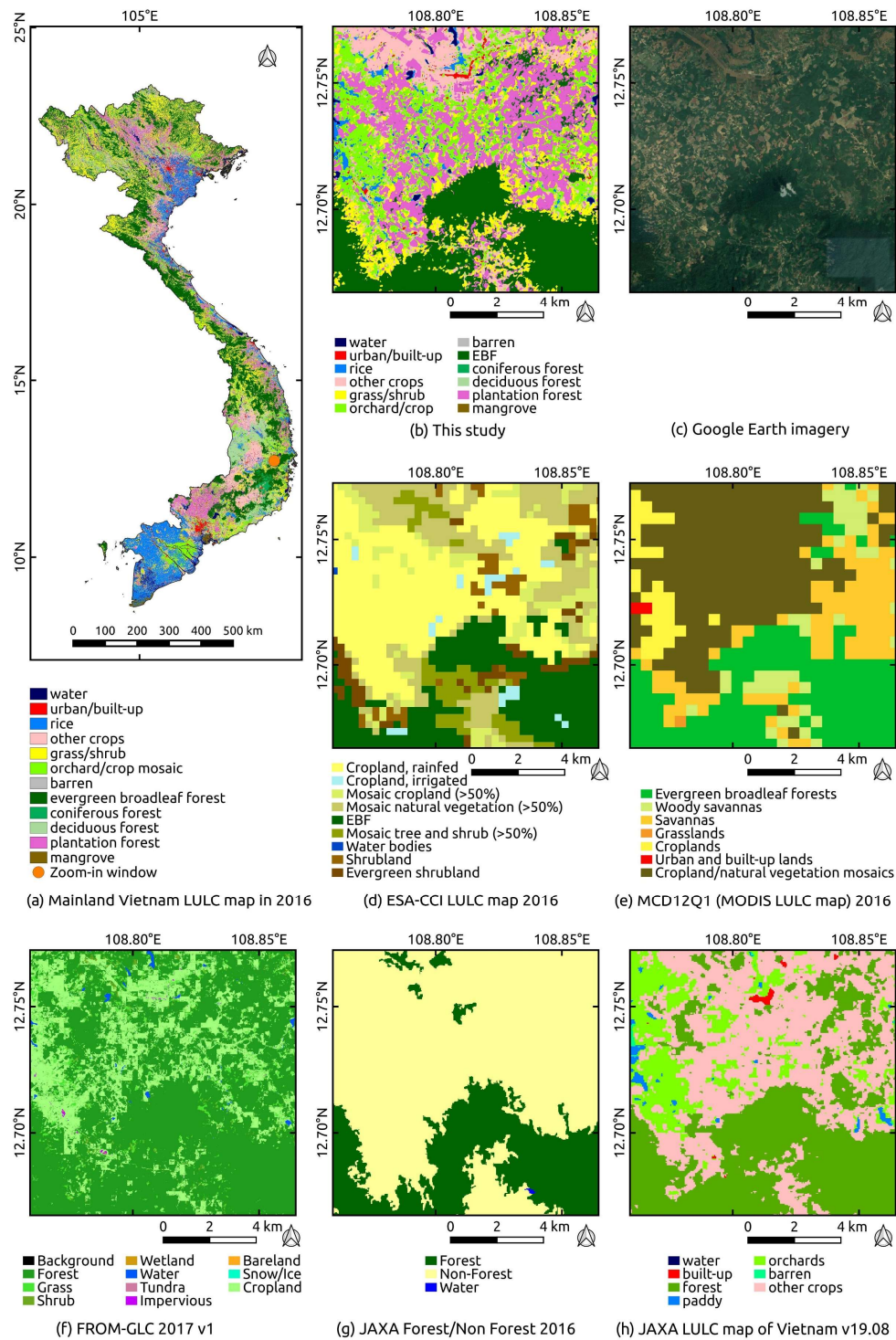


Figure 3.5. The resultant Vietnam LULC map 2016 and its comparison to other LULC products. (a) The overall mainland Vietnam LULC map in 2016; (b) The LULC map of this study in the zoom-in window; (c) The Google Earth imagery in the zoom-in window; (d) ESA-CCI LULC map 2016 in the zoom-in window; (e) MCD12Q1 (MODIS LULC map) 2016 in the zoom-in window; (f) FROM-GLC 2017 v1 LULC map in the zoom-in window; (g) JAXA Forest/Non-Forest map 2016 in the zoom-in window; (h) JAXA LULC map of Vietnam 2016 (version 19.08) in the zoom-in window.

### 3.3.3. Comparison of forest areas between this study's map in 2016 and Vietnam national statistical data

The comparison between this study and Vietnam national statistical data of the total forest area, the natural forest area, and the plantation forest area is shown Figure 3.6. For the natural forest area in this study, the classes including EBFs, deciduous forests, and coniferous forests were merged into one class which represented the natural forests in Vietnam and then the area and the standard error were measured. The total forest area in this study was measured by summing up all the forest classes in the resultant map.

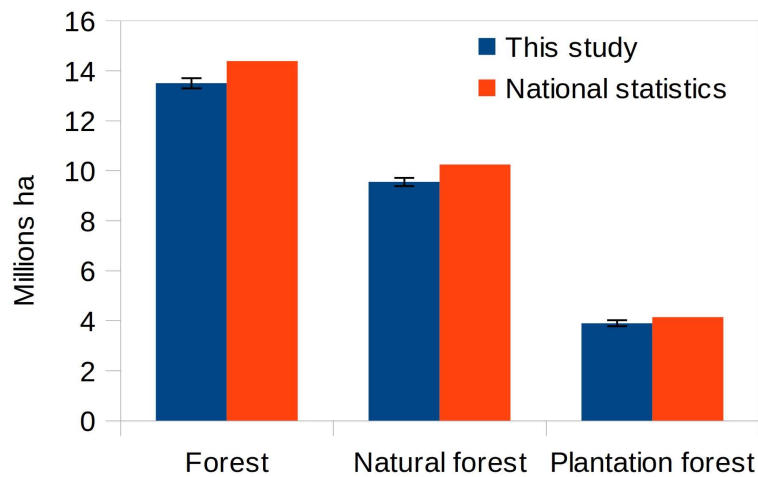


Figure 3.6. Comparison of forest areas between this study's LULC map in 2016 with Vietnam national statistical data.

Overall, this study's areas were lower than those of the national statistics with minor differences (smaller than 8% in all the three forest areas). The total forest area, the natural forest area, and the plantation forest area in this study's map of 2016 were  $13.50 \times 10^6$  ha ( $\pm 0.20 \times 10^6$  ha),  $9.55 \times 10^6$  ha ( $\pm 0.16 \times 10^6$  ha), and  $3.89 \times 10^6$  ha ( $\pm 0.11 \times 10^6$  ha) respectively, whereas those of the national statistical data were about  $14.38 \times 10^6$  ha,  $10.24 \times 10^6$  ha, and  $4.14 \times 10^6$  ha respectively (VNFOREST, 2020a). The differences in forest areas between this map and the national statistics may come from the error of this map and the difference in the definition of land use/land cover

used by each of the sources. The national statistics counted all the land areas assigned as forest land, even when there was no tree stands at that time. For this study's map, forest areas were estimated based on actual forest covers detected by the remote sensing data.

### **3.3.4. Comparison between this study's map and the Vietnam Forest Resource (VFR) Map 2016**

The resultant LULC map was compared with the forest map of the government of Vietnam, namely the Vietnam Forest Resource Map (2016). The VFR Map was established under a Vietnam national forest inventory program and it has been opened to the public (VNFOREST, 2020b). The category system of the VFR Map included 17 classes. The source of the VFR Map also provided a simplified forest map with three classes including natural forests (a merged class from many natural forest classes), plantation forests, and bare land. I estimated 10-km resolution fractional cover maps of the natural forests and plantation forests of this study's map and the simplified VFR Map (Figure 3.7a–d). The natural forest class in this study's map was merged from the EBFs, deciduous forests, and coniferous forests. The fractional difference maps (absolute value of the subtraction) between this study and the VFR Map (Figures 3.7e and 3.7f) was then derived to examine the degree of consistency between this study's result and the official map.

This study's maps and the VFR Maps had a good consistency at a 10-km resolution (Figure 3.7). Most of the area over mainland Vietnam had a fractional cover difference of less than 10% in terms of both natural forests and plantation forests. However, several areas revealed a substantial fractional difference, shown as zoom-in sites in Figures 3.7e and 3.7f. I compared my LULC map with the VFR Map at the three sites to explore the causes of these differences (Figure 3.8).



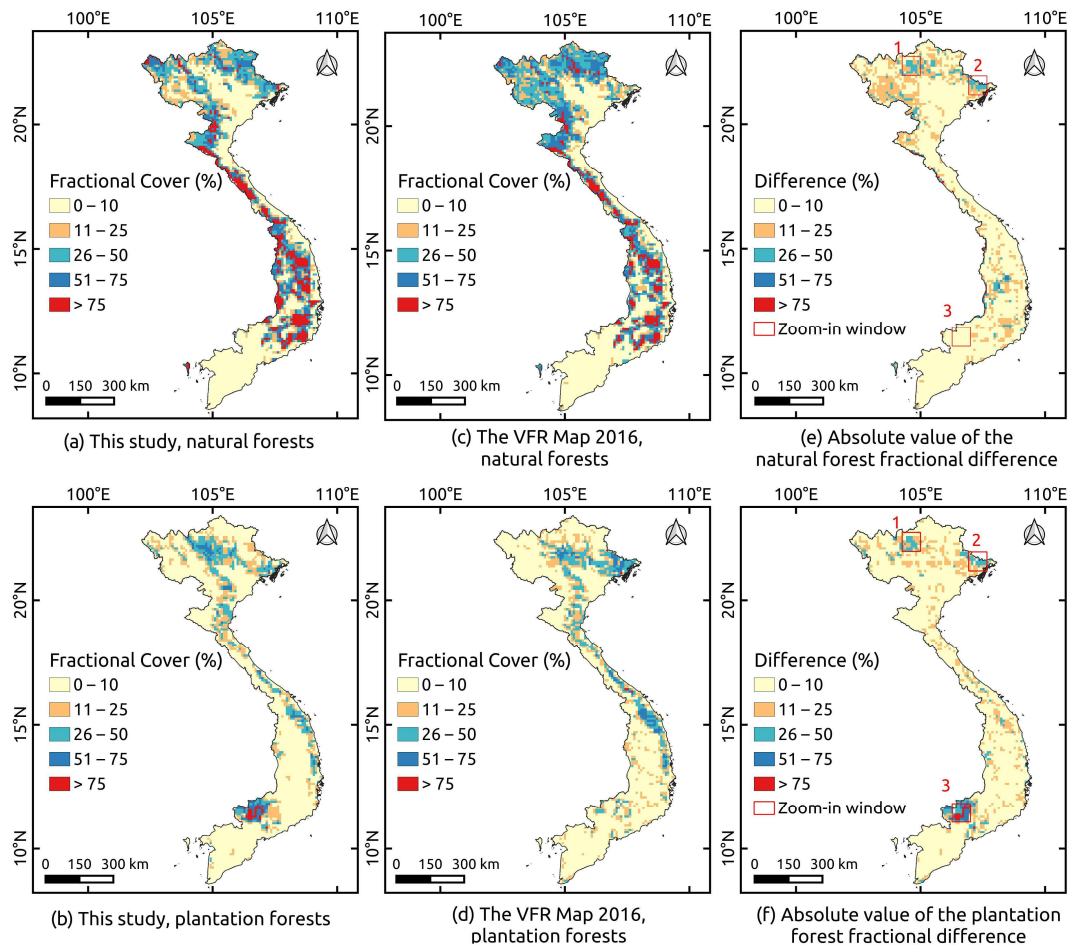


Figure 3.7. Comparison of the 10-km resolution forest fraction maps between this study and the Vietnam Forest Resource (VFR) Map in 2016 and their forest fraction differences. (a) Natural forest fractional cover map of this study; (b) Plantation forest fractional cover map of this study; (c) Natural forest fractional cover map of the VFR Map 2016; (d) Plantation forest fractional cover map of the VFR Map 2016; (e) Absolute value of the natural forest fractional difference between this study's map and the VFR Map 2016; (f) Absolute value of the plantation forest fractional difference between this study's map and the VFR Map 2016.

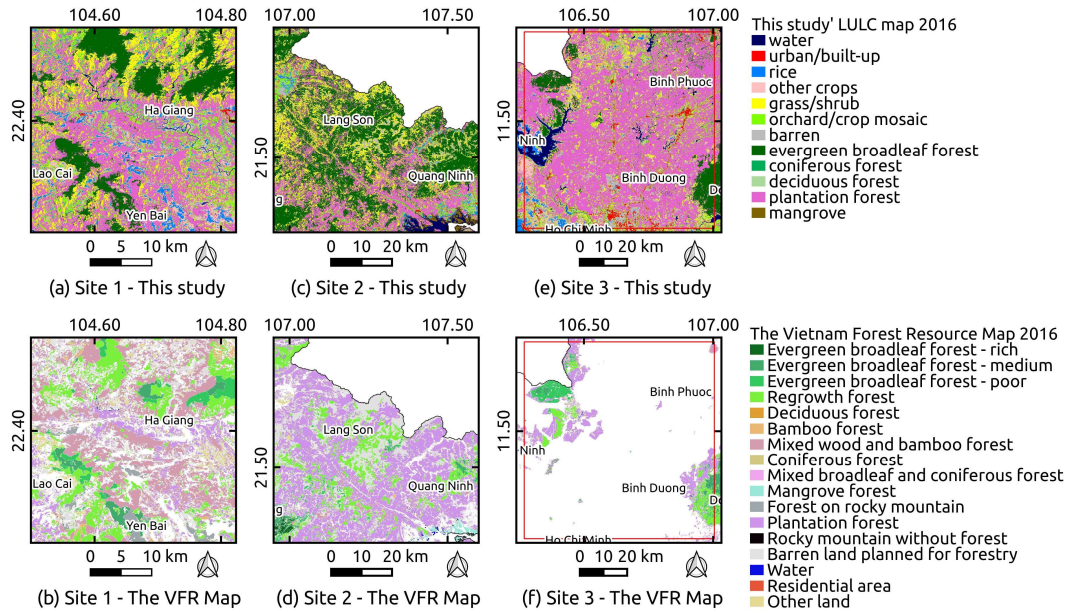


Figure 3.8. The three zoom-in sites in the VFR Map 2016 and in this study's map 2016. (a) Site 1 of this study's map; (b) Site 1 of the VFR map; (c) Site 2 of this study's map; (d) Site 2 of the VFR map; (e) Site 3 of this study's map; (f) Site 3 of the VFR map

In the following discussion, I assumed that the VFR Map properly reflected the reality of the forest status of Vietnam in 2016. As for Site 1 (Yen Bai, Ha Giang provinces), many plantation forest areas in this study's map (Figure 3.8a) were presented as mixed wood and bamboo forest in the VFR Map (Figure 3.8b). The natural bamboo forests have some similar characteristics to plantation forests such as a low biomass, low moisture content, and bamboo trees having similar trunk sizes. Therefore, the natural bamboo forests are likely to be confused with plantation forests in the classification process.

For Site 2 (Lang Son, Quang Ninh provinces), areas shown as natural forest (EBF) in this study map (Figure 3.8c) were presented as plantation forests in the VFR Map (Figure 3.8d). Interestingly, there was a nature-oriented reforestation project aided by the government of Germany from 1995 to 2005 conducted in this region (Bac Giang, Quang Ninh, Lang Son provinces) (Sturm & Apel, 2006). According to Sturm and Apel (2006), the project aimed for planting near-natural forests with multiple functions of forest ecosystems and attempting to harmonize the ecological, economic, and social

requirements of the region. Therefore, the structures and characteristics of these planted forests in Site 2 were identical to natural forests. This similarity caused the misclassification of the near-natural planted forests, in which they were detected as natural EBFs in this study's map.

For Site 3 (Binh Duong, Binh Phuoc provinces), the rubber plantation forests in this study's map (Figure 3.8e) were not presented in the VFR Map (Figure 3.8f). The cause of this disagreement came from the fact that the Vietnamese government's forest data excluded rubber plantations. In Vietnam's national statistics, rubber plantation areas have been considered as agricultural lands (perennial industrial crops) (GSO, 2019). However, according to the FAO (FAO, 2018) and the country report of Vietnam for the FAO Forest Resources Assessment 2020 (FAO, 2020a), the definition of forest considered rubber to constitute plantation forests. This study followed the FAO definitions to consider rubber as a plantation forest.

### **3.4. Discussion**

#### **3.4.1. Advantages and potential applications of the resultant LULC map**

In terms of methodology, the advantage of this map was demonstrated by the comprehensiveness of the mapping approach. Based on the hypothesis on the ultimate differences between natural forests and plantation forests, the comprehensiveness of the approach consisted of (1) combining the advantages of various sensors using the probabilistic integration at the decision level; (2) using time-series data; (3) using remote sensing indices.

In terms of product quality, the advantage of this study's LULC map was highlighted by a comparison with previous JAXA LULC maps of Vietnam and other LULC products. This map has a higher resolution (10 m), which is currently the best resolution among JAXA LULC products and other global LULC products. While all the previous JAXA LULC maps of Vietnam categorized forests as one class, this study's map has four forest classes, which can offer better support for forest monitoring

initiatives such as REDD+, land use, land use change, and forestry (LULUCF), the national forest inventory, etc. In addition, this map was one of the first regional maps that distinguished natural forests and plantation forests, in which plantation forests were comprised of various foliage types including evergreen broadleaf, deciduous, and coniferous foliage. This salient point would open a potential direction for mapping natural forests and planted forests at a global scale to improve the accuracy of carbon emission assessments, the detection of deforestation, and assessments of biodiversity loss. As for the classification accuracy, the major forest classes, such as EBFs and plantation forests, had high accuracies (PA, UA) ranging from 86.0% to 95.3%. In terms of mapping the forest/non-forest cover, this study's map (merging all forest classes as one and merging all non-forest classes as the other), showed a very higher accuracy (95.7%, Appendix Table A2). In addition, the higher-accuracy mangrove cover class in this map can facilitate studies associated with blue carbon assessments (Dat Pham et al., 2019) or mangrove ecosystem services (T. D. Pham et al., 2018; Van et al., 2015).

### **3.4.2. Limitations and challenges of this study's map**

The comparison between this study's map and the VFR Map revealed several limitations and challenges in distinguishing natural forests and plantation forests. The misclassification of the natural bamboo forests was one of the challenges as bamboo forests and plantation forests had similar features in this study's classification design. Bamboo forests have been considered one important carbon pool because of their strong carbon sequestration capacity (Du et al., 2018). According to Du et al. (2018), bamboo forests in Vietnam occupied  $1.018 \times 10^6$  ha, which accounted for about 3.33% of the total bamboo forest area over the world and about 10% of the total natural forest area of Vietnam. Therefore, bamboo forests should be considered as a future target for this study's approach. Potential solutions to overcome the misclassification of the bamboo forests would be using the leaf area index (LAI) information or adopting the approach of global bamboo forest mapping by Du et al. (2018).

Another challenge was the misclassification of the nature-like planted forests. The establishment of these planted forests involved the use of indigenous species and the

incorporation of natural succession (Sturm & Apel, 2006). Hence, the characteristics of these forests and natural forests were mostly identical. Therefore, the detection of the nature-like planted forests would require human knowledge-embedded information as ancillary data along with Earth observation imagery.

The misclassification of the grass/shrub class indicated another limitation of this study's map. The error matrix (Appendix Table A1) showed that the grass/shrub class was mostly confused with EBFs, orchard/crop mosaics, and barren land. The reason for this misclassification may come from the imperfect training data of the grass/shrub class, which were possibly created by an inaccurate visual interpretation. In some cases, the interpreters were not highly confident in identifying whether an area in a satellite image is a rich shrubland or a degraded forest. Similarly, sparse grasslands and bare lands were sometimes difficult to distinguish from each other by satellite image interpretation. The quality of the training data can be improved by increasing the ground-truth data or consulting various sources such as available open reference data.

### **3.4.3. Future research directions**

In terms of time-series scalability, this study can be replicated for historical high-resolution remote sensing observations such as ALOS/AVNIR2 and ALOS/PALSAR (2006–2011). Thus, such expected high-resolution time-series LULC maps would provide the long-term changes of natural forests and plantation forests in Vietnam. These forest changes, in turn, would offer various research directions for identifying the links between forest resources and social-economic issues. For example, previous studies on plantation forests in Vietnam indicated that the expansion of plantation forests in Vietnam had a strong relationship with the expansion of plantation farm-based smallholders (Sandewall et al., 2010) and the vulnerability of resource-poor local people (Thulstrup, 2014).

Another future work would be to improve the detail level and accuracy of future LULC maps. Recent studies on carbon emissions from land cover changes in Vietnam, like Avitabile et al. (2016), and the REDD+ readiness status (Maraseni et al., 2020) have called for highly reliable and detailed LULC and forest maps. Carbon emission

assessments would be more accurate if the input LULC maps contained sub-categories of natural forests such as bamboo, biomass-rich forests, biomass-medium forests, biomass-poor forests, and regrowth forests. Similarly, separating plantation forests into single tree species sub-categories such as rubber, acacia, eucalyptus, pine, etc., would be of importance. Although the VFR Map has a high level of detail, it is expensive because its establishment relies on satellite imagery with a visual interpretation of numerous forestry staff and specialists, and it has been carried out at five-year intervals. Therefore, the expected improved LULC product would provide more timely and objective data to policymakers and the land science community with low cost.

Future research initiatives will have more opportunities for improvement since, along with current data archives, this research direction will have the opportunity to use new data from future satellites such as Landsat 9 (optical, 2021), NISAR (L-band SAR, 2021), BIOMASS (P-band SAR, 2021), Tandem-L (L-band SAR, 2023), ALOS-3 (optical, future), ALOS-4 (L-band SAR, future) and a new Vietnamese satellite, LOTUSat-1 (X-band SAR, 2023). Moreover, the continued evolution of advanced deep learning algorithms would provide new classification methods for improving LULC map production.

### **3.5. Summary**

This chapter demonstrated a comprehensive approach to create a high-resolution LULC map which aimed at distinguishing natural forests and plantation forests (acacia, rubber, eucalyptus, and others) in Vietnam. This approach comprised of integrating various data products from multiple sensors (PALSAR-2/ScanSAR, PALSAR-2 mosaic, Sentinel-1, Sentinel-2, Landsat 8, AW3D30) at the decision level, after applying the probabilistic classifier for each data, taking advantage of time-series data and remote sensing spectral indices. A ROC analysis showed that the integration of all the sensor data displayed a better classification performance than any individual sensor's data. In addition, the PALSAR-2/ScanSAR and Sentinel-2 data showed better classification performances in forest classes compared to the data products from other sensors.

The high-resolution LULC map over mainland Vietnam in 2016 was produced with 12 classes and an overall accuracy of 85.6%. The major forest classes such as EBFs and plantation forests reached high accuracies of more than 86%. The comparison of the natural and plantation forest fractional covers between this study's map with Vietnam's national statistics and the Vietnam Forest Resources Maps 2016 showed good agreement except for the limitation of the bamboo forest misclassification (confused with plantation forests). This study confirmed the feasibility of producing highly detailed and accurate forest type maps in the forthcoming big data era of Earth observation. There is also a further need to reproduce the resultant map in historical periods to have spatially explicit insights into changes in plantation forests and natural forests in Vietnam.

## **Chapter 4. A spatiotemporal Analysis of Deforestation in Vietnam over the Last Two Decades**

### **Publications (under review):**

- **Hoang T.T.**, Phan C.D., Tadono T., Nasahara K.N. (2021) A spatiotemporal analysis of deforestation in Vietnam over the last two decades, Remote Sensing, (under review in Remote Sensing)



## 4.1. Background

Deforestation is a critical environmental issue that exerts negative impacts on global climate change, biodiversity, and local communities. For example, in 2019 the Intergovernmental Panel on Climate Change (IPCC) reported that agriculture, forestry, and other land use (AFOLU) including deforestation and forest degradation accounted for 23% of global anthropogenic greenhouse gas emissions (IPCC, 2019). Furthermore, by investigating 875 sample sites across the tropics, Alroy (2017) found that approximately 41% of tree and animal species are absent from disturbed forests in comparison to undisturbed forests. Despite efforts by national governments and international bodies to halt the issue, tropical deforestation has continued apace, making the development of effective countermeasures a significant challenge (Seymour & Harris, 2019).

Vietnam has experienced a forest transition from net forest loss to net forest gain since the 1990s (Keenan et al., 2015). However, deforestation continues to persist in this country. For example, Khuc et al. (2018) identified 1.77 million ha of deforestation in Vietnam between 2000 and 2010 based on national forest maps obtained from the Vietnamese government. Furthermore, according to data released by the Vietnamese government, the Central Highlands region, which is considered the most severely deforested region in Vietnam, lost 524,000 ha of natural forest between 2009 and 2019 (GSO, 2020). Deforestation in Vietnam has led to numerous detrimental impacts including habitat fragmentation and biodiversity loss (Meyfroidt & Lambin, 2008b), the intensification of natural disasters such as floods, flash floods (Bradshaw et al., 2007), and a changing water cycle and altered flow regimes (N. C. Q. Truong et al., 2018; Ziegler et al., 2004).

Precise deforestation monitoring and quantitative understanding of deforestation are fundamental to inform sustainable forest management (Geist & Lambin, 2002; Hosonuma et al., 2012; Kissinger et al., 2012). However, current deforestation data have substantial limitations that decline the reliability of the deforestation information. Remote sensing-based maps have presented large uncertainty in deforestation areas (H. Chen et al., 2020), which included both overestimation and underestimation in Global

Forest Change (GFC) data (Galiatsatos et al., 2020; Sannier et al., 2016) and Land Cover project of the Climate Change Initiative (CCI-LC) data (ESA, 2015a), respectively. Whereas, forest census-based data have presented the limitation on the land-use based definition. By the definition, “forest” in this data represents a forestland registered by the government, even if there is no tree. This limitation led to inaccurate estimates of the actual forest cover.

In addition, patch size is one of the important pattern metrics that can reflect the characteristics of deforestation. For example, Kalamandeen et al. (2018) and Rosa et al. (2012) pointed out that the change in patch size of deforestation in Brazilian Amazon was coincident with implementation of new conservation policies. Forest disturbance regimes of Europe was mapped using several pattern metrics that included disturbance mean patch size (MPS) (Senf & Seidl, 2020). The increasing trends in patch size of tropical deforestation can signal an increasing trend of industrial-scale drivers, according to Austin et al. (2017).

As for Vietnam, previous studies on the characterization of deforestation mostly focused on identifying its direct and indirect drivers (Cochard et al., 2017; Curtis et al., 2018; Khuc et al., 2018; T. T. Pham et al., 2019) and explaining its mechanisms in some local study cases (Meyfroidt et al., 2013; Tachibana et al., 2001). However, spatiotemporal presentations of drivers of deforestation in entire Vietnam has remained unknown. Such information would enrich the knowledge of deforestation in Vietnam and provides a good reference for policy designs and action plans of conservation.

Recently, the Japan Aerospace Exploration Agency (JAXA) released a new high-resolution LULC map for 2016 covering all of Vietnam (version 20.06) (Hoang et al., 2020). This map has a 10-m spatial resolution with fine discrimination of natural forests and plantation forests. Importantly, the mapping approach used to produce this map can be applied to historical remote sensing data to create historical LULC maps, from which deforestation can be quantified based on post-classification comparisons of natural forest extent.

This study aimed to address the following three main research questions: (1) whether the high-resolution LULC mapping approach suggested by Hoang et al. (2020)

(Hoang et al., 2020) can provide better deforestation detection in comparison to other currently available data including GFC (Hansen et al., 2013) and CCI-LC (ESA, 2015a) data, and statistical forest data from the government of Vietnam (GSO, 2020); (2) how deforestation mean patch size (MPS) has varied spatially and temporally in Vietnam over the last two decades; and (3) whether there is a link between spatiotemporal variations in the MPS of deforestation and its direct drivers during this period. To address these questions, the following four specific objectives were adopted: (1) to create a high-resolution LULC map for 2007 based on the JAXA 2016 high-resolution LULC mapping approach (Hoang et al., 2020); (2) to create a deforestation map for the period between 2007 and 2016 based on the two LULC maps and in comparison with the GFC and CCI-LC datasets, and national governmental statistics; (3) analyze spatial variations in deforestation MPS in association with spatial patterns of deforestation drivers; and (4) analyze temporal variations in the deforestation MPS for the period 2001–2019 alongside variations in deforestation drivers.

## **4.2. Materials and method**

### **4.2.1. Satellite data and preprocessing**

One important goal of this study was to establish a deforestation map for mainland Vietnam between 2007 and 2016. The deforestation map was created using a post-classification comparison of two high-resolution LULC maps for these years. The 2016 map was the JAXA high-resolution LULC map (version 20.06) (Hoang et al., 2020), which was created based on a comprehensive mapping approach that included integrating information from time-series data of various sensors and making use of spectral and radar indices. By using this mapping approach, this study also created a map for 2007. For this, all input data were transformed to the geographic latitude/longitude WGS84 coordinate system. The LULC classification process for 2007 was conducted for each  $1^\circ \times 1^\circ$  tile (Figure 2.1a) rather than the entire Vietnam area.

#### **(a) ALOS/PALSAR RTC data**

The Phased Array type L-band Synthetic Aperture Radar (PALSAR) is a radar imaging sensor onboard the Advanced Land Observing Satellite (ALOS) operating from

2006 to 2011, managed by the JAXA. PALSAR Radiometrically Terrain Corrected (RTC) data were produced by the ASF under the Radiometric Terrain Correction Project, which corrected the geometry and radiometry of PALSAR data and published these in GeoTiff format (ASF, 2014). Here, I obtained 626 high-resolution (12.5 m) PALSAR RTC scenes in the Fine Beam Dual (FBD) mode including both polarizations of horizontal transmit–horizontal receive (HH) and horizontal transmit–vertical receive (HV) for 2007 over Vietnam (Figure 4.1a). For classification purposes, the pixel values (DN) in gamma-0 power were transformed to the decibel scale (unit in decibel [dB]) (Equation (3.7)). The pixels affected by layover and shadowing are masked in this data product. A Lee filter (Lee, 1980) with a  $7 \times 7$  moving window was applied to suppress the speckle noise in the gamma-0 images. Radar indices were estimated and then stacked with the two original gamma-0 HH and HV images. The radar indices included the ratio (RAT, Equation (3.8)), normalized difference index (NDI, Equation (3.9)), and NL Index (NLI, Equation (3.10)). These indices have proven to be useful in mapping natural forests and plantation forests (De Alban et al., 2018; Hoang et al., 2020; Sarzynski, Giam, Carrasco, et al., 2020). The images were then trimmed into  $1^\circ \times 1^\circ$  tiles (Figure 2.1a).

#### **(b) ALOS/AVNIR-2 ORI data**

High-spatial-resolution (10 m) Advanced Visible and Near Infrared Radiometer type 2 (AVNIR-2) Ortho Rectified Image (ORI) data from the ALOS satellite are available for 2006–2011 with a 46-day revisit cycle and a 70-km swath width. These data have four spectral bands in the visible and infrared regions (Table 4.1). The AVNIR-2 ORI data were created from AVNIR-2 level 1B1 after stereo-matching with a digital surface model (DSM) constructed using Panchromatic Remote-Sensing Instrument for Stereo Mapping (PRISM) data. In total, 177 scenes from 2007 with cloud covers of less than 30% were used to create the LULC map (Figure 4.1b). The spectral reflectance of each band was calculated based on the provided parameters enclosed with the data header files (JAXA, 2008, 2020b; Tadono et al., 2009). To remove these cloud covers, I adjusted the too-bright threshold values of the visible spectral bands to mask the bright pixels (Vermote et al., 2014). The images were then trimmed into  $1^\circ \times 1^\circ$  tiles (Figure 2.1a). Along with the four original bands, vegetation indices were used

including the Normalized Difference Vegetation Index (NDVI, Equation (3.14)) (Rouse et al., 1973; Tucker, 1979), the Enhanced Vegetation Index (EVI, Equation (3.15)) (A. Huete et al., 2002; A. R. Huete et al., 1997), the Soil and Atmosphere Resistant Vegetation Index (SARVI, Equation (3.19)) (A. R. Huete et al., 1997), the Green-Red Vegetation Index (GRVI, Equation (4.1)) (Tucker, 1979), the Modified Soil-adjusted Vegetation Index (MSAVI, Equation (4.2)) (Qi et al., 1994), and the Normalized Difference Water Index (NDWI, Equation (4.3)) (McFeeters, 1996). The AVNIR-2 ORI data for the Vietnam region were provided by the JAXA under the "Generation of the Precise Land Cover Map" research agreement with a support by JAXA/EORC Ecology Group.

$$GRVI = \frac{Green - Red}{Green + Red} \quad (4.1)$$

$$MSAVI = \frac{2NIR + 1 - \sqrt{(2NIR + 1)^2 - 8 \times (NIR - Red)}}{2} \quad (4.2)$$

$$NDWI = \frac{Green - NIR}{Green + NIR} \quad (4.3)$$

Where: Green, Red, and NIR are described in Table 4.1.

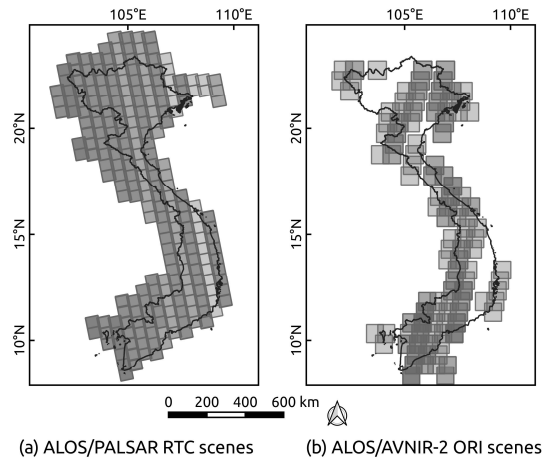


Figure 4.1. (a) Coverage of 626 ALOS/PALSAR RTC scenes and (b) 177 ALOS/AVNIR-2 ORI scenes.

### (c) Landsat-5 and Landsat-7 data

Landsat-5 and Landsat-7 surface reflectance products collected from the Google Earth Engine (GEE) were used to fill the data gaps in the ALOS/AVNIR-2 ORIs (Figure 4.1b). Moreover, spectral bands in the shortwave and thermal IR regions of the

Landsat data can provide more information about the land surface than AVNIR-2 data. The Landsat surface reflectance product embedded the atmospheric corrections using LEDAPS codes (USGS, 2020a) with cloud and cloud shadow masking using the CFMASK algorithm (Foga et al., 2017). After applying the cloud and cloud shadow masking flags, eight median composite images were generated with 1.5-month intervals, which were trimmed into  $1^\circ \times 1^\circ$  tiles (Figure 2.1a). Seven spectral bands (Table 4.1) were used along with 10 remote sensing indices including the NDVI (Equation (3.14)), EVI (Equation (3.15)), SARVI (Equation (3.19)), Land Surface Water Index (LSWI, Equation (3.16)) (X. Xiao et al., 2002), Aerosol Free Vegetation Index (AFVI, Equation (3.17)) (Karnieli et al., 2001), Atmospherically Resistant Vegetation Index (ARVI, Equation (3.18)) (Kaufman & Tanré, 1992), Moisture Stress Index (MSI, Equation (3.20)) (Hunt & Rock, 1989), Soil-Adjusted Total Vegetation Index (SATVI, Equation (3.21)) (Hagen et al., 2012), Normalized Difference Tillage Index (NDTI, Equation (3.22)) (Daughtry et al., 2005), and the Index-Based Built-Up Index (IBI, Equation (3.23)) (Xu, 2008).

Table 4.1. Spectral bands of ALOS/AVNIR-2 ORI (JAXA, 2020b), Landsat-5, and Landsat-7 (USGS, 2020b) used in this study

<b>Data</b>	<b>Band</b>	<b>Spectral Range (nm)</b>	<b>Electromagnetic Region</b>
ALOS/AVNIR-2 ORI	Band 1	420–500	Blue
	Band 2	520–600	Green
	Band 3	610–690	Red
	Band 4	760–890	NIR (Near Infrared)
Landsat-5 & Landsat-7	Band 1	450–520	Blue
	Band 2	520–600	Green
	Band 3	630–690	Red
	Band 4	760–900	NIR (Near Infrared)
	Band 5	1,550–1,750	SWIR1 (Shortwave Infrared 1)
	Band 6	10,400–12,500	TIR (Thermal Infrared)
	Band 7	2,080–2,350	SWIR2 (Shortwave Infrared 2)

#### **(d) Auxiliary data**

The open digital surface model AW3D30 produced by the JAXA (JAXA, 2020a), the Defense Meteorological Satellite Program Operational Line Scanner (DMSP-OLS)

nighttime lights produced by the National Oceanic and Atmospheric Administration (NOAA) (WorldPop, 2018b), and the distance to OpenStreetMap (OSM) major roads (WorldPop, 2018a) were used as auxiliary data when establishing the 2007 LULC map. These datasets were chosen to reflect human accessibility and presence, to enhance the separability of natural land cover (e.g., natural forests and grass/shrubland) from human-impacted land-cover types (e.g., plantation forests, crops, orchards, and urban/built-up areas) in the LULC mapping (Hoang et al., 2018, 2020).

#### **(e) Global Forest Change data v1.7 (Hansen)**

The year of gross forest cover loss event ('lossyear') dataset produced by Hansen et al. (2013) was used as a comparison to this study's deforestation area results, and to analyze temporal variations in deforestation MPS during the period 2001–2019. The lossy data of the GFC were defined as “a stand-replacement disturbance, or a change from a forest to non-forest state” with a 30-m resolution. As this study adopted the FAO definition of deforestation (FAO, 2018), which excludes temporary forest cover loss, this study used these data with natural forest masks from the 2007 and 2016 LULC maps to exclude temporary clearing of plantation forests after harvesting cycles.

### **4.2.2. Methods**

#### **(a) Establishing the high-resolution LULC map in 2007**

The creation of the 2007 high-resolution LULC map followed the same mapping approach of the 2016 map (Hoang et al., 2020) created by integrating information from various data sources (Figure 4.3). The details of this classification method are described by Hoang et al. (2020) and Hashimoto et al. (2014). Briefly, to integrate the various information types, a probabilistic classification model was applied to each of the individual inputs, and then an integration procedure was performed by multiplying the resulting probability of each of the classified outputs. The classification model was based on kernel density estimation (KDE) with a Bayesian inference (Hashimoto et al., 2014). In the classification process, first, the KDE was used to estimate the likelihood of each LULC category based on training data. Then, the posterior probability values of each LULC category at corresponding pixel values were estimated based on Bayes'



theorem with the likelihood as the input. The integration was conducted by multiplying the component posterior probability values from each single-date image of each sensor's data. This classification method has been widely used for creating high-resolution LULC products for Japan (Hashimoto et al., 2014; Katagi et al., 2018) and Vietnam (Hoang et al., 2018, 2020; D. C. Phan et al., 2018; V. T. Truong et al., 2019), and the products have been published as open LULC data by the JAXA (JAXA, 2020d).

The LULC maps for 2007 and 2016 categorized 12 LULC types, namely water, urban/built-up areas, rice, other crops, grass/shrub, orchard/crop mosaic, barren, EBF, coniferous forest, deciduous forest, plantation forest, and mangrove. The definitions of these categories are described in detail by Hoang et al. (2020).

#### **(b) Deforestation mapping for 2007–2016 and comparisons with other datasets**

The creation of the deforestation map for the period 2007–2016 adopted a post-classification comparison approach, which is a widely used change detection method (P. Coppin et al., 2004; P. R. Coppin & Bauer, 1996; Hussain et al., 2013; Singh, 1989). This approach compares classified maps to identify the changes between the categories of the maps. One important advantage of this is that the individual classification of each map can minimize the impact of different observation conditions, such as atmospheric disturbance and different sensors.

Here, deforestation was defined as the loss of natural forests by conversion to other LULC types. To minimize the inclusion of small tree loss areas, which are not defined as forests by the FAO (FAO, 2018), this study only considered deforestation areas greater than or equal to 1 ha. Temporary loss of plantation forests, such as clearing areas after a harvesting cycle, was also not classified as deforestation. Thus, to identify the deforestation areas, I created 100-m-resolution natural forest fractional cover maps. The fractional cover of natural forest was taken as the ratio of natural forest area within a 100 m × 100 m square to an area of 100 m × 100 m. The 100-m fractional cover maps for 2007 and 2016 were estimated based on the original 10-m natural forest classes of the LULC maps. The natural forest classes in the LULC maps included EBF, coniferous forest, and deciduous forest. A fractional cover difference map was then derived by subtraction. This difference map indicated that the degree of change in forest fractional

cover varied from -1 (complete gain) to 1 (complete loss). Next, I identified the threshold of forest fractional cover difference that gave the best accuracy for deforestation detection. For this, I created 11 deforestation maps corresponding to 11 fractional cover difference thresholds from 0.50 to 1.00 (intervals of 0.05). These maps were then validated using a reference dataset described in section 4.2.3. The results showed a forest fractional cover difference of  $> 0.7$  was optimal, giving a user accuracy (UA) of 69.2% and producer accuracy (PA) of 85.6% (Table 4.2).

Table 4.2. Accuracies and errors of deforestation map for Vietnam between 2007 and 2016 corresponding with various fractional cover difference thresholds

Difference of forest fractional cover thresholds	User's Accuracy (%)	Producer's Accuracy (%)	Commission error (%)	Omission error (%)
0.50	57.7	100.0	42.3	0.0
0.55	60.9	98.0	39.1	2.0
0.60	63.7	94.6	36.3	5.4
0.65	65.8	89.6	34.2	10.4
0.70	69.2	85.6	30.8	14.4
0.75	68.4	76.2	31.6	23.8
0.80	74.0	73.3	26.0	26.7
0.85	76.6	66.3	23.4	33.7
0.90	76.7	56.9	23.3	43.1
0.95	77.6	48.0	22.4	52.0
1.00	83.0	41.1	17.0	58.9

This study compared the calculated deforestation area between 2007 and 2016 with GFC data, CCI-LC data, and national governmental statistics. First, the deforestation area based on the created map was estimated using an error-adjusted estimator of area following Olofsson et al. (2013). The error-adjusted estimator was calculated from the deforestation area in the map and the error matrix (Appendix Table A3). For the comparison with GFC data, the deforestation area was estimated based on the GFC lossy data for the period 2007–2016 after being masked by natural forest extent derived from the 2007 LULC map to exclude areas temporary plantation clearing. For the CCI-LC data, the deforestation area was estimated based on a post-classification comparison of forest classes in CCI-LC maps for the same period (2007–2016). Forest classes were chosen to correspond to the equivalent forest category in the IPCC land

categories according to the CCI-LC product user guide (ESA, 2017). For the comparison with national statistics (GSO, 2020), as deforestation data are not directly available, this study used the net change in natural forest area as a substitute, which was estimated by subtracting the 2016 natural forest area from the equivalent 2007 area.

### **(c) Spatial variations in deforestation MPS**

The MPSs of deforestation were mapped for Vietnam using the constructed 2007–2016 deforestation map. For this, I divided mainland Vietnam into hexagon grids with a maximal diameter of 30 km. The deforestation MPS in each hexagon was then calculated as the ratio of the total deforestation area to the number of deforestation patches within each hexagon. Hexagons were used to minimize spatial differences between complex landforms (Birch et al., 2007; Senf & Seidl, 2020).

Spatial variations in deforestation MPS were investigated at a regional scale across the four main regions of Vietnam (Figure 4.2). By considering MPS values within each region as one sample set, I statistically compared the sample sets using the non-parametric Wilcoxon rank-sum test (as the data were not normally distributed). I hypothesized that there was a link between the MPS of deforestation and the drivers of deforestation. Based on this hypothesis, I explained differences in deforestation MPS among the regions using evidence of differences in deforestation drivers from previous studies.

The first source of evidence of drivers of deforestation was the global map of primary drivers of forest cover loss for the period 2001–2015 by Curtis et al. (2018). This global map presents the following five dominant direct drivers of forest cover loss: (i) commodity-driven deforestation, defined as the permanent conversion from forest to non-forest land use such as agriculture, mining, and infrastructure; (ii) shifting agriculture, defined as conversion from forest to agriculture that is later abandoned, followed by forest regrowth; (iii) forestry, defined as the operation of managed forests and tree plantations; (iv) wildfire, defined as large-scale forest loss by burning with no human conversion or agricultural practices afterward; and (v) urbanization, defined as the conversion from forest to urban areas. The creation of the map was based on a statistical model using various geospatial datasets. As the resolution of this map is 10

km, it is suitable for regional-scale analyses. The overall accuracy of the map was 89%, and is published as open-source data via the online platform Global Forest Watch (<https://www.globalforestwatch.org/map/>).

For Vietnam, all categories of forest loss drivers are available except for wildfire. Here, I used classes commodity-driven deforestation, shifting agriculture, and urbanization but excluded the forestry class as, as previously noted, the temporary loss of plantation forests was not considered as deforestation in this study. By overlaying this map for the Vietnam area on this study's 2007–2016 deforestation map, I estimated the percentages of deforestation areas caused by their corresponding drivers for each of the regions. These percentages were then used to explain the differences in the MPS of deforestation among the regions.

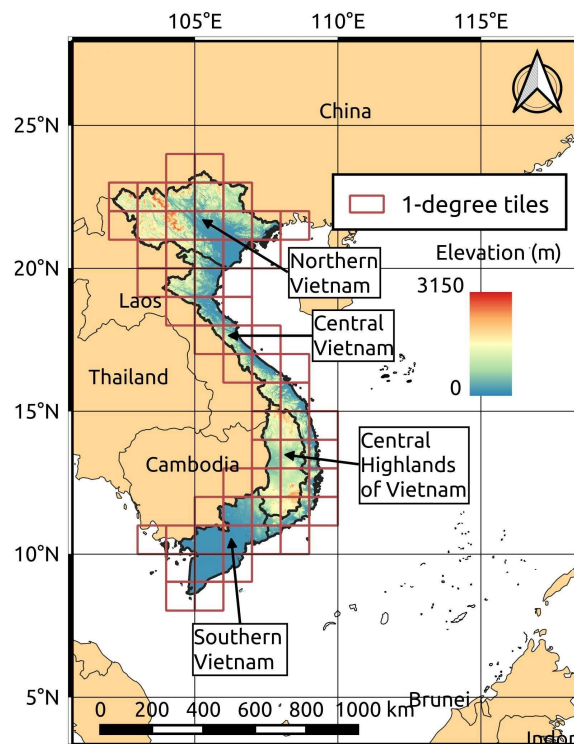


Figure 4.2. Four main regions of Vietnam

#### **(d) Temporal variations in deforestation MPS**

Annual maps of deforestation MPS for the period 2001–2019 were created using the annual GFC lossy maps with natural forest masks derived from this study’s LULC maps. Specifically, the natural forest extent in 2007 was used to mask the GFC lossy maps from 2001 to 2010, and the natural forest extent in 2016 was used to mask the GFC maps from 2011 to 2019. This approach may encounter potential issues such as the potential overestimation of forest loss area of GFC data as previously noted, and the possible insufficiency of using natural forest masking layers of two years 2007 and 2016 as natural forest extents may have annual changes. However, in this analysis, I focused on comparing the trends of deforestation MPS at the regional scale. Therefore, even if the GFC data may bring the overestimation, the consistent use of this data can still reflect the trends. The insufficiency issue of masking layers can be negligible since the annual changes of natural forest could be minimized in regional estimations and comparison.

To identify significant changes in deforestation MPS over time, I generated mean maps for 5-year periods, that is, 2001–2005, 2006–2010, 2011–2015, and 2016–2019. Then, for each of the regions, the deforestation MPS values for each of these periods was considered as a sample set and compared using the Wilcoxon rank-sum test. This comparison identified the trajectories of deforestation MPS by identifying significant changes over time. Based on the hypothesized link between deforestation MPS and deforestation drivers, I explained the observed trajectories in each region using evidence of temporal changes in deforestation drivers from previous studies.

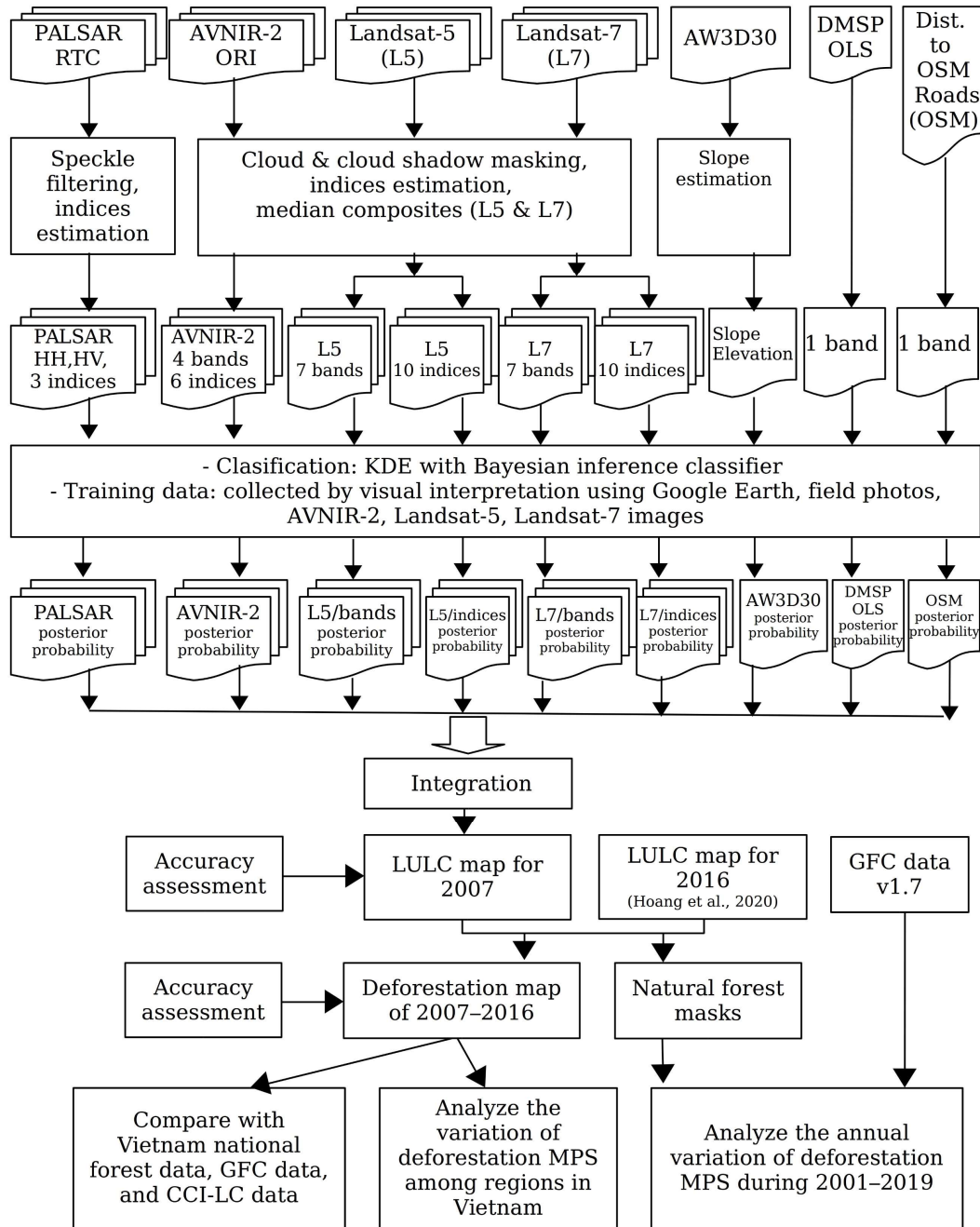


Figure 4.3. The overall workflow of Chapter 4

### 4.2.3. Reference Data

Reference data included a training dataset for the automated classification of the 2007 LULC map, a validation dataset for accuracy assessment of this map, and a

validation dataset for the accuracy assessment of the deforestation 2007–2016 map (see Section 4.2.2b). All the reference data were created based on visual interpretation using high-resolution Google Earth satellite images and other satellite images in 2007 and 2016, such as Landsat-5 (2007), AVNIR-2 (2007), Sentinel-2 (2016), and Landsat-8 (2016). This visual interpretation was supported by geotagged photos collected in field surveys described by Hoang et al. (2020).

To train the classification process of the 2007 LULC map, I created 113,181 training data points for the 12 LULC categories (Appendix Figure A1a). The validation data for this map were created based on the method described by Olofsson et al. (2013, 2014). Briefly, stratified random sampling was first used to randomly create 100 sampling points in each of the 12 strata corresponding to the 12 LULC classes, giving 1,200 data points in total (Appendix Figure A1a). Next, the sampling points were labeled based on visual interpretation using satellite images from 2007, such as Landsat-5 and AVNIR-2 imagery. Finally, accuracy assessment metrics including overall accuracy (OA), PA, and UA, and their standard errors were estimated and described in an error matrix (Appendix Table A4).

For the accuracy assessment of this study's deforestation map, I created 8,550 validation points including 202 deforestation points and 8,348 non-deforestation points (Appendix Figure A1c) following Olofsson et al. (2013, 2014). The corresponding error matrix is provided in Appendix Table A3.

## **4.3. Results and Discussion**

### **4.3.1. High-resolution 2007 LULC map and LULC changes between 2007 and 2016**

The generated 10-m resolution 2007 LULC map is shown in Figure 4.4a. Details of the accuracy assessment of the map are provided in Appendix Table A4. The overall accuracy of the map was 85.0%. The EBF class, which accounts for 88% of the total natural forest area, had high UA and PA (94.0% and 86.2%, respectively). Other minor natural forest classes, such as coniferous forest and deciduous forest, had a UA lower



than 80%. The plantation forest class also had high UA and PA (87.0% and 85.0%, respectively). The errors of forest classes mainly came from misclassifications, either among the forest classes or between the forest classes and grass/shrub class. The 10-m resolution 2016 LULC map created by Hoang et al. (2020) is shown in Figure 4.4b for comparison.

Overall LULC net changes in Vietnam between 2007 and 2016 (Figure 4.5) were derived from the two LULC maps. The LULC categories showing substantial increases were urban/built-up areas, other crops, and plantation forest, which increased by 200,000 ha, 255,000 ha, and 1,152,000 ha, respectively. The LULC categories showing substantial decreases were orchard/crop mosaic, barren, and EBF, which decreased by 508,000 ha, 178,000 ha, and 649,000 ha, respectively. Of these changes, the decrease in EBFs reflects deforestation in Vietnam during the study period, accounting for 88% of the total natural forest area across the entire country (see Section 4.3.2). For the “other crop” category, changes were in agreement with the increase in perennial crop cover in Vietnam in recent decades, which is considered one of the drivers of deforestation (Kissinger, 2020; Nghiem et al., 2020). The decrease in barren and grass/shrub areas, and the increase of plantation forest area, in Figure 4.5 might reflect reforestation programs that have been implemented since the 1990s (Cochard et al., 2017; Dao Minh et al., 2017). For example, plantation forest area was boosted in recent decades by reforestation Program 327 (1992–1997), Program 661 (1998–2010), and Program 147 (2007–2015) (T. T. Nguyen & Masuda, 2018). In addition, the observed changes in the other LULC categories are in agreement with the results of previous research. For example, the decrease in orchard/crop mosaic area tallies with the results of LULC changes in Central Vietnam between 2007 and 2017 reported by Phan et al. (2018) (D. C. Phan et al., 2018). Furthermore, the increase in urban/built-up areas supports the findings of Fan et al. (2019) and Dung et al. (2016), who reported an urban expansion in Vietnam in recent years.

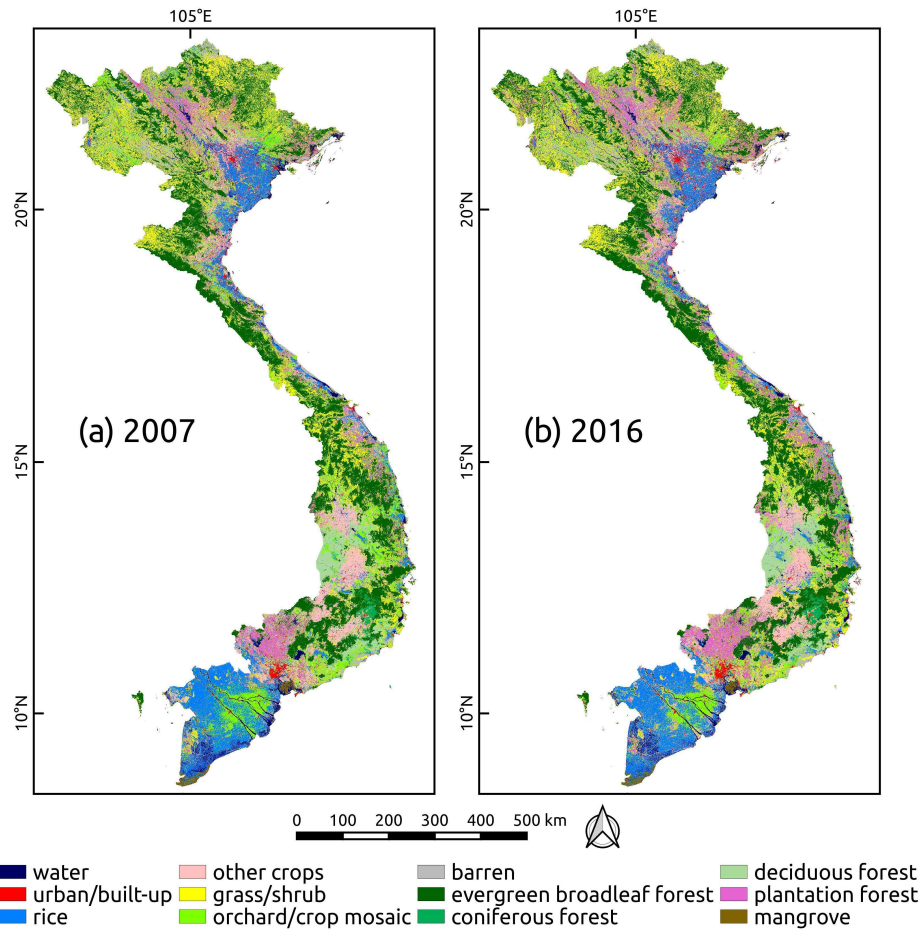


Figure 4.4. High-resolution LULC maps for (a) 2007 and (b) 2016 (Chapter 3) (Hoang et al., 2020).

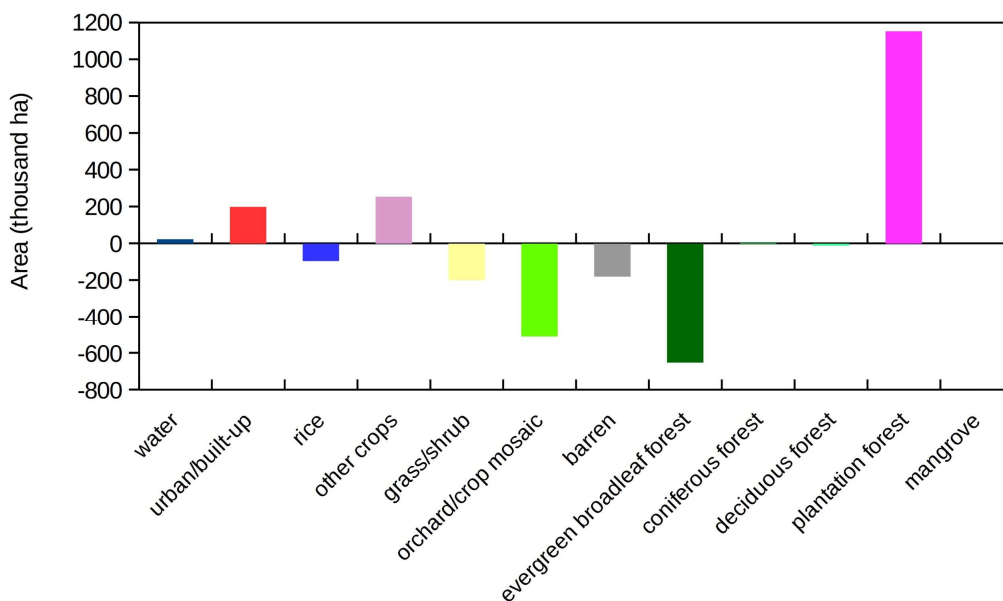


Figure 4.5. Overall LULC net changes in Vietnam between 2007 and 2016 estimated from LULC maps for 2007 and 2016 (Chapter 3) (Hoang et al., 2020).

### 4.3.2. 2007–2016 deforestation map and comparison with other data

The generated 2007–2016 deforestation map is shown in Figure 4.6a. The map identified a deforestation area of  $686,000 \pm 65,000$  ha in mainland Vietnam. The Central Highlands was the region with the largest deforestation area at  $399,000 \pm 48,000$  ha. In comparison, the estimated deforestation areas in Northern Vietnam, Central Vietnam, and Southern Vietnam were  $151,000 \pm 54,000$  ha,  $200,000 \pm 42,000$  ha, and  $48,000 \pm 14,000$  ha, respectively. The uncertainties of these estimations represent the 95% confidence interval.

Aside from the accuracy assessment mentioned in section 4.2.3, the deforestation map was compared with deforestation information from local news in Vietnamese online media. The results showed that the deforestation map was in agreement with the local news. For example, [thoibaonghang.vn](http://thoibaonghang.vn) (2015) reported that the natural forest area of Dak Nong province, Central Highlands decreased by 140,000 ha between 2005–2015 (from 360,000 ha to 220,000 ha). The decrease was mainly due to the conversion from natural forests to perennial plantations such as coffee, pepper, and orchards. The

information in the news was relatively consistent with the result of this study's maps which indicated approximately 85,000 ha of forest loss by the conversion to croplands between 2007–2016 (Appendix Figure A2). For Southern Vietnam, [tuoitre.vn](http://tuoitre.vn) (2010) reported a conversion from natural forests to farm-based rubber plantations in Bu Dang district, Binh Phuoc province circa 2010. The legal loophole which allowed poor-quality natural forests to be converted to rubber plantations was considered an indirect cause of deforestation in this area. This conversion from natural forests to plantation forests was well presented in this study's maps (Appendix Figure A3). For the northwest of Vietnam, [baotainguyenmoitruong.vn](http://baotainguyenmoitruong.vn) (2016) informed that Muong Nhe district in Dien Bien province was considered a small-scale deforestation hot spot. The deforestation situation was mainly attributed to the demand for cultivation land of immigrants from other provinces. Between 2011–2016, there were approximately 2000 immigrants settled down in Muong Nhe district. The information on deforestation in Muong Nhe was in agreement with the results of this study's maps which showed the conversion from natural forests to croplands, orchards, and plantation forests (Appendix Figure A4). For the northeast of Vietnam, [thienhien.net](http://thienhien.net) (2008) informed a conversion from natural forests to acacia plantation by local residents circa 2008 in Son Dong district, Bac Giang province. The cause of this change was due to the high economic value of acacia plantation which overweighed the benefit from natural forests which had been allocated to each local household. The conversion was continued until 2017, reported by [kinhtenongthon.vn](http://kinhtenongthon.vn) (2017). The conversion was also reflected in this study's maps by the change from natural forests to plantation forests in Appendix Figure A5. For Central Vietnam, [nongnghiep.vn](http://nongnghiep.vn) (2015) informed the deforestation case in Yen Hop commune, Quy Hop district, Nghe An province circa 2015 which was due to natural forest logging and then growing acacia plantation by local people. The underlying cause of this change was also due to the high benefit of acacia plantation. This deforestation case was indicated in this study's maps by the conversion from natural forests to plantation forests in Appendix Figure A6.

I compared the deforestation areas derived from this study's map with other data for the entire mainland Vietnam (Figure 4.6b) and for the Central Highlands, which is a recognized deforestation hotspot (Figure 4.6c). In comparison with the national statistics, for the entire country (Figure 4.6b), my estimated deforestation area (686,000

$\pm 65,000$  ha) is far higher than the net change in natural forest area reported in the national statistics (41,000 ha); for the Central Highlands (Figure 4.6c), my estimate ( $399,000 \pm 48,000$  ha) is remarkably close to the reported net change in natural forest area (444,000 ha). The possible reason for the difference—particularly for the whole-country values—may be due to limitations in the national statistics, which are based on the national forest censuses that adopt a land-use definition for forestland. Under such a definition, "forest" represents forestland, which is registered by the government even where no trees are present (Hoang et al., 2020). Therefore, these national statistics do not likely accurately record true forest loss unless that loss is caused by the land use-conversion allowed by the government. Moreover, reforestation programs in Vietnam could have increased the area of natural forestlands (Crowther et al., 2020). These forest gain areas could compensate forest loss areas. Therefore, the net change in natural forest areas, in this case, was low. In the case of the Central Highlands, deforestation has been mainly caused by the rapid expansion in the growth of perennial crops (e.g., coffee and rubber). This has been supported by government policies and legal loopholes, which have allowed the conversion of natural forests to rubber plantations according to Kissinger et al. (2020). As a result, the conversion from natural forest to cropland in the Central Highlands would be officially recorded in the national statistics. Moreover, the natural forest gain in Central Highlands was negligible due to lacking of economic incentives and weak local governance (thienhien.net, 2020). Thus, for Central Highlands, the net change of natural forest area could be close to the true area of deforestation areas.

In comparison with other remote sensing-based data, my estimated deforestation area is appropriately half that of the GFC data both for the entire country and the Central Highlands region (Figures 4.6b and 4.6c). In contrast, my estimates are far higher than the CCI-LC data suggest (Figures 4.6b and 4.6c). This difference might reflect the limitations of these remote sensing-based datasets, such as overestimation by the GFC data and the coarse resolution of the CCI-LC data.

Assuming that the net change in natural forest areas in the Central Highlands region recorded in the national statistics accurately reflect the true deforestation area, my map provides the best estimates in comparison with the other remote sensing-based

datasets. A reliable reference dataset of deforestation over Vietnam is now needed to enable more comprehensive evaluations.

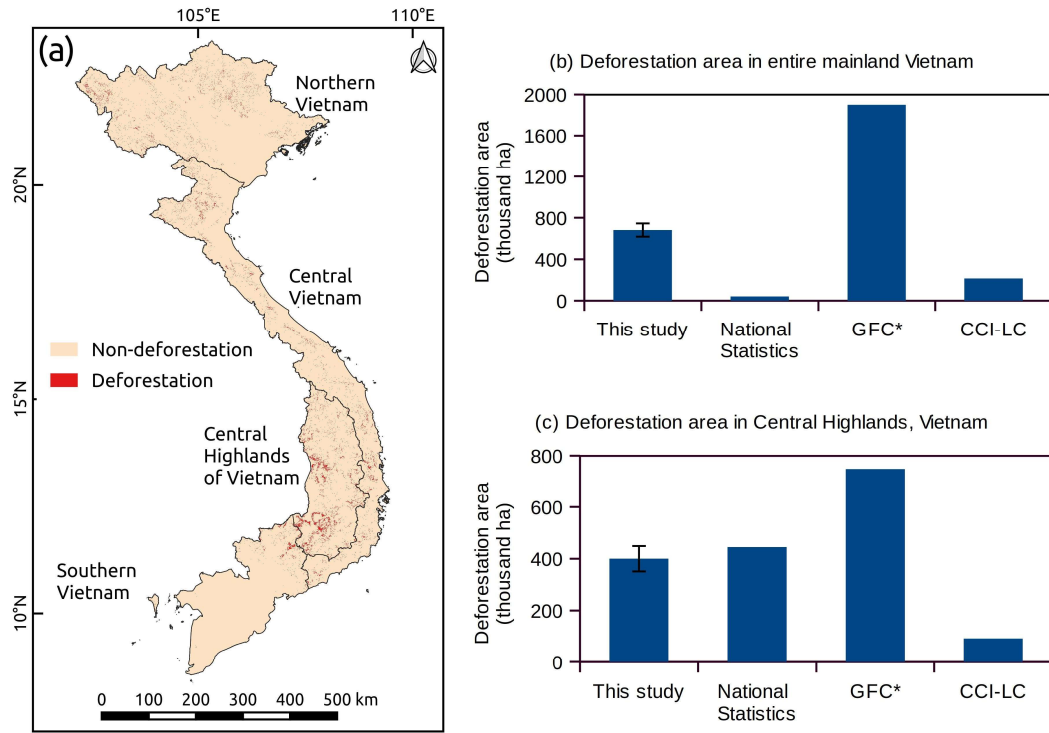


Figure 4.6. (a) 2001–2016 deforestation map derived in this study; (b) a comparison of the estimated total deforestation area for mainland Vietnam (2007–2016) with national statistics (net change in natural forest area), GFC\* (year of gross forest cover loss event data with a natural forest mask from the 2007 LULC map 2007 created in this study), and CCI-LC; (c) a comparison of estimated the deforestation area in the Central Highlands of Vietnam (2007–2016).

### 4.3.3. Spatial variations in deforestation MPS

Spatial variations in the MPS of deforestation for the period 2007–2016 are illustrated in Figure 4.7a with corresponding for each study region in Figures 4.7b–e. To examine the significance of the observed differences, the results of a statistical comparison are shown in Table 4.3. These show that the MPS values of deforestation in the Central Highlands are significantly greater than those of all other regions ( $p < 0.001$ ). Furthermore, the MPS values of Deforestation for Northern Vietnam are significantly lower than those of all other regions ( $p < 0.001$ ) except for Southern Vietnam ( $p = 0.206$ ).

Based on the hypothesized link between deforestation MPS and deforestation drivers, the observed differences among the regions can be explained based on evidence from previous research. For this, the percentages of deforestation areas caused by their corresponding drivers for each of the regions were estimated using this study's deforestation map and the map of primary drivers of forest cover loss by Curtis et al. (2018) (Figure 4.8). The distributions of the percentages corresponding to each of the regions in Figure 4.8a and the regional means of deforestation MPSs (2007–2016) in ascending order (Figure 4.8b) indicate the link between MPS and deforestation drivers. That is, the percentages of shifting agriculture-driven deforestation are likely negatively correlated to regional mean deforestation MPS, whereas the percentages of commodity-driven deforestation are likely positively correlated to regional mean deforestation MPS.

According to Li et al. (2014), shifting agriculture in Vietnam is mostly practiced by ethnic minority households in upland areas for subsistence food production. Therefore, shifting agriculture-driven deforestation may result in dispersed, small patch sizes. On the other hand, commodity-driven deforestation mainly involves market-based farming of crops and plantation forests, or the construction of hydropower plants (Meyfroidt et al., 2013; Nghiem et al., 2020; T. T. Pham et al., 2019). Thus, commodity-driven deforestation may result in larger patch sizes in comparison with shifting agriculture-driven deforestation and centralized distributions. Based on this assessment, the deforestation MPS map quantitatively captures the spatial heterogeneity of deforestation drivers in Vietnam.

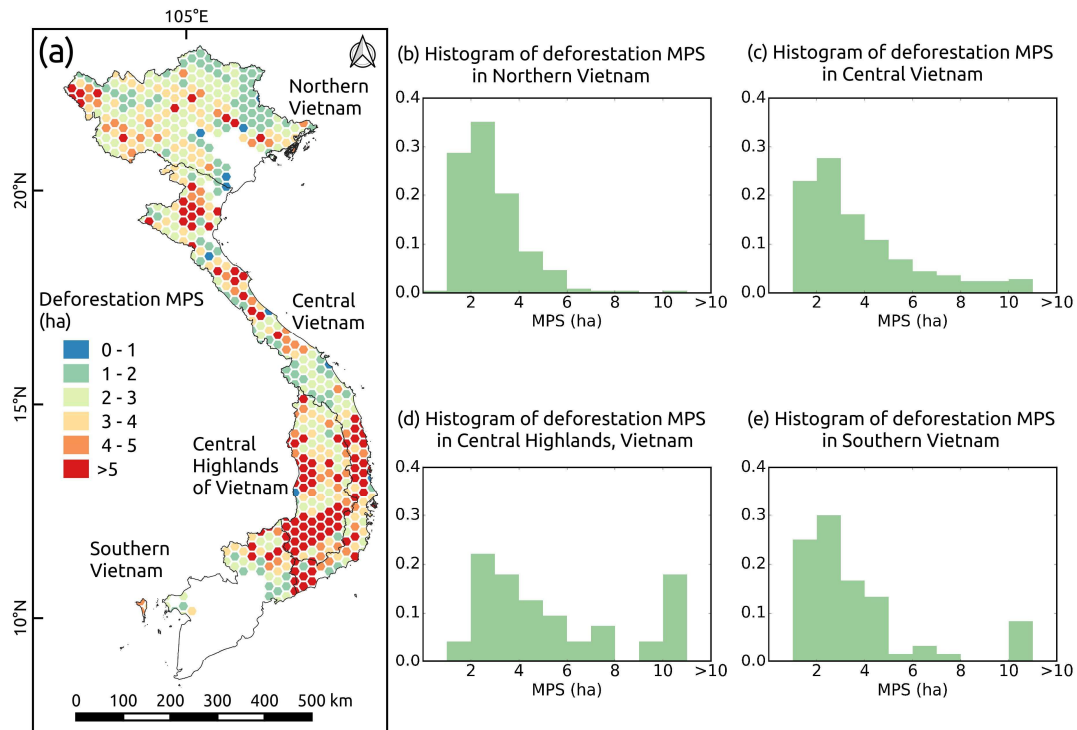


Figure 4.7. (a) Deforestation mean patch size (MPS) map for Vietnam for the period 2007–2016; (b) histogram of deforestation MPS in Northern Vietnam; (c) histogram of deforestation MPS in Central Vietnam; (d) histogram of deforestation MPS in the Central Highlands region of Vietnam; (e) histogram of deforestation MPS in Southern Vietnam

Table 4.3. Comparison of deforestation MPS in Northern Vietnam, Central Vietnam, the Central Highlands of Vietnam, and Southern Vietnam. Statistical significance of differences was estimated using the Wilcoxon rank-sum test.

Pair of regions	Regional mean of deforestation MPS (respectively) (ha)		Statistical Significance
Northern Vietnam ( $n=236$ ) & Central Vietnam ( $n=249$ )	3.079	4.043	$p < 0.001$
Northern Vietnam ( $n=236$ ) & Central Highlands ( $n=95$ )	3.079	7.175	$p < 0.001$
Northern Vietnam ( $n=236$ ) & Southern Vietnam ( $n=60$ )	3.079	4.030	$p = 0.206$
Central Vietnam ( $n=249$ ) & Central Highlands ( $n=95$ )	4.043	7.175	$p < 0.001$
Central Vietnam ( $n=249$ ) & Southern Vietnam ( $n=60$ )	4.043	4.030	$p = 0.371$
Central Highlands ( $n=95$ ) & Southern Vietnam ( $n=60$ )	7.175	4.030	$p < 0.001$



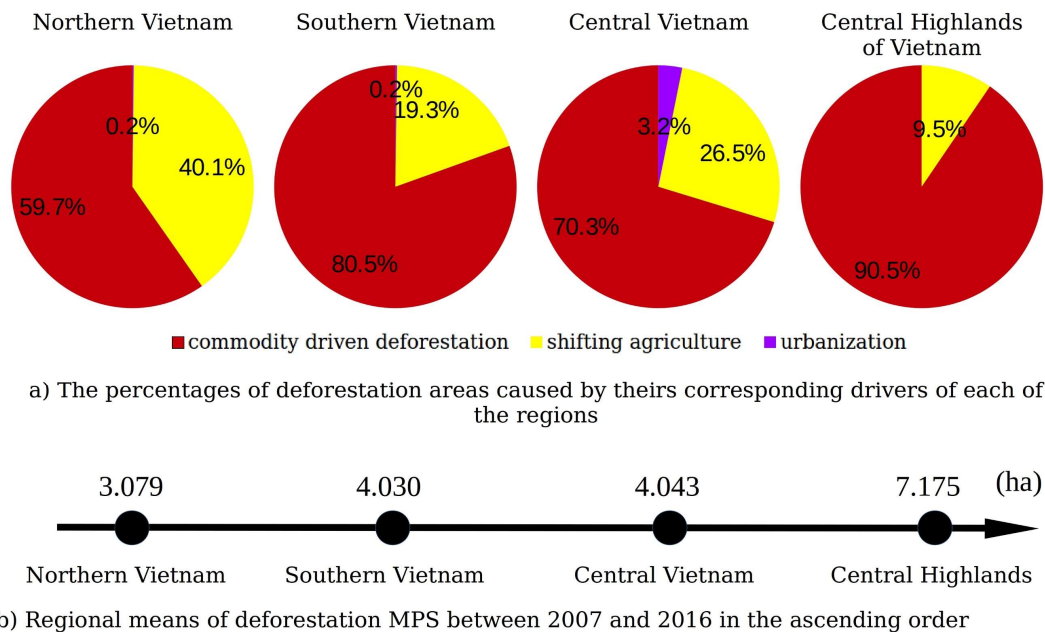


Figure 4.8. (a) Percentages of deforestation areas caused by corresponding drivers (Curtis et al., 2018) in different regions and (b) regional deforestation mean patch size (MPS) between 2007 and 2016 in the ascending order.

#### 4.3.4. Temporal variations in deforestation MPS

The temporal variations in deforestation patch size are illustrated using annual maps of the deforestation MPS (2001–2019) in Figure 4.9, with statistical comparisons between 5-year means for each main region of Vietnam shown in Table 4.4. The trajectories of the regional means in each region are also shown in Figure 4.10. The observed temporal trends fall into two categories. First, Northern Vietnam and Central Vietnam show steadily increasing trends ( $p < 0.05$  in most cases). Second, the Central Highlands and Southern Vietnam show a sharp increase between 2001 and 2010, and then a decreasing trend until 2019.

As with the spatial patterns discussed in Section 4.3.3, these trajectories can be explained by temporal trends in deforestation drivers. For Northern Vietnam and Central Vietnam, evidence from previous studies indicates that there has been a transition from subsistence farming shifting agriculture to market-based farming of

perennial crops and plantation forests in recent decades (Nghiem et al., 2020; M. P. Nguyen et al., 2018; T. T. Nguyen & Masuda, 2018; T. T. Pham et al., 2019; Sandewall et al., 2010; Van Khuc et al., 2020). For example, Nguyen et al. (2018) showed that loopholes in the forestry policy of Program 147, which supported the conversion of poor-quality natural forests to plantation forests, were a cause of deforestation in Bac Kan Province, Northern Vietnam between 2008 and 2020. Furthermore, Nghiem et al. (2020) reported that the expansion of coffee plantations has contributed to forest loss in Son La Province, Northern Vietnam, and Sandewall et al. (2010) indicated a transition from shifting cultivation to farm-based plantations in the mountainous areas of Phu Tho Province, Tuyen Quang Province, and Lao Cai Province in Northern Vietnam. Khuc et al. (2020) also highlight the expansion of plantation forests in Nghe An Province, Central Vietnam, and suggested that switching from shifting cultivation to plantation forests increases the income of households. As discussed in Section 4.3.3, shifting agriculture-driven deforestation is likely to generate smaller MPSs than commodity driven-deforestation. Therefore, such transitions from shifting agriculture to commodity-based plantations are in agreement with the observed steady increase in deforestation MPS in the regions between 2001 and 2019.

For the Central Highlands region and Southern Vietnam, evidence from previous studies shows that there has been an expansion in perennial crop agriculture from the late 2000s. For example, Meyfroidt et al. (2013) reported a rapid expansion in perennial crops causing significant deforestation between 2000 and 2010 in the Central Highlands, with the deforested area doubling between 2001–2005 and 2006–2010. The same authors also highlight that this agricultural expansion has resulted in the replacement of shifting agriculture with market-based plantations. Moreover, Kissinger (2020) provide evidence of the expansion of perennial crop cultivation in the Central Highlands between 2005 and 2015, with the areas of rubber, coffee, and pepper plantations increasing by 198%, 29%, and 106%, respectively. In Southern Vietnam, deforestation is mainly caused by the conversion of natural forests to rubber plantations in Binh Phuoc, Tay Ninh, and Binh Duong Provinces (baodatviet.vn, 2016; Fox & Castella, 2013; laodong.vn, 2018; Phuc & Nghi, 2014). Such expansion in the extent of perennial crop plantations is in agreement with the observed MPS trajectories in these two regions. The decreasing deforestation MPS trend in the Central Highlands region and Southern

Vietnam during 2016–2019 may indicate some degree of mitigation driven by active policy responses from the Vietnamese government (Kissinger, 2020; T. T. Pham et al., 2019).

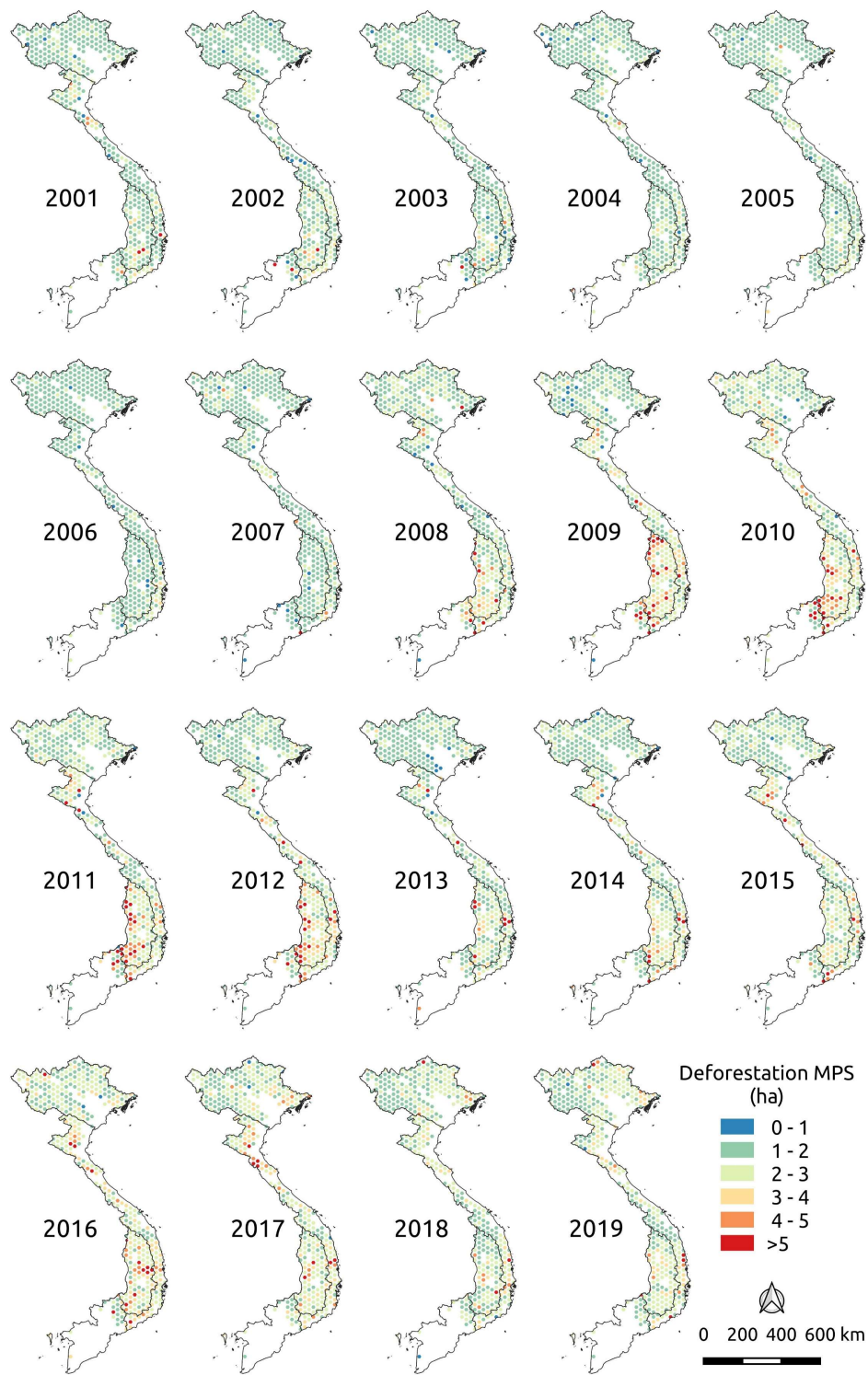


Figure 4.9. Annual maps of deforestation mean patch size (MPS) during the period 2001–2019 created from GFC year of gross forest cover loss event data with natural forest masks from the 2007 LULC map created in this study and the 2016 LULC map created by Hoang et al., (2020).

Table 4.4. Differences in 5-year means (2001–2005, 2006–2010, 2011–2015, and 2016–2019) of deforestation mean patch size (MPS) for the main regions in Vietnam. The statistical significance of the differences was estimated using the Wilcoxon rank-sum test.

Regions	Pair of 5-year period	Regional mean of deforestation MPS of each 5-year period (respectively) (ha)		Statistical Significance
Northern Vietnam ( <i>n</i> =236)	2001–2005 & 2006–2010	1.700	1.880	<i>p</i> < 0.001
	2001–2005 & 2011–2015	1.700	1.853	<i>p</i> < 0.001
	2001–2005 & 2016–2019	1.700	2.183	<i>p</i> < 0.001
	2006–2010 & 2011–2015	1.880	1.853	<i>p</i> = 0.729
	2006–2010 & 2016–2019	1.880	2.183	<i>p</i> < 0.001
	2011–2015 & 2016–2019	1.853	2.183	<i>p</i> < 0.001
Central Vietnam ( <i>n</i> =249)	2001–2005 & 2006–2010	1.903	2.209	<i>p</i> < 0.001
	2001–2005 & 2011–2015	1.903	2.460	<i>p</i> < 0.001
	2001–2005 & 2016–2019	1.903	2.579	<i>p</i> < 0.001
	2006–2010 & 2011–2015	2.209	2.460	<i>p</i> = 0.001
	2006–2010 & 2016–2019	2.209	2.579	<i>p</i> < 0.001
	2011–2015 & 2016–2019	2.460	2.579	<i>p</i> = 0.035
Central Highlands of Vietnam ( <i>n</i> =95)	2001–2005 & 2006–2010	1.951	2.678	<i>p</i> < 0.001
	2001–2005 & 2011–2015	1.951	3.028	<i>p</i> < 0.001
	2001–2005 & 2016–2019	1.951	2.646	<i>p</i> < 0.001
	2006–2010 & 2011–2015	2.678	3.028	<i>p</i> = 0.065
	2006–2010 & 2016–2019	2.678	2.646	<i>p</i> = 0.968
	2011–2015 & 2016–2019	3.028	2.646	<i>p</i> = 0.095
Southern Vietnam ( <i>n</i> =60)	2001–2005 & 2006–2010	2.140	2.718	<i>p</i> = 0.239
	2001–2005 & 2011–2015	2.140	2.669	<i>p</i> = 0.255
	2001–2005 & 2016–2019	2.140	2.249	<i>p</i> = 0.316
	2006–2010 & 2011–2015	2.718	2.669	<i>p</i> = 0.946
	2006–2010 & 2016–2019	2.718	2.249	<i>p</i> = 0.935
	2011–2015 & 2016–2019	2.669	2.249	<i>p</i> = 0.704

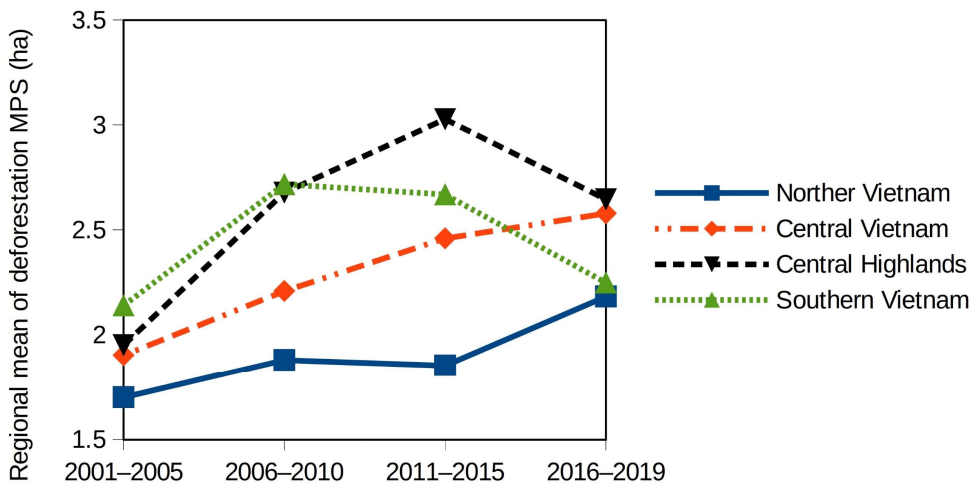


Figure 4.10. Trajectories of regional deforestation MPS means for the main regions of Vietnam during the last two decades.

#### 4.4. Summary

This chapter created a high-resolution 2007 LULC map for Vietnam following the mapping approach of the JAXA to comprehensively distinguish natural forests and plantation forests (Hoang et al., 2020). The resulting map had an overall accuracy of 85%, and accuracies of the major forest classes such as EBFs and plantation forests were higher than 85%. By analyzing the LULC net change between the 2007 LULC map and the 2016 JAXA map, I identified a marked reduction in the area of EBFs (a loss of 649,000 ha) and an increase in the area of plantation forests (a gain of 1,152,000 ha).

Based on the loss of natural forest areas derived from the LULC maps, I generated a deforestation map for the 2007–2016 period. The deforestation category of the resulting map had a user accuracy and producer accuracy of 69.2% and 85.6%, respectively. In comparison with other datasets, this study found that for Central Highlands deforestation hotspot, my estimated deforestation area ( $399,000 \pm 48,000$  ha) is closest to that reported in official national statistics (444,000 ha), while GFC data and CCI-LC data yield overestimations and underestimations results in comparison to the national statistics, respectively. Although there is still a need for reliable deforestation datasets in Vietnam, my comparisons demonstrate the potential advantages of this study’s mapping approach for the regional-scale detection of deforestation.

Based on this study's deforestation map and GFC data with natural forest masks, I created maps of deforestation MPS for the period 2001–2019. My results demonstrate a clear association between spatiotemporal variations in deforestation MPS and drivers of deforestation in Vietnam. Specifically, shifting agriculture-driven deforestation is likely associated with smaller MPSs than commodity driven-deforestation. Temporally, the transition from shifting agriculture to commodity-based plantations in Northern Vietnam and Central Vietnam is indicated by a steadily increasing trend in deforestation MPS. Furthermore, the booming expansion of perennial crops in Central Highlands and Southern Vietnam well matches the deforestation MPS trajectories.

Understanding the drivers of deforestation is essential for designing forest conservation policies. It is recommended that zero-deforestation commitments should be taken into account in land-use planning relevant to commodity-based plantations.

## **Chapter 5. Discussion**



The changes of plantation forests and natural forests in Vietnam in recent decades with their profound impacts have raised an urgent demand for highly accurate and detailed monitoring. To this end, this study provided a comprehensive solution comprising of mapping, change analysis, and investigating the causes of the changes based on Earth observation data. The results of this study would be a potential reference for policymaking in the forestry sector in Vietnam. Aside from the achievements, limitations and caveats are worth mentioning for future work.

For the first research question mentioned in section 1.2, this study addressed the challenge of mapping different types of plantation forests and natural forests in various geographical regions in Vietnam by the comprehensive approach which integrated time-series data from various sensors. Overall, the main target of this research question was achieved. The major natural forest category—EBF, and plantation forest had high accuracies of more than 85%. The resulting map presented its advantages when compared to other LULC map products or forest map products. The advantages were, i.e., 10-m resolution, which is currently the best resolution among open LULC data products, and the discrimination of natural forest and plantation forest classes which facilitates deforestation monitoring. As for limitations, natural bamboo forests were likely to be confused with plantation forests, and nature-like planted forests were likely to be confused with natural forests. Potential solutions for the misclassification of bamboo would be using leaf area index (LAI) information or adopting the approach of global bamboo forest mapping by Du et al. (2018). To detect the nature-like planted forests, human knowledge-based information would be the solution. Besides, increasing forest categories would be of future work. The number of forest categories of this study (4 categories) was lower than that of the Vietnam Forest Map of the Vietnamese government (11 categories). The development of new satellite images and advanced deep learning classification methods would offer opportunities for highly detailed and accurate forest mapping.

For the second research question, this study showed that in the deforestation hot spot—Central Highlands, the deforestation area between 2007 and 2016 of this study's map was closer to national statistics in comparison with other remote sensing-based data. The limitation in this comparison was that there was no reference for the

deforestation area in the national statistics. Therefore, for the national statistics, the net change of natural forest area was used as a substitution for deforestation area. Since in Central Highlands, the natural forest gain was negligible, the net change of natural forest area can reflect the deforestation area. This result indicated the potential advantage of this study's map in comparison with other remote sensing-based data in deforestation detection. However, there is a need for a reliable reference of deforestation area over entire Vietnam.

For the third research question, this study showed that the spatiotemporal variations in deforestation mean patch size (MPS) were connected with spatiotemporal variations in the main direct drivers of deforestation among the regions in Vietnam. The connection was that deforestation MPS were negatively correlated to the involvement of shifting agriculture, and positively correlated to the involvement of commodity-driven deforestation. This result suggests that maps of deforestation MPS can be potential representations for the deforestation drivers. Moreover, the temporal trends of deforestation MPS can track the temporal changes of drivers of deforestation in Vietnam such as the transition from shifting agriculture to commodity-driven deforestation in Northern Vietnam and Central Vietnam, or the booming expansion of perennial crops in Central Highlands over the last two decades. In this analysis, the support of natural forest extents from this study's LULC maps in the deforestation MPS mapping was essential. Therefore, the discrimination of natural forests and plantation forests in the objective 1 played a key role throughout this study. However, the limitation of this result was no ground-truth verification of the spatiotemporal variations in the drivers. Evidence of the drivers was collected from data and documents of previous studies. Therefore, the involvement of ground-truth data for the drivers of deforestation would be of future work.

## **Chapter 6. Conclusion**

This study aimed for analyzing changes of natural forests and plantation forests in Vietnam using remote sensing data. The overall goal comprised of specific objectives, i.e., (i) to establish a comprehensive and geographically transferable approach to produce the high-resolution LULC map in 2016 which distinguish various types of plantation forests and natural forests over entire mainland Vietnam; (ii) to establish an approach to create a deforestation map based on two LULC maps (2007 and 2016) which were created based on the approach in objective (i) and comparing the deforestation area of this study's map with other data; and (iii) to investigate spatiotemporal variations in the deforestation mean patch size and its link with spatiotemporal variations in drivers of deforestation of the main regions in Vietnam during 2001–2019.

The results of this study indicate that:

1. This study demonstrated a comprehensive approach to create high-resolution LULC maps which aimed for distinguishing natural forests and plantation forests (acacia, rubber, eucalyptus, and others) among various geographical regions in Vietnam. The comprehensive approach comprised of integrating various data from multiple sensors at the decision level, taking advantage of using time-series data, and taking advantage of using remote sensing indices.
2. Based on the mapping approach, this study created two high-resolution LULC maps in 2007 and 2016. The resultant LULC maps provide a reliable reference for forest changes analysis. The major forest classes such as EBFs and plantation forests have accuracies of more than 85%. The LULC maps have been published on the JAXA website as open Vietnam LULC data of JAXA:  
[https://www.eorc.jaxa.jp/ALOS/en/lulc/lulc\\_vnm\\_v2006.htm](https://www.eorc.jaxa.jp/ALOS/en/lulc/lulc_vnm_v2006.htm)
3. In comparison other widely-used LULC maps and forest maps, the resultant LULC maps have advantages in the discrimination of natural forest and plantation forest classes, which facilitates deforestation monitoring, and high-resolution (10 m).

4. Based on post-classification comparison, this study identified that the major natural forest category—EBF decreased by 649 thousand ha and plantation forests increased by 1,152 thousand ha over entire Vietnam between 2007 and 2016.
5. This study found that for Central Highlands deforestation hotspot, the estimated deforestation area of this study ( $399,000 \pm 48,000$  ha) is closest to that reported in official national statistics (444,000 ha) in comparison with other datasets. Assuming that in the case of Central Highlands, the national statistics properly reflected the reality of deforestation area, this result indicated the potential advantage of this study's map in comparison with other remote sensing-based data in deforestation detection.
6. Spatiotemporal variations in deforestation MPS over Vietnam were analyzed at the regional scale in Vietnam. The analysis demonstrated a link between spatiotemporal variations in deforestation MPS and drivers of deforestation in Vietnam. That is, shifting agriculture-driven deforestation is likely associated with smaller MPSs than commodity driven-deforestation.
7. Based on the hypothesized link, the deforestation MPS well represented the temporal changes in drivers of deforestation in Vietnam in the last two decades. Specifically, the transition from shifting agriculture to commodity-based plantations in Northern Vietnam and Central Vietnam is indicated by a steadily increasing trend in deforestation MPS. Furthermore, the booming expansion of perennial crops in Central Highlands and Southern Vietnam well matches the deforestation MPS trajectories.

## Acknowledgement

I would like to express my sincere gratitude to the Japanese Government, JICA, and the Project for Human Resource Development Scholarship by Japanese Grant Aid (JDS) for providing me the scholarship (No. B0012018VNMD04), which support me to achieve my Ph.D. degree in the Graduate School of Life and Environmental Sciences, University of Tsukuba.

I express my deepest gratitude to my supervisor, Prof. Kenlo Nasahara for his support, encouragement, and his inspiration not only in the Ph.D. program but also in my life and my scientific career. I would like to thank Prof. Tomoko Akitsu, Prof. Maki Tsujimura, Prof. Mitsuru Hirota, and other faculty members for their valuable comments and instructive suggestions on my thesis as well as my research progress. I also thank my fellow laboratory members including Jin Katagi and Hiroki Mizuochi who helped me on technical issues of my initial stage, Duong Cao Phan and Truong Van Think who collaborated with me in my field trips and publications, and many other members for their kindly helps.

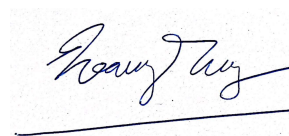
I would like to thank Prof. Nguyen Van Thang, the Director General of my home country organization (Viet Nam Institute of Meteorology, Hydrology and Climate Change), and other colleagues who supported me in taking the opportunity to study the Ph.D. program in Japan.

I would like to thank Dr. Takeo Tadono, Dr. Masato Hayashi, and other scientists, researchers in JAXA/EORC ecosystem & forest group for their support and valuable comments, suggestions for my study. I would like to thank JAXA for providing PALSAR-2/ScanSAR, and AVNIR-2 ORI data in the Vietnam region under the research agreement of “Generation of the Precise Land Cover Map” between JAXA and the University of Tsukuba, as well as JAXA ALOS-2 RA6 (PI#3283, Kenlo Nasahara).

Special thanks go to JDS staff and JICE for their support during the time I stay in Japan.

Last but not least, to my family and their enthusiastic support.

Tsukuba, Japan, January 31, 2021



HOANG THANH TUNG

## Reference

- Almeida-Filho, R., Shimabukuro, Y. E., Rosenqvist, A., & Sánchez, G. A. (2009). Using dual-polarized ALOS PALSAR data for detecting new fronts of deforestation in the Brazilian Amazônia. *International Journal of Remote Sensing*. <https://doi.org/10.1080/01431160902777175>
- Alroy, J. (2017). Effects of habitat disturbance on tropical forest biodiversity. *Proceedings of the National Academy of Sciences of the United States of America*. <https://doi.org/10.1073/pnas.1611855114>
- Anselmetti, F. S., Hodell, D. A., Ariztequi, D., Brenner, M., & Rosenmeier, M. F. (2007). Quantification of soil erosion rates related to ancient Maya deforestation. *Geology*. <https://doi.org/10.1130/G23834A.1>
- ASF. (2014). *ALOS PALSAR – Radiometric Terrain Correction*. <https://asf.alaska.edu/data-sets/derived-data-sets/alos-palsar-rtc/alos-palsar-radiometric-terrain-correction/>
- Austin, K. G., González-Roglich, M., Schaffer-Smith, D., Schwantes, A. M., & Swenson, J. J. (2017). Trends in size of tropical deforestation events signal increasing dominance of industrial-scale drivers. *Environmental Research Letters*, *12*(5). <https://doi.org/10.1088/1748-9326/aa6a88>
- Avitabile, V., Schultz, M., Herold, N., de Bruin, S., Pratihast, A. K., Manh, C. P., Quang, H. V., & Herold, M. (2016). Carbon emissions from land cover change in Central Vietnam. *Carbon Management*. <https://doi.org/10.1080/17583004.2016.1254009>
- baodatviet.vn. (2016). *Binh Phuoc sawing forests to plant rubber: Poor-quality forest, or not? (In Vietnamese, published on 2016-08-23)*. <https://baodatviet.vn/chinh-tri-xa-hoi/tin-tuc-thoi-su/binh-phuoc-cua-rung-trong-cao-su-rung-ngheo-ma-khong-ngheo-3316994/>
- baotainguyenmoitruong.vn. (2016). *Muong Nhe, Dien Bien: Forests turn to swidden (in Vietnamese, published on 2016-11-16)*. <https://baotainguyenmoitruong.vn/muong-nhe-dien-bien-rung-thanh-nuong-ray-235879.html>
- Barlow, J., Lennox, G. D., Ferreira, J., Berenguer, E., Lees, A. C., Nally, R. Mac, Thomson, J. R., Ferraz, S. F. D. B., Louzada, J., Oliveira, V. H. F., Parry, L., Ribeiro De Castro Solar, R., Vieira, I. C. G., Aragaõ, L. E. O. C., Begotti, R. A., Braga, R. F., Cardoso, T. M., Jr, R. C. D. O., Souza, C. M., ... Gardner, T. A. (2016). Anthropogenic disturbance in tropical forests can double biodiversity loss from deforestation. *Nature*. <https://doi.org/10.1038/nature18326>
- Birch, C. P. D., Oom, S. P., & Beecham, J. A. (2007). Rectangular and hexagonal grids used for observation, experiment and simulation in ecology. *Ecological Modelling*.

<https://doi.org/10.1016/j.ecolmodel.2007.03.041>

- Bradshaw, C. J. A., Sodhi, N. S., Peh, K. S. H., & Brook, B. W. (2007). Global evidence that deforestation amplifies flood risk and severity in the developing world. *Global Change Biology*. <https://doi.org/10.1111/j.1365-2486.2007.01446.x>
- Campbell, A., Clark, S., Coad, L., Miles, L., Bolt, K., & Roe, D. (2008). Protecting the future: Carbon, forests, protected areas and local livelihoods. *Biodiversity*. <https://doi.org/10.1080/14888386.2008.9712916>
- Carnus, J. M., Parrotta, J., Brockerhoff, E., Arbez, M., Jactel, H., Kremer, A., Lamb, D., O'Hara, K., & Walters, B. (2006). Planted forests and biodiversity. *Journal of Forestry*. <https://doi.org/10.1093/jof/104.2.65>
- Chen, B., Li, X., Xiao, X., Zhao, B., Dong, J., Kou, W., Qin, Y., Yang, C., Wu, Z., Sun, R., Lan, G., & Xie, G. (2016). Mapping tropical forests and deciduous rubber plantations in Hainan Island, China by integrating PALSAR 25-m and multi-temporal Landsat images. *International Journal of Applied Earth Observation and Geoinformation*. <https://doi.org/10.1016/j.jag.2016.03.011>
- Chen, G., Powers, R. P., de Carvalho, L. M. T., & Mora, B. (2015). Spatiotemporal patterns of tropical deforestation and forest degradation in response to the operation of the Tucuruí hydroelectricdam in the Amazon basin. *Applied Geography*. <https://doi.org/10.1016/j.apgeog.2015.06.001>
- Chen, H., Zeng, Z., Wu, J., Peng, L., Lakshmi, V., Yang, H., & Liu, J. (2020). Large uncertainty on forest area change in the early 21st century among widely used global land cover datasets. *Remote Sensing*. <https://doi.org/10.3390/rs12213502>
- Cheng, Y., Yu, L., Xu, Y., Lu, H., Cracknell, A. P., Kanniah, K., & Gong, P. (2018). Mapping oil palm extent in Malaysia using ALOS-2 PALSAR-2 data. *International Journal of Remote Sensing*. <https://doi.org/10.1080/01431161.2017.1387309>
- Cochard, R., Ngo, D. T., Waeber, P. O., & Kull, C. A. (2017). Extent and causes of forest cover changes in Vietnam's provinces 1993–2013: a review and analysis of official data. *Environmental Reviews*, 25(2), 199–217. <https://doi.org/10.1139/er-2016-0050>
- Coppin, P., Jonckheere, I., Nackaerts, K., Muys, B., & Lambin, E. (2004). Digital change detection methods in ecosystem monitoring: A review. *International Journal of Remote Sensing*. <https://doi.org/10.1080/0143116031000101675>
- Coppin, P. R., & Bauer, M. E. (1996). Digital Change Detection in Forest Ecosystems with Remote Sensing Imagery. *Remote Sensing Reviews*. <https://doi.org/10.1080/02757259609532305>
- Crowther, J., Zimmer, H., Le Thi, H., Quang, T. Lo, & Nichols, J. D. (2020). Forestry



- in Vietnam: The potential role for native timber species. In *Forest Policy and Economics*. <https://doi.org/10.1016/j.forpol.2020.102182>
- Curtis, P. G., Slay, C. M., Harris, N. L., Tyukavina, A., & Hansen, M. C. (2018). Classifying drivers of global forest loss. *Science*, *361*(6407), 1108–1111. <https://doi.org/10.1126/science.aau3445>
- Dao Minh, T., Yanagisawa, M., & Kono, Y. (2017). Forest transition in Vietnam: A case study of Northern mountain region. *Forest Policy and Economics*. <https://doi.org/10.1016/j.forpol.2016.09.013>
- Dat Pham, T., Xia, J., Thang Ha, N., Tien Bui, D., Nhu Le, N., & Tekeuchi, W. (2019). A review of remote sensing approaches for monitoring blue carbon ecosystems: Mangroves, sea grasses and salt marshes during 2010–2018. In *Sensors (Switzerland)*. <https://doi.org/10.3390/s19081933>
- Daughtry, C. S. T., Hunt, E. R., Doraiswamy, P. C., & McMurtrey, J. E. (2005). Remote sensing the spatial distribution of crop residues. *Agronomy Journal*. <https://doi.org/10.2134/agronj2003.0291>
- De Alban, J. D. T., Connette, G. M., Oswald, P., & Webb, E. L. (2018). Combined Landsat and L-band SAR data improves land cover classification and change detection in dynamic tropical landscapes. *Remote Sensing*. <https://doi.org/10.3390/rs10020306>
- De Jong, W., Do, D., & Trieu, V. (2006). *Forest rehabilitation in Viet Nam: histories, realities and future*. CIFOR. [http://www.cifor.cgiar.org/publications/pdf\\_files/Books/BDeJong0601.pdf](http://www.cifor.cgiar.org/publications/pdf_files/Books/BDeJong0601.pdf)
- Deng, X., Guo, S., Sun, L., & Chen, J. (2020). Identification of Short-Rotation Eucalyptus Plantation at Large Scale Using Multi-Satellite Imageries and Cloud Computing Platform. *Remote Sensing*, *12*(13), 2153. <https://doi.org/10.3390/rs12132153>
- Dong, J., Xiao, X., Chen, B., Torbick, N., Jin, C., Zhang, G., & Biradar, C. (2013). Mapping deciduous rubber plantations through integration of PALSAR and multi-temporal Landsat imagery. *Remote Sensing of Environment*. <https://doi.org/10.1016/j.rse.2013.03.014>
- Dong, J., Xiao, X., Sheldon, S., Biradar, C., Duong, N. D., & Hazarika, M. (2012). A comparison of forest cover maps in Mainland Southeast Asia from multiple sources: PALSAR, MERIS, MODIS and FRA. *Remote Sensing of Environment*, *127*, 60–73. <https://doi.org/10.1016/j.rse.2012.08.022>
- Dong, J., Xiao, X., Sheldon, S., Biradar, C., & Xie, G. (2012). Mapping tropical forests and rubber plantations in complex landscapes by integrating PALSAR and MODIS imagery. *ISPRS Journal of Photogrammetry and Remote Sensing*, *74*, 20–33. <https://doi.org/10.1016/j.isprsjprs.2012.07.004>

- Dong, J., Xiao, X., Sheldon, S., Biradar, C., Zhang, G., Duong, N. D., Hazarika, M., Wikantika, K., Takeuchi, W., & Moore, B. (2014). A 50-m forest cover map in Southeast Asia from ALOS/PALSAR and its application on forest fragmentation assessment. *PLoS ONE*, 9(1). <https://doi.org/10.1371/journal.pone.0085801>
- Du, H., Mao, F., Li, X., Zhou, G., Xu, X., Han, N., Sun, S., Gao, G., Cui, L., Li, Y., Zhu, D., Liu, Y., Chen, L., Fan, W., Li, P., Shi, Y., & Zhou, Y. (2018). Mapping Global Bamboo Forest Distribution Using Multisource Remote Sensing Data. *IEEE Journal of Selected Topics in Applied Earth Observations and Remote Sensing*. <https://doi.org/10.1109/JSTARS.2018.2800127>
- Dung, P. T., Chuc, M. D., Thanh, N. T. N., Hung, B. Q., & Chung, D. M. (2016). Optimizing GLCNMO version 2 method to detect Vietnam's urban expansion. *Proceedings - 2016 8th International Conference on Knowledge and Systems Engineering, KSE 2016*. <https://doi.org/10.1109/KSE.2016.7758072>
- ESA. (2014a). *Copernicus Open Access Hub*. <https://scihub.copernicus.eu/>
- ESA. (2014b). *Sentinel-1 Data products*. <https://sentinel.esa.int/web/sentinel/missions/sentinel-1/data-products>
- ESA. (2015a). *Land cover - Climate Change Initiative*. <https://www.esa-landcover-cci.org/>
- ESA. (2015b). *Sentinel-2, Spatial and Spectral Resolutions*. <https://sentinel.esa.int/web/sentinel/missions/sentinel-2/instrument-payload/resolution-and-swath>
- ESA. (2015c). *Sentinel-2 MSI, Cloud Masks*. <https://sentinel.esa.int/web/sentinel/technical-guides/sentinel-2-msi/level-1c/cloud-masks>
- ESA. (2017). Land Cover CCI Product User Guide - Version 2.0. In *Esa*.
- Fan, H., Fu, X., Zhang, Z., & Wu, Q. (2015). Phenology-based vegetation index differencing for mapping of rubber plantations using landsat OLI data. *Remote Sensing*, 7(5), 6041–6058. <https://doi.org/10.3390/rs70506041>
- Fan, P., Ouyang, Z., Nguyen, D. D., Nguyen, T. T. H., Park, H., & Chen, J. (2019). Urbanization, economic development, environmental and social changes in transitional economies: Vietnam after Doimoi. *Landscape and Urban Planning*. <https://doi.org/10.1016/j.landurbplan.2018.10.014>
- FAO. (2012). Global ecological zones for FAO forest reporting: 2010 Update. In *Forest resources Assessment Working Paper 179*. FAO. <http://www.fao.org/docrep/017/ap861e/ap861e00.pdf>
- FAO. (2018). Global Forest Resources Assessment 2020: Terms and Definition. In

*Resources Assessment Working Paper 188.*

- FAO. (2020a). *Global Forest Resources Assessment - Vietnam report*.
- FAO. (2020b). Global Forest Resources Assessment 2020 Key Findings. In *Global Forest Resources Assessment 2020*. FAO. <https://doi.org/10.4060/ca8753en>
- Filgueiras, R., Mantovani, E. C., Althoff, D., Fernandes Filho, E. I., & da Cunha, F. F. (2019). Crop NDVI monitoring based on sentinel 1. *Remote Sensing*. <https://doi.org/10.3390/rs11121441>
- Flores-Anderson, A. I., Herndon, K. E., Thapa, R. B., & Cherrington, E. (2019). The SAR Handbook: Comprehensive Methodologies for Forest Monitoring and Biomass Estimation. In *THE SAR HANDBOOK Comprehensive Methodologies for Forest Monitoring and Biomass Estimation*. SERVIR. <https://doi.org/10.25966/nr2c-s697>
- Foga, S., Scaramuzza, P. L., Guo, S., Zhu, Z., Dilley, R. D., Beckmann, T., Schmidt, G. L., Dwyer, J. L., Joseph Hughes, M., & Laue, B. (2017). Cloud detection algorithm comparison and validation for operational Landsat data products. *Remote Sensing of Environment*. <https://doi.org/10.1016/j.rse.2017.03.026>
- Fox, J., & Castella, J. C. (2013). Expansion of rubber (*Hevea brasiliensis*) in Mainland Southeast Asia: What are the prospects for smallholders? *Journal of Peasant Studies*. <https://doi.org/10.1080/03066150.2012.750605>
- Friedl, M., & Sulla-Menashe, D. (2019). *MCD12Q1 MODIS/Terra+Aqua Land Cover Type Yearly L3 Global 500m SIN Grid V006*. <https://doi.org/https://doi.org/10.5067/MODIS/MCD12Q1.006>
- Friedl, Mark a., Sulla-Menashe, D., Tan, B., Schneider, A., Ramankutty, N., Sibley, A., & Huang, X. (2010). MODIS Collection 5 global land cover: Algorithm refinements and characterization of new datasets. *Remote Sensing of Environment*, *114*(1), 168–182. <https://doi.org/10.1016/j.rse.2009.08.016>
- Galiatsatos, N., Donoghue, D. N. M., Watt, P., Bholanath, P., Pickering, J., Hansen, M. C., & Mahmood, A. R. J. (2020). An assessment of global forest change datasets for national forest monitoring and reporting. *Remote Sensing*. <https://doi.org/10.3390/rs12111790>
- Geist, H. J., & Lambin, E. F. (2002). Proximate causes and underlying driving forces of tropical deforestation. *American Institute of Biological Sciences*, *52*(2), 143–150. [https://doi.org/10.1641/0006-3568\(2002\)052\[0143:PCAUDF\]2.0.CO;2](https://doi.org/10.1641/0006-3568(2002)052[0143:PCAUDF]2.0.CO;2)
- Gong, P., Liu, H., Zhang, M., Li, C., Wang, J., Huang, H., Clinton, N., Ji, L., Li, W., Bai, Y., Chen, B., Xu, B., Zhu, Z., Yuan, C., Ping Suen, H., Guo, J., Xu, N., Li, W., Zhao, Y., ... Song, L. (2019). Stable classification with limited sample: transferring a 30-m resolution sample set collected in 2015 to mapping 10-m resolution global land cover in 2017. *Science Bulletin*.

- <https://doi.org/10.1016/j.scib.2019.03.002>
- Google Earth Engine. (2020a). *Reducing an ImageCollection*.  
[https://developers.google.com/earth-engine/ic\\_reducing](https://developers.google.com/earth-engine/ic_reducing)
- Google Earth Engine. (2020b). *Sentinel-1 Algorithms*.  
<https://developers.google.com/earth-engine/sentinell>
- Gregorio, A. Di. (2016). Land Cover Classification System. In *October*. FAO.
- Griffin, A. R., Nambiar, E. S., Harwood, C. E., & See, L. S. (2015). Sustaining the future of Acacia plantation forestry – a synopsis. *Southern Forests*.  
<https://doi.org/10.2989/20702620.2015.1011380>
- GSO. (2019). *Statistical Yearbook of Vietnam 2019*. General Statistics Office of Vietnam.  
[https://www.gso.gov.vn/default\\_en.aspx?tabid=515&idmid=5&ItemID=19299](https://www.gso.gov.vn/default_en.aspx?tabid=515&idmid=5&ItemID=19299)
- GSO. (2020). *Area of forest as of 31 December by province*.  
[https://www.gso.gov.vn/en/px-web/?pxid=E0641&theme=Agriculture%2CForestry and Fishing](https://www.gso.gov.vn/en/px-web/?pxid=E0641&theme=Agriculture%2CForestry%20and%20Fishing)
- Gutiérrez-Vélez, V. H., & DeFries, R. (2013). Annual multi-resolution detection of land cover conversion to oil palm in the Peruvian Amazon. *Remote Sensing of Environment*. <https://doi.org/10.1016/j.rse.2012.10.033>
- Ha, D. T., & Shively, G. (2008). Coffee boom, coffee bust and smallholder response in Vietnam's Central Highlands. *Review of Development Economics*.  
<https://doi.org/10.1111/j.1467-9361.2007.00391.x>
- Hagen, S. C., Heilman, P., Marsett, R., Torbick, N., Salas, W., Van Ravensway, J., & Qi, J. (2012). Mapping total vegetation cover across western rangelands with moderate-resolution imaging spectroradiometer data. *Rangeland Ecology and Management*, 65, 456–467. <https://doi.org/10.2111/REM-D-11-00188.1>
- Hansen, M. C., Potapov, P. V., Moore, R., Hancher, M., Turubanova, S. a, Tyukavina, A., Thau, D., Stehman, S. V, Goetz, S. J., Loveland, T. R., Kommareddy, A., Egorov, A., Chini, L., Justice, C. O., & Townshend, J. R. G. (2013). High-Resolution Global Maps of 21st-Century Forest Cover Change. *Science (New York, N.Y.)*, 850(November), 2011–2014. <https://doi.org/10.1126/science.1244693>
- Haralick, R. M., Dinstein, I., & Shanmugam, K. (1973). Textural Features for Image Classification. *IEEE Transactions on Systems, Man and Cybernetics*.  
<https://doi.org/10.1109/TSMC.1973.4309314>
- Harwood, C. E., & Nambiar, E. (2014). Sustainable plantation forestry in South-East Asia. In *ACIAR Technical Reports No. 84*. Australian Centre for International Agricultural Research.

- Hashimoto, S., Tadono, T., Onosato, M., & Hori, M. (2014). A New Method to Derive Precise Land-use and Land-cover Maps Using Multi-temporal Optical Data. *Journal of The Remote Sensing of Japan*, 34(2), 102–112.
- Hoang, T. T., Nasahara, K. N., & Katagi, J. (2018). Analysis of Land Cover Change in Northern Vietnam Using High Resolution Remote Sensing Data. In D. Tien Bui, A. Ngoc Do, H.-B. Bui, & N.-D. Hoang (Eds.), *Advances and Applications in Geospatial Technology and Earth Resources* (Vol. 1). Springer International Publishing. [https://doi.org/10.1007/978-3-319-68240-2\\_9](https://doi.org/10.1007/978-3-319-68240-2_9)
- Hoang, T. T., Truong, V. T., Hayashi, M., Tadono, T., & Nasahara, K. N. (2020). New JAXA high-resolution land use/land cover map for Vietnam aiming for natural forest and plantation forest monitoring. *Remote Sensing*. <https://doi.org/10.3390/RS12172707>
- Hornung, M., Stevens, P. A., & Reynolds, B. . (1987). The effects of forestry on soils, soil water and surface water chemistry. In J. E. G. Good (Ed.), *Environmental Aspects of Plantation Forestry in Wales* (pp. 64–69). NERC/ITE.
- Hosonuma, N., Herold, M., De Sy, V., De Fries, R. S., Brockhaus, M., Verchot, L., Angelsen, A., & Romijn, E. (2012). An assessment of deforestation and forest degradation drivers in developing countries. *Environmental Research Letters*, 7(4), 044009. <https://doi.org/10.1088/1748-9326/7/4/044009>
- Huete, A., Didan, K., Miura, T., Rodriguez, E. P., Gao, X., & Ferreira, L. G. (2002). Overview of the radiometric and biophysical performance of the MODIS vegetation indices. *Remote Sensing of Environment*. [https://doi.org/10.1016/S0034-4257\(02\)00096-2](https://doi.org/10.1016/S0034-4257(02)00096-2)
- Huete, A. R., Liu, H. Q., Batchily, K., & Van Leeuwen, W. (1997). A comparison of vegetation indices over a global set of TM images for EOS-MODIS. *Remote Sensing of Environment*. [https://doi.org/10.1016/S0034-4257\(96\)00112-5](https://doi.org/10.1016/S0034-4257(96)00112-5)
- Hunt, E. R., & Rock, B. N. (1989). Detection of changes in leaf water content using Near- and Middle-Infrared reflectances. *Remote Sensing of Environment*. [https://doi.org/10.1016/0034-4257\(89\)90046-1](https://doi.org/10.1016/0034-4257(89)90046-1)
- Hussain, M., Chen, D., Cheng, A., Wei, H., & Stanley, D. (2013). Change detection from remotely sensed images: From pixel-based to object-based approaches. In *ISPRS Journal of Photogrammetry and Remote Sensing*. <https://doi.org/10.1016/j.isprsjprs.2013.03.006>
- IPCC. (2019). Climate change and Land. In *IPCC Special Report*. <https://doi.org/10.4337/9781784710644>
- Isaacson, S., Ephrath, J. E., Rachmilevitch, S., Maman, S., Ginat, H., & Blumberg, D. G. (2017). Long and short term population dynamics of acacia trees via remote sensing and spatial analysis: Case study in the southern Negev Desert. *Remote*

- Sensing of Environment*. <https://doi.org/10.1016/j.rse.2017.05.035>
- JAXA/EORC. (2016). *JAXA Homepage of High-Resolution Land Use and Land Cover Map Products*. [https://www.eorc.jaxa.jp/ALOS/en/lulc/lulc\\_vnm.htm](https://www.eorc.jaxa.jp/ALOS/en/lulc/lulc_vnm.htm)
- JAXA. (2008). *ALOS Data Users Handbook* (Issue March).  
[http://www.eorc.jaxa.jp/ALOS/en/doc/fdata/ALOS\\_HB\\_RevC\\_EN.pdf](http://www.eorc.jaxa.jp/ALOS/en/doc/fdata/ALOS_HB_RevC_EN.pdf)
- JAXA. (2015). *PALSAR-2 Basic Observation Scenario Map/User Guideline*.  
[https://www.eorc.jaxa.jp/ALOS-2/en/obs/pal2\\_obs\\_guide.htm](https://www.eorc.jaxa.jp/ALOS-2/en/obs/pal2_obs_guide.htm)
- JAXA. (2019). *Global 25m Resolution PALSAR-2 / PALSAR Mosaic and Forest / Non-Forest Map ( FNF ) Dataset Description*.
- JAXA. (2020a). *ALOS Global Digital Surface Model “ALOS World 3D - 30m (AW3D30).”* <https://www.eorc.jaxa.jp/ALOS/en/aw3d30/index.htm>
- JAXA. (2020b). *AVNIR-2 Ortho Rectified Image Product Format Description* (Issue June).
- JAXA. (2020c). *Global PALSAR-2/PALSAR/JERS-1 Mosaic and Forest/Non-Forest map*. [https://www.eorc.jaxa.jp/ALOS/en/palsar\\_fnf/fnf\\_index.htm](https://www.eorc.jaxa.jp/ALOS/en/palsar_fnf/fnf_index.htm)
- JAXA. (2020d). *Homepage of High-Resolution Land Use and Land Cover Map Products*. [https://www.eorc.jaxa.jp/ALOS/en/lulc/lulc\\_index.htm](https://www.eorc.jaxa.jp/ALOS/en/lulc/lulc_index.htm)
- Kalamandeen, M., Gloor, E., Mitchard, E., Quincey, D., Ziv, G., Spracklen, D., Spracklen, B., Adami, M., Aragaõ, L. E. O. C., & Galbraith, D. (2018). Pervasive Rise of Small-scale Deforestation in Amazonia. *Scientific Reports*.  
<https://doi.org/10.1038/s41598-018-19358-2>
- Karnieli, A., Kaufman, Y. J., Remer, L., & Wald, A. (2001). AFRI - Aerosol free vegetation index. *Remote Sensing of Environment*. [https://doi.org/10.1016/S0034-4257\(01\)00190-0](https://doi.org/10.1016/S0034-4257(01)00190-0)
- Katagi, J., Nasahara, K. N., Kobayashi, K., Dotsu, M., & Tadono, T. (2018). Reduction of misclassification caused by mountain shadow in a high resolution land use and land cover map using multi-temporal optical images. *Journal of The Remote Sensing Society of Japan*, 38(1), 30–34.
- Kaufman, Y. J., & Tanré, D. (1992). Atmospherically Resistant Vegetation Index (ARVI) for EOS-MODIS. *IEEE Transactions on Geoscience and Remote Sensing*.  
<https://doi.org/10.1109/36.134076>
- Keenan, R. J., Reams, G. A., Achard, F., Freitas, J. V. De, Grainger, A., & Lindquist, E. (2015). Dynamics of global forest area : Results from the FAO Global Forest Resources Assessment 2015. *Forest Ecology and Management*, 352, 9–20.  
<https://doi.org/10.1016/j.foreco.2015.06.014>

- Khuc, Q. Van, Tran, B. Q., Meyfroidt, P., & Paschke, M. W. (2018). Drivers of deforestation and forest degradation in Vietnam: An exploratory analysis at the national level. *Forest Policy and Economics*, 90(January), 128–141. <https://doi.org/10.1016/j.forpol.2018.02.004>
- kinhtenongthon.vn. (2017). *Forests in Son Dong was “butchered” (in Vietnamese, published on 2017-10-08)*. <https://kinhtenongthon.vn/rung-son-dong-bi-“xe-thit”-post16090.html>
- Kissinger, G. (2020). Policy Responses to Direct and Underlying Drivers of Deforestation: Examining Rubber and Coffee in the Central Highlands of Vietnam. *Forests*, 11(7), 733. <https://doi.org/10.3390/f11070733>
- Kissinger, G., Herold, M., & De Sy, V. (2012). Drivers of Deforestation and Forest Degradation: A Synthesis Report for REDD+ Policymakers. In *Kissinger, G Herold, M De Sy, Veronique*.
- Kou, W., Xiao, X., Dong, J., Gan, S., Zhai, D., Zhang, G., Qin, Y., & Li, L. (2015). Mapping deciduous rubber plantation areas and stand ages with PALSAR and landsat images. *Remote Sensing*. <https://doi.org/10.3390/rs70101048>
- laodong.vn. (2018). *Binh Phuoc: Unusual around deforestation (In Vietnamese, published on 2018-10-10)*. <https://laodong.vn/phong-su/binh-phuoc-bat-thuong-quanh-vu-pha-rung-634999.ldo>
- le Maire, G., Dupuy, S., Nouvellon, Y., Loos, R. A., & Hakamada, R. (2014). Mapping short-rotation plantations at regional scale using MODIS time series: Case of eucalypt plantations in Brazil. *Remote Sensing of Environment*, 152, 136–149. <https://doi.org/10.1016/j.rse.2014.05.015>
- Lee, J. Sen. (1980). Digital Image Enhancement and Noise Filtering by Use of Local Statistics. *IEEE Transactions on Pattern Analysis and Machine Intelligence*. <https://doi.org/10.1109/TPAMI.1980.4766994>
- Li, G., Lu, D., Moran, E., Dutra, L., & Batistella, M. (2012). A comparative analysis of ALOS PALSAR L-band and RADARSAT-2 C-band data for land-cover classification in a tropical moist region. *ISPRS Journal of Photogrammetry and Remote Sensing*. <https://doi.org/10.1016/j.isprsjprs.2012.03.010>
- Li, P., Feng, Z., Jiang, L., Liao, C., & Zhang, J. (2014). A review of swidden agriculture in Southeast Asia. In *Remote Sensing*. <https://doi.org/10.3390/rs6021654>
- Maraseni, T. N., Poudyal, B. H., Rana, E., Chandra Khanal, S., Ghimire, P. L., & Subedi, B. P. (2020). Mapping national REDD+ initiatives in the Asia-Pacific region. *Journal of Environmental Management*. <https://doi.org/10.1016/j.jenvman.2020.110763>
- Masemola, C., Azong, M., & Ramoelo, A. (2020). *ISPRS Journal of Photogrammetry*

- and Remote Sensing Towards a semi-automated mapping of Australia native invasive alien Acacia trees using Sentinel-2 and radiative transfer models in South Africa. *ISPRS Journal of Photogrammetry and Remote Sensing*, 166(April), 153–168. <https://doi.org/10.1016/j.isprsjprs.2020.04.009>
- Mather, A. S. (2007). Recent Asian forest transitions in relation to forest transition theory. *International Forestry Review*. <https://doi.org/10.1505/ifor.9.1.491>
- McElwee, P. (2009). Reforesting “Bare Hills” in Vietnam: Social and Environmental Consequences of the 5 Million Hectare Reforestation Program. *AMBIO: A Journal of the Human Environment*, 38(6), 325–333. <https://doi.org/10.1579/08-R-520.1>
- McFeeters, S. K. (1996). The use of the Normalized Difference Water Index (NDWI) in the delineation of open water features. *International Journal of Remote Sensing*. <https://doi.org/10.1080/01431169608948714>
- Meyfroidt, P., & Lambin, E. F. (2008a). The causes of the reforestation in Vietnam. *Land Use Policy*, 25(2), 182–197. <https://doi.org/10.1016/j.landusepol.2007.06.001>
- Meyfroidt, P., & Lambin, E. F. (2008b). Forest transition in Vietnam and its environmental impacts. *Global Change Biology*, 14(6), 1319–1336. <https://doi.org/10.1111/j.1365-2486.2008.01575.x>
- Meyfroidt, P., Vu, T. P., & Hoang, V. A. (2013). Trajectories of deforestation, coffee expansion and displacement of shifting cultivation in the Central Highlands of Vietnam. *Global Environmental Change*, 23(5), 1187–1198. <https://doi.org/10.1016/j.gloenvcha.2013.04.005>
- Miettinen, J., & Liew, S. C. (2011). Separability of insular Southeast Asian woody plantation species in the 50 m resolution ALOS PALSAR mosaic product. *Remote Sensing Letters*, 2(4), 299–307. <https://doi.org/10.1080/01431161.2010.520345>
- Minderhoud, P. S. J., Erkens, G., Pham, V. H., Bui, V. T., Erban, L., Kooi, H., & Stouthamer, E. (2017). Impacts of 25 years of groundwater extraction on subsidence in the Mekong delta, Vietnam. *Environmental Research Letters*. <https://doi.org/10.1088/1748-9326/aa7146>
- Morales, R. M., Idol, T., & Friday, J. B. (2011). Assessment of Acacia koa forest health across environmental gradients in hawai'i using fine resolution remote sensing and GIS. *Sensors*. <https://doi.org/10.3390/s110605677>
- Mustalahti, I. (2011). *Footprints in Forests: Effects and Impacts of Finnish Forestry Assistance*.
- Nambiar, E. S., Harwood, C. E., & Kien, N. D. (2015). Acacia plantations in Vietnam: research and knowledge application to secure a sustainable future. *Southern Forests*, 77(1), 1–10. <https://doi.org/10.2989/20702620.2014.999301>



- Nghiem, T., Kono, Y., & Leisz, S. J. (2020). Crop boom as a trigger of smallholder livelihood and land use transformations: The case of coffee production in the Northern Mountain Region of Vietnam. *Land*. <https://doi.org/10.3390/land9020056>
- Nguyen. (2017). Historic drought and salinity intrusion in the Mekong Delta in 2016: Lessons learned and response solutions. *Vietnam Journal of Science, Technology and Engineering*. [https://doi.org/10.31276/vjste.59\(1\).93](https://doi.org/10.31276/vjste.59(1).93)
- Nguyen, M. N., Nguyen, P. T. B., Van, T. P. D., Phan, V. H., Nguyen, B. T., Pham, V. T., & Nguyen, T. H. (2020). An understanding of water governance systems in responding to extreme droughts in the Vietnamese Mekong Delta. *International Journal of Water Resources Development*. <https://doi.org/10.1080/07900627.2020.1753500>
- Nguyen, M. P., Catacutan, D. C., Do, H. T., & Mulia, R. (2018). Drivers of forest changes : mapping actors and motivations in Bac Kan province , Northeast Viet Nam. In R. Mulia & E. Simelton (Eds.), *Towards low-emission landscapes in Viet Nam* (pp. 23–43). World Agroforestry (ICRAF).
- Nguyen, T. T., & Masuda, M. (2018). Land Use After Forestland Allocation and the Potential for Farm Forestry in a Mountainous Region of Northeast Vietnam. *Small-Scale Forestry*, 17(4), 485–503. <https://doi.org/10.1007/s11842-018-9399-0>
- nongnghiep.vn. (2015). *Forests in Yen Hop call for help (in Vietnamese, published on 2015-11-27)*. <https://nongnghiep.vn/rung-yen-hop-keu-cuu-d153277.html>
- Olofsson, P., Foody, G. M., Herold, M., Stehman, S. V., Woodcock, C. E., & Wulder, M. a. (2014). Good practices for estimating area and assessing accuracy of land change. *Remote Sensing of Environment*, 148, 42–57. <https://doi.org/10.1016/j.rse.2014.02.015>
- Olofsson, P., Foody, G. M., Stehman, S. V., & Woodcock, C. E. (2013). Making better use of accuracy data in land change studies : Estimating accuracy and area and quantifying uncertainty using stratified estimation. *Remote Sensing of Environment*, 129, 122–131. <https://doi.org/10.1016/j.rse.2012.10.031>
- Pham, T. D., Kaida, N., Yoshino, K., Nguyen, X. H., Nguyen, H. T., & Bui, D. T. (2018). Willingness to pay for mangrove restoration in the context of climate change in the Cat Ba biosphere reserve, Vietnam. *Ocean and Coastal Management*. <https://doi.org/10.1016/j.ocecoaman.2018.07.005>
- Pham, T. T., Hoang, T. L., Nguyen, D. T., Dao, T. L. C., Ngo, H. C., & Pham, V. H. (2019). The context of REDD+ in Vietnam: Drivers, agents and institutions [2nd edition]. In *The context of REDD+ in Vietnam: Drivers, agents and institutions 2nd edition*. <https://doi.org/10.17528/cifor/007402>
- Phan, D. C., Ta, T. H., Nasahara, K. N., & Tadono, T. (2018). JAXA high-resolution land use / land cover map for Central Vietnam in 2007 and 2017 . *Remote Sensing*,

10, 1406. <https://doi.org/10.3390/rs10091406>

- Phan, T. T. H. (2017). Identifying illicit timber trade between Vietnam and China. *World Customs Journal*, 11(1), 13–22.
- Phuc, T. X., & Nghi, T. H. (2014). *Rubber Expansion and Forest Protection in Vietnam*. *Rubber Expansion and Forest Protection in Vietnam*. [http://www.forest-trends.org/documents/files/doc\\_4671.pdf](http://www.forest-trends.org/documents/files/doc_4671.pdf)
- Phuong, V. T. (2007). Forest Environment of Vietnam: Features of Forest Vegetation and Soils. *Forest Environments in the Mekong River Basin*, 189–200. [https://doi.org/10.1007/978-4-431-46503-4\\_17](https://doi.org/10.1007/978-4-431-46503-4_17)
- Poortinga, A., Tenneson, K., Shapiro, A., Nguyen, Q., Aung, K. S., Chishtie, F., & Saah, D. (2019). Mapping plantations in Myanmar by fusing Landsat-8, Sentinel-2 and Sentinel-1 data along with systematic error quantification. *Remote Sensing*. <https://doi.org/10.3390/rs11070831>
- Qi, J., Chehbouni, A., Huete, A. R., Kerr, Y. H., & Sorooshian, S. (1994). A modified soil adjusted vegetation index. *Remote Sensing of Environment*. [https://doi.org/10.1016/0034-4257\(94\)90134-1](https://doi.org/10.1016/0034-4257(94)90134-1)
- Qin, Y., Xiao, X., Dong, J., Zhang, G., Roy, P. S., Joshi, P. K., Gilani, H., Murthy, M. S. R., Jin, C., Wang, J., Zhang, Y., Chen, B., Menarguez, M. A., Biradar, C. M., Bajgain, R., Li, X., Dai, S., Hou, Y., Xin, F., & Moore, B. (2016). Mapping forests in monsoon Asia with ALOS PALSAR 50-m mosaic images and MODIS imagery in 2010. *Scientific Reports*, 6(July 2015). <https://doi.org/10.1038/srep20880>
- Qin, Y., Xiao, X., Dong, J., Zhang, G., Shimada, M., Liu, J., Li, C., Kou, W., & Moore, B. (2015). Forest cover maps of China in 2010 from multiple approaches and data sources: PALSAR, Landsat, MODIS, FRA, and NFI. *ISPRS Journal of Photogrammetry and Remote Sensing*, 109, 1–16. <https://doi.org/10.1016/j.isprsjprs.2015.08.010>
- Räsänen, T. A., Koponen, J., Lauri, H., & Kumm, M. (2012). Downstream Hydrological Impacts of Hydropower Development in the Upper Mekong Basin. *Water Resources Management*. <https://doi.org/10.1007/s11269-012-0087-0>
- Rivera, A., Bravo, C., & Buob, G. (2020). Climate Change and Land. In *IPCC Special Report*. IPCC. <https://doi.org/10.1002/9781118786352.wbieg0538>
- Rosa, I. M. D., Souza, C., & Ewers, R. M. (2012). Changes in Size of Deforested Patches in the Brazilian Amazon. *Conservation Biology*. <https://doi.org/10.1111/j.1523-1739.2012.01901.x>
- Rouse, J. W., Haas, R. H., Schell, J. A., & Deering, D. . (1973). Monitoring vegetation systems in the Great Plains with ERTS (Earth Resources Technology Satellite). *Third Earth Resources Technology Satellite-1 Symposium*.

- Salati, E., & Nobre, C. A. (1991). Possible climatic impacts of tropical deforestation. *Climatic Change*. <https://doi.org/10.1007/BF00142225>
- Sandewall, M., Ohlsson, B., Sandewall, R. K., & Viet, L. S. (2010). The expansion of farm-based plantation forestry in Vietnam. *Ambio*. <https://doi.org/10.1007/s13280-010-0089-1>
- Sannier, C., McRoberts, R. E., & Fichet, L. V. (2016). Suitability of Global Forest Change data to report forest cover estimates at national level in Gabon. *Remote Sensing of Environment*, *173*, 326–338. <https://doi.org/10.1016/j.rse.2015.10.032>
- Sarzynski, T., Giam, X., & Carrasco, L. (2020). Combining Radar and Optical Imagery to Map Oil Palm Plantations in Sumatra, Indonesia, Using the Google Earth Engine. *Remote Sensing*, *12*, 1220.
- Sarzynski, T., Giam, X., Carrasco, L., & Huay Lee, J. S. (2020). Combining radar and optical imagery to map oil palm plantations in Sumatra, Indonesia, using the Google Earth Engine. *Remote Sensing*. <https://doi.org/10.3390/rs12071220>
- Senf, C., Pflugmacher, D., van der Linden, S., & Hostert, P. (2013). Mapping rubber plantations and natural forests in Xishuangbanna (Southwest China) using multi-spectral phenological metrics from modis time series. *Remote Sensing*, *5*(6), 2795–2812. <https://doi.org/10.3390/rs5062795>
- Senf, C., & Seidl, R. (2020). Mapping the forest disturbance regimes of Europe. *Nature Sustainability*. <https://doi.org/10.1038/s41893-020-00609-y>
- Seymour, F., & Harris, N. L. (2019). Reducing tropical deforestation. In *Science*. <https://doi.org/10.1126/science.aax8546>
- Shimada, M., Itoh, T., Motooka, T., Watanabe, M., Shiraishi, T., Thapa, R., & Lucas, R. (2014). New global forest/non-forest maps from ALOS PALSAR data (2007-2010). *Remote Sensing of Environment*, *155*, 13–31. <https://doi.org/10.1016/j.rse.2014.04.014>
- Singh, A. (1989). Review Article Digital change detection techniques using remotely-sensed data. *International Journal of Remote Sensing*, *10*(6), 989–1003. <https://doi.org/10.1080/01431168908903939>
- Small, D. (2011). Flattening gamma: Radiometric terrain correction for SAR imagery. *IEEE Transactions on Geoscience and Remote Sensing*. <https://doi.org/10.1109/TGRS.2011.2120616>
- Sturm, K., & Apel, U. (2006). Forest restoration through nature-oriented reforestation practices in North Eastern Vietnam. *International Forestry Review*. <https://doi.org/10.1505/ifor.8.3.350>
- Tachibana, T., Nguyen, T. M., & Otsuka, K. (2001). Agricultural intensification versus

- extensification: A case study of deforestation in the Northern-hill region of Vietnam. *Journal of Environmental Economics and Management*.  
<https://doi.org/10.1006/jeem.1998.1131>
- Tadono, T., Shimada, M., Murakami, H., & Takaku, J. (2009). Calibration of PRISM and AVNIR-2 onboard ALOS daichi. *IEEE Transactions on Geoscience and Remote Sensing*. <https://doi.org/10.1109/TGRS.2009.2025270>
- Law on Forest Protection and Development*, (2004) (testimony of The Government of Vietnam).
- The Government of Vietnam. (2014). *Vietnam's Fifth National Report to the United Nations Convention on Biological Diversity*. MONRE.  
<https://www.cbd.int/doc/world/vn/vn-nr-05-en.pdf>
- Thenkabail, P. S., Stucky, N., Griscom, B. W., Ashton, M. S., Diels, J., Van der Meer, B., & Enclona, E. (2004). Biomass estimations and carbon stock calculations in the oil palm plantations of African derived savannas using IKONOS data. *International Journal of Remote Sensing*.  
<https://doi.org/10.1080/01431160412331291279>
- thiennhien.net. (2008). *Bac Giang: Preventing deforestation in Son Dong (in Vietnamese, published on 2008-08-12)*.  
<https://www.thiennhien.net/2008/08/12/bac-giang-ngan-chan-tinh-trang-chat-pha-rung-tu-nhien-o-son-dong/>
- thiennhien.net. (2020). *How to keep forests in Central Highlands? (in Vietnamese, published on 2020-07-06)*. <https://www.thiennhien.net/2020/07/06/cach-nao-giu-duoc-rung-tay-nguyen/>
- thoibaonganhang.vn. (2015). *Deforestation become hot in Dak Nong (in Vietnamese, published on 2015-09-23)*. <https://thoibaonganhang.vn/dak-nong-nong-chuyen-pha-rung-39665.html>
- Thulstrup, A. W. (2014). Plantation livelihoods in central Vietnam: Implications for household vulnerability and community resilience. *Norsk Geografisk Tidsskrift*.  
<https://doi.org/10.1080/00291951.2013.870928>
- Thulstrup, A. W., Casse, T., & Nielsen, T. T. (2013). The push for plantations: Drivers, rationales and social vulnerability in Quang Nam Province, Vietnam. *Environmental Science and Engineering (Subseries: Environmental Science)*.  
[https://doi.org/10.1007/978-3-642-35804-3\\_4](https://doi.org/10.1007/978-3-642-35804-3_4)
- Torbick, N., Ledoux, L., Salas, W., & Zhao, M. (2016). Regional mapping of plantation extent using multisensor imagery. *Remote Sensing*.  
<https://doi.org/10.3390/rs8030236>
- Truong, N. C. Q., Nguyen, H. Q., & Kondoh, A. (2018). Land use and land cover

- changes and their effect on the flow regime in the upstream Dong Nai River Basin, Vietnam. *Water (Switzerland)*. <https://doi.org/10.3390/w10091206>
- Truong, V. T., Hoang, T. T., Cao, D. P., Hayashi, M., Tadono, T., & Nasahara, K. N. (2019). JAXA annual forest cover maps for Vietnam during 2015-2018 Using ALOS-2/PALSAR-2 and auxiliary data. *Remote Sensing*, *11*(20). <https://doi.org/10.3390/rs11202412>
- Tucker, C. J. (1979). Red and photographic infrared linear combinations for monitoring vegetation. *Remote Sensing of Environment*. [https://doi.org/10.1016/0034-4257\(79\)90013-0](https://doi.org/10.1016/0034-4257(79)90013-0)
- tuoitre.vn. (2010). *Deforestation for farming (in Vietnamese, published on 2010-07-06)*. <https://tuoitre.vn/pha-rung-lam-trang-trai-388535.htm>
- USGS/NASA. (2020). *Landsat Missions*. <https://www.usgs.gov/land-resources/nli/landsat>
- USGS. (2019). Product Guide: Landsat 8 Surface Reflectance Code (Lasrc) Product. In *USGS*. USGS.
- USGS. (2020a). *Landsat 4-7 Collection 1 (C1) Surface Reflectance (LEDAPS) Product Guide (LSDS-1370 Version 3.0)* (Vol. 1, Issue August).
- USGS. (2020b). *What are the band designations for the Landsat satellites?* [https://www.usgs.gov/faqs/what-are-band-designations-landsat-satellites?qt-news\\_science\\_products=0#qt-news\\_science\\_products](https://www.usgs.gov/faqs/what-are-band-designations-landsat-satellites?qt-news_science_products=0#qt-news_science_products)
- Van Khuc, Q., Le, T. A. T., Nguyen, T. H., Nong, D., Tran, B. Q., Meyfroidt, P., Tran, T., Duong, P. B., Nguyen, T. T., Tran, T., Pham, L., Leu, S., Phuong Thao, N. T., Huu-Dung, N., Dao, T. K., Hong, N. Van, Minh Nguyet, B. T., Nguyen, H. S., & Paschke, M. W. (2020). Forest cover change, households' livelihoods, trade-offs, and constraints associated with plantation forests in poor upland-rural landscapes: Evidence from north central Vietnam. *Forests*, *11*(5). <https://doi.org/10.3390/F11050548>
- Van, T. T., Wilson, N., Thanh-Tung, H., Quisthoudt, K., Quang-Minh, V., Xuan-Tuan, L., Dahdouh-Guebas, F., & Koedam, N. (2015). Changes in mangrove vegetation area and character in a war and land use change affected region of Vietnam (Mui Ca Mau) over six decades. *Acta Oecologica*. <https://doi.org/10.1016/j.actao.2014.11.007>
- Vermote, E., Justice, C., & Csiszar, I. (2014). Early evaluation of the VIIRS calibration, cloud mask and surface reflectance Earth data records. *Remote Sensing of Environment*. <https://doi.org/10.1016/j.rse.2014.03.028>
- VNFOREST. (2020a). *Annual forest dynamics data of Vietnam (in Vietnamese)*. <http://www.kiemlam.org.vn/Desktop.aspx/List/So-lieu-dien-bien-rung-hang-nam/>

- VNFOREST. (2020b). *Forestry Data Sharing System*. <http://maps.vnforest.gov.vn/>
- WorldPop. (2018a). *Distance to OSM major roads 2016*.  
<https://www.worldpop.org/doi/10.5258/SOTON/WP00644>
- WorldPop. (2018b). *DMSP-OLS night-time lights (2000-2011)*.  
<https://www.worldpop.org/doi/10.5258/SOTON/WP00644>
- Xiao, C., Li, P., & Feng, Z. (2019). Monitoring annual dynamics of mature rubber plantations in Xishuangbanna during 1987-2018 using Landsat time series data: A multiple normalization approach. *International Journal of Applied Earth Observation and Geoinformation*. <https://doi.org/10.1016/j.jag.2018.12.006>
- Xiao, X., Boles, S., Frohling, S., Salas, W., Moore, I., Li, C., He, L., & Zhao, R. (2002). Landscape-scale characterization of cropland in China using Vegetation and Landsat TM images. *International Journal of Remote Sensing*.  
<https://doi.org/10.1080/01431160110106069>
- Xu, H. (2008). A new index for delineating built-up land features in satellite imagery. *International Journal of Remote Sensing*.  
<https://doi.org/10.1080/01431160802039957>
- Ziegler, A. D., Giambelluca, T. W., Tran, L. T., Vana, T. T., Nullet, M. A., Fox, J., Vien, T. D., Pinthong, J., Maxwell, J. F., & Evett, S. (2004). Hydrological consequences of landscape fragmentation in mountainous northern Vietnam: Evidence of accelerated overland flow generation. *Journal of Hydrology*.  
<https://doi.org/10.1016/j.jhydrol.2003.09.027>
- Zweig, M. H., & Campbell, G. (1993). Receiver-operating characteristic (ROC) plots: A fundamental evaluation tool in clinical medicine. *Clinical Chemistry*, 39, 561–577.  
<https://doi.org/10.1093/clinchem/39.4.561>

## Appendices

Appendix Table A1. Error matrix of the resultant LULC map of 2016

		Reference												Total	$W_i$	UA [%]	OA [%]
		Water	Urban	Rice	Crops	Grass/ Shrub	Orchard/ Crop	Barren	EBF	CF	DF	PF	MGR				
Map	Water	141	2	0	4	0	0	3	0	0	0	0	0	150	0.032	94.0 ± 1.9	
	Urban	0	134	0	3	3	5	4	0	0	0	1	0	150	0.025	89.3 ± 2.5	
	Rice	20	3	274	2	1	0	0	0	0	0	0	0	300	0.127	91.3 ± 1.6	
	Crops	5	15	0	273	3	2	0	0	0	0	2	0	300	0.112	91.0 ± 1.7	
	Grass/Shrub	0	1	1	15	236	4	2	34	0	0	7	0	300	0.150	78.7 ± 2.4	
	Orchard/Crop mosaic	1	7	2	24	16	236	8	1	0	0	5	0	300	0.112	78.7 ± 2.4	
	Barren	0	6	0	13	18	2	111	0	0	0	0	0	150	0.043	74.0 ± 3.6	
	EBF	0	0	0	0	1	0	0	286	2	3	8	0	300	0.243	95.3 ± 1.2	
	Coniferous forest (CF)	1	1	0	2	0	0	2	19	114	1	10	0	150	0.006	76.0 ± 3.5	
	Deciduous forest (DF)	0	0	2	16	1	2	16	3	0	110	0	0	150	0.029	73.3 ± 3.6	
	Plantation forest (PF)	2	1	0	1	8	8	0	22	0	0	258	0	300	0.113	86.0 ± 2.0	
	Mangrove (MGR)	3	0	0	6	0	1	0	0	0	0	1	139	150	0.007	92.7 ± 2.1	
	Total	173	170	279	359	287	260	146	365	116	114	292	139	2700	1		
	PA [%]	72.1 ± 5.3	64.0 ± 6.3	98.6 ± 1.9	79.5 ± 2.7	87.3 ± 3.2	92.1 ± 3.3	79.0 ± 5.4	89.6 ± 1.7	73.8 ± 18.8	89.6 ± 7.4	88.0 ± 3.3	100.0 ± 2.3			85.6 ± 0.7	

PA = Producer's Accuracy, UA = User's Accuracy, OA = Overall Accuracy,  $W_i$  = area weight

EBF = Evergreen broadleaf forest

Appendix Table A2. Error matrix of the of the resultant LULC map in 2016 in terms of Forest/Non-Forest

		Reference			PA [%]
		Non-Forest	Forest	Total	
Map	Non-Forest	1749	51	1800	97.2
	Forest	64	836	900	92.9
	Total	1813	887	2700	
	UA [%]	96.5	94.3		OA = 95.7%

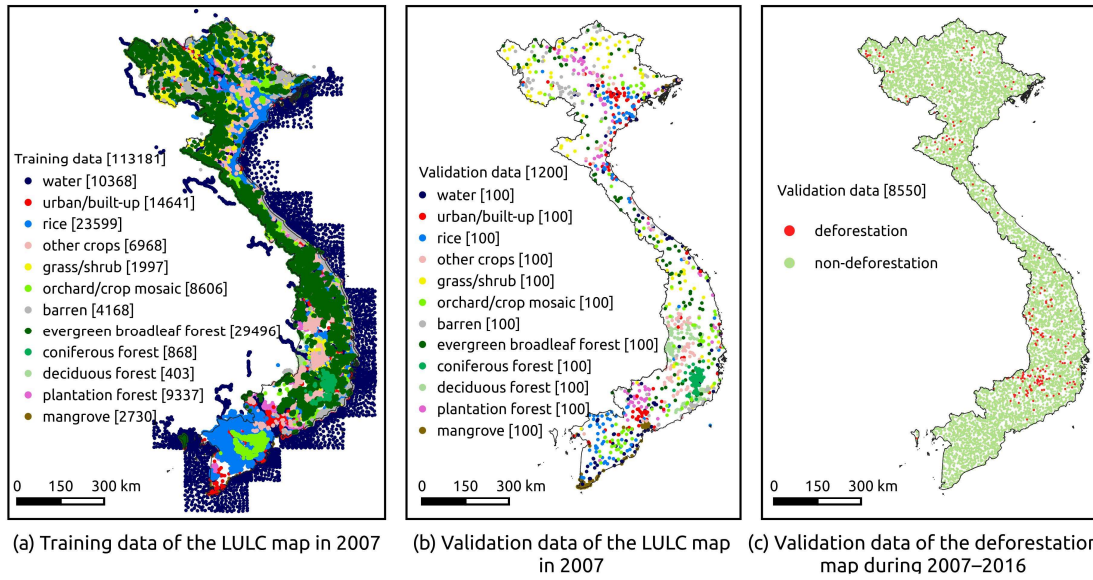


Appendix Table A3. Error matrix of deforestation map in Vietnam between 2007–2016 with fractional cover difference threshold of 0.70

		Reference			$W_i$	UA [%]
		DF	Non-DF	Total		
Map	DF	173	77	250	0.024	69.2 ± 2.9
	Non-DF	29	8271	8300	0.976	99.7 ± 0.1
	Total	202	8348	8550		
	PA [%]	85.6 ± 2.6	99.1 ± 0.1			

DF = Deforestation; Non-DF = Non-deforestation

PA = Producer's Accuracy, UA = User's Accuracy, OA = Overall Accuracy,  $W_i$  = area weight

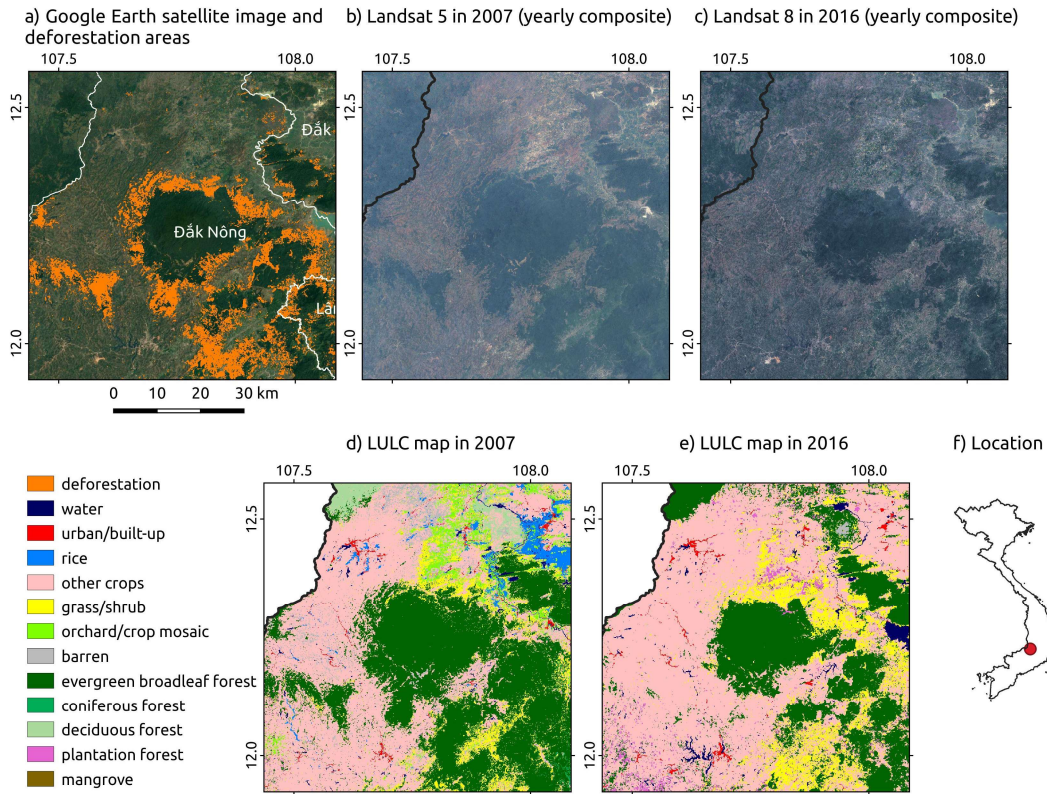


Appendix Figure A1. (a) Distribution and quantity of training data of the LULC map in 2007; (b) Distribution and quantity of validation data of the LULC map in 2007; (c) Distribution and quantity of validation data of the deforestation map between 2007–2016. The number of data points were described in square brackets.

Appendix Table A4. Error matrix of the resultant LULC map 2007

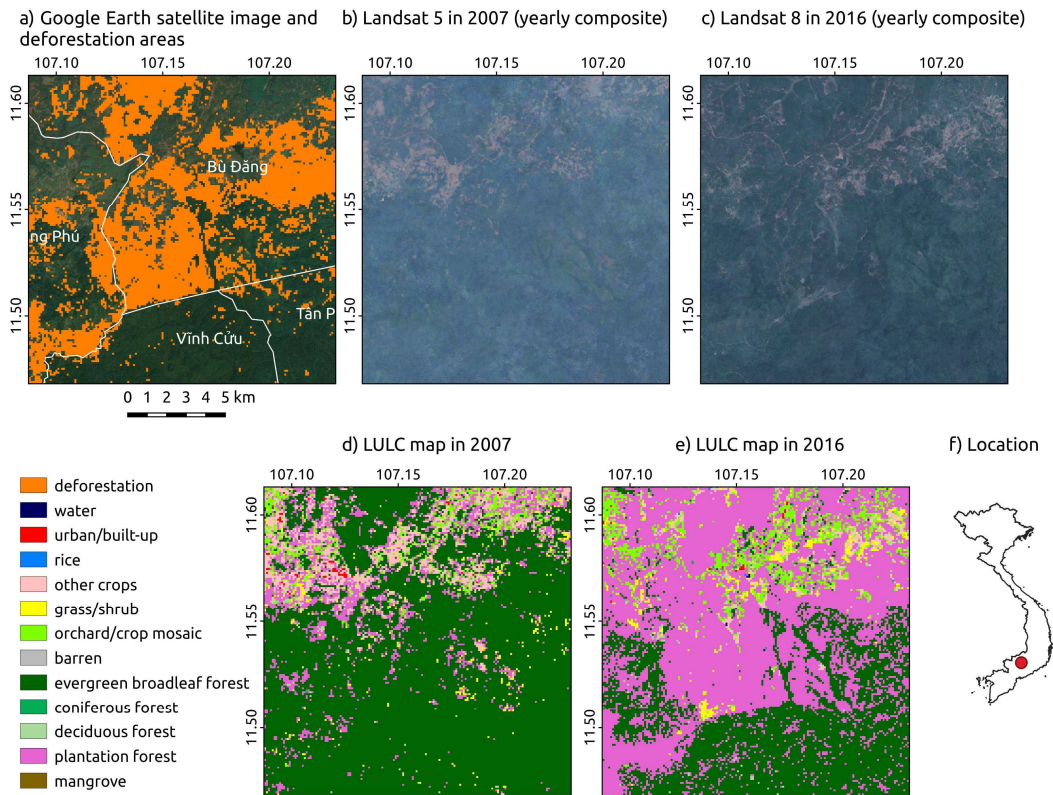
		Reference												Total	$W_i$	UA [%]	OA [%]
		Water	Urban	Rice	Crops	Grass/ Shrub	Orchard/ Crop	Barren	EBF	CF	DF	PF	MGR				
Map	Water	93	2	2	0	0	0	3	0	0	0	0	0	100	0.032	93.0 ± 2.6	
	Urban	0	91	0	2	2	2	3	0	0	0	0	0	100	0.019	91.0 ± 2.9	
	Rice	3	1	92	1	0	2	0	0	0	0	0	1	100	0.130	92.0 ± 2.7	
	Crops	0	2	2	91	0	2	1	0	0	0	2	0	100	0.104	91.0 ± 2.9	
	Grass/Shrub	0	0	0	2	76	0	0	19	0	0	3	0	100	0.156	76.0 ± 4.3	
	Orchard/Crop mosaic	0	0	0	8	5	78	5	0	0	0	4	0	100	0.127	78.0 ± 4.2	
	Barren	0	0	0	9	13	1	77	0	0	0	0	0	100	0.049	77.0 ± 4.2	
	EBF	0	0	0	0	6	0	0	94	0	0	0	0	100	0.262	94.0 ± 2.4	
	Coniferous forest (CF)	0	0	0	1	4	1	0	10	75	3	6	0	100	0.006	75.0 ± 4.4	
	Deciduous forest (DF)	0	0	0	12	8	0	0	7	0	73	0	0	100	0.029	73.0 ± 4.5	
	Plantation forest (PF)	0	1	0	0	2	1	0	9	0	0	87	0	100	0.079	87.0 ± 3.4	
	Mangrove (MGR)	3	1	0	0	0	2	1	0	0	0	0	93	100	0.007	93.0 ± 2.6	
	Total	99	98	96	126	116	89	90	139	75	76	102	94	1200	1		
	PA [%]	87.8 ± 5.8	78.1 ± 7.6	97.8 ± 1.2	80.6 ± 3.2	78.3 ± 3.8	93.8 ± 2.3	80.6 ± 5.3	86.2 ± 2.0	100.0 ± 0.0	99.1 ± 0.5	85.0 ± 4.1	83.9 ± 13.5			85.0 ± 1.2	

PA = Producer's Accuracy, UA = User's Accuracy, OA = Overall Accuracy,  $W_i$  = area weight  
 EBF = Evergreen broadleaf forest



Appendix Figure A2. Deforestation between 2007–2016 identified by this study’s land use/land cover (LULC) maps in Dak Nong province, Central Highlands, Vietnam. (a) Google Earth satellite and the deforestation areas; (b) Landsat 5 image in 2007; (c) Landsat 8 image in 2016; (d) The LULC map in 2007; (e) The LULC map in 2016; (f) The location of Dak Nong province.

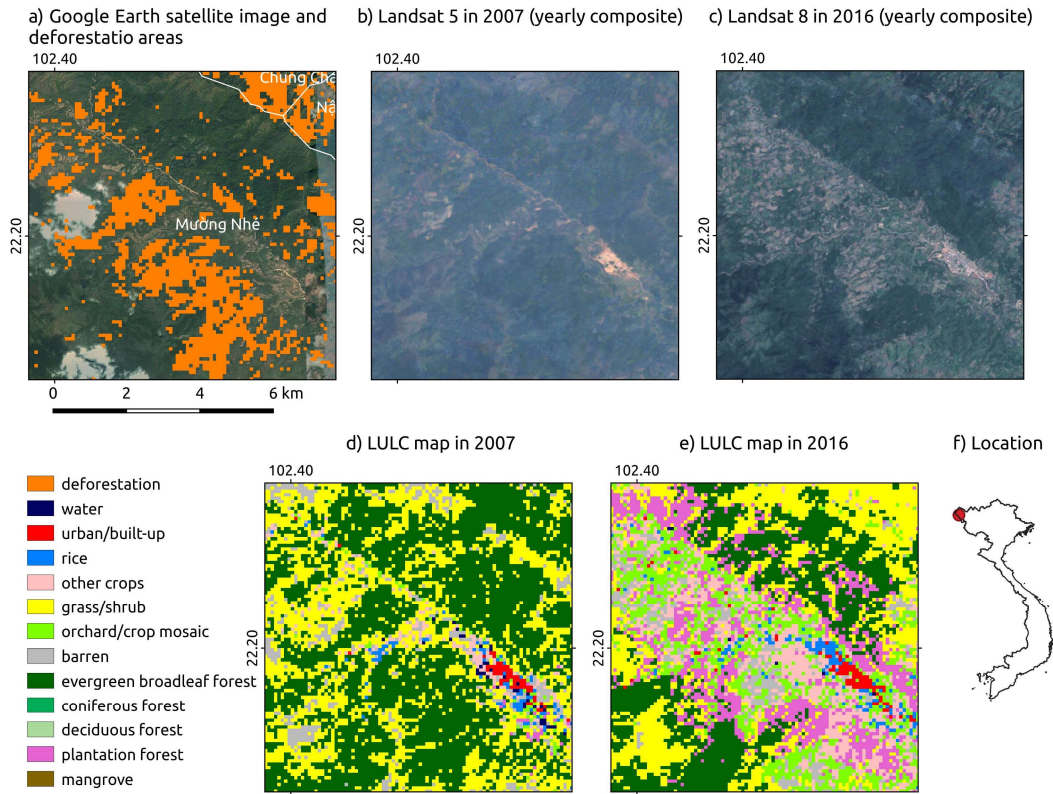
Thoibaonghang.vn (2015) reported that the natural forest area of Dak Nong province, Central Highlands decreased by 140,000 ha between 2005–2015 (from 360,000 ha to 220,000 ha). The decrease was mainly due to the conversion from natural forests to perennial plantations such as coffee, pepper, and orchards. The information in the news was relatively consistent with the result of this study’s maps which indicated approximately 85,000 ha of forest loss by the conversion to croplands between 2007–2016 (Appendix Figure A2a,d,e).



Appendix Figure A3. Deforestation between 2007–2016 identified by this study’s land use/land cover (LULC) maps in Bu Dang district, Binh Phuoc province, Vietnam. (a) Google Earth satellite and the deforestation areas; (b) Landsat 5 image in 2007; (c) Landsat 8 image in 2016; (d) The LULC map in 2007; (e) The LULC map in 2016; (f) The location of Bu Dang district, Binh Phuoc province, Vietnam.

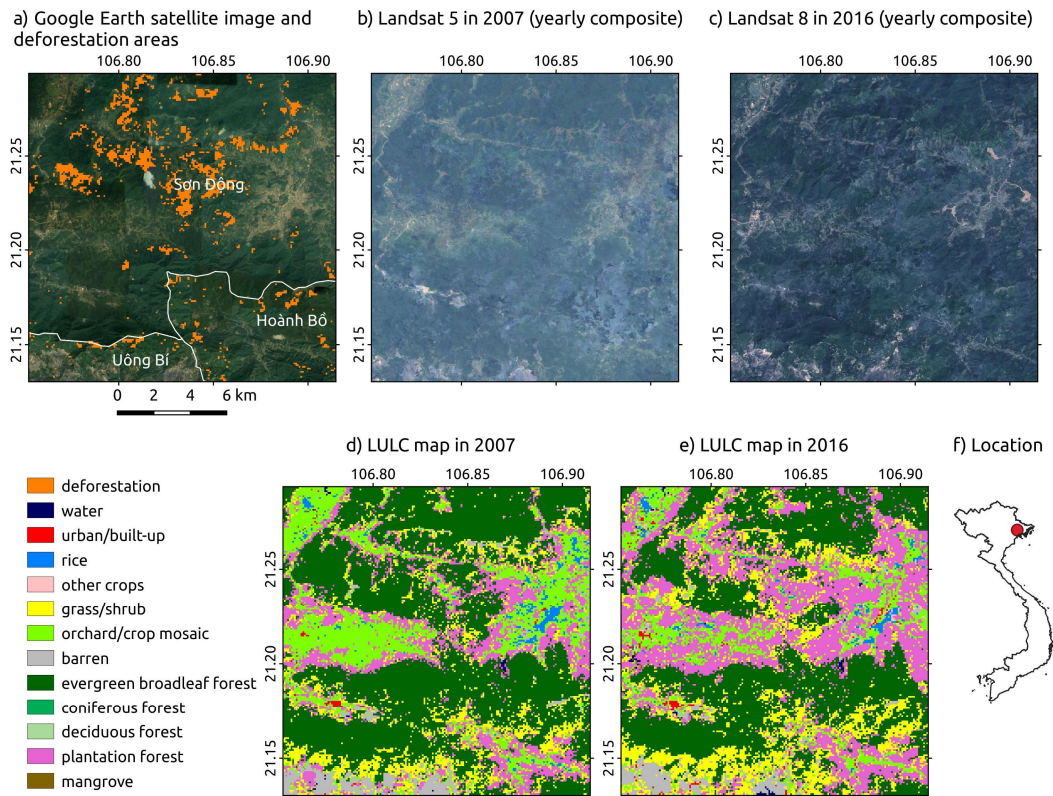
TuoiTre.vn (2010) reported a conversion from natural forests to farm-based rubber plantations in Bu Dang district, Binh Phuoc province circa 2010. The legal loophole which allowed poor-quality natural forests to be converted to rubber plantations was considered an indirect cause of deforestation in this area. This conversion from natural forests to plantation forests was well presented in this study’s maps (Appendix Figures A3d and A3e).





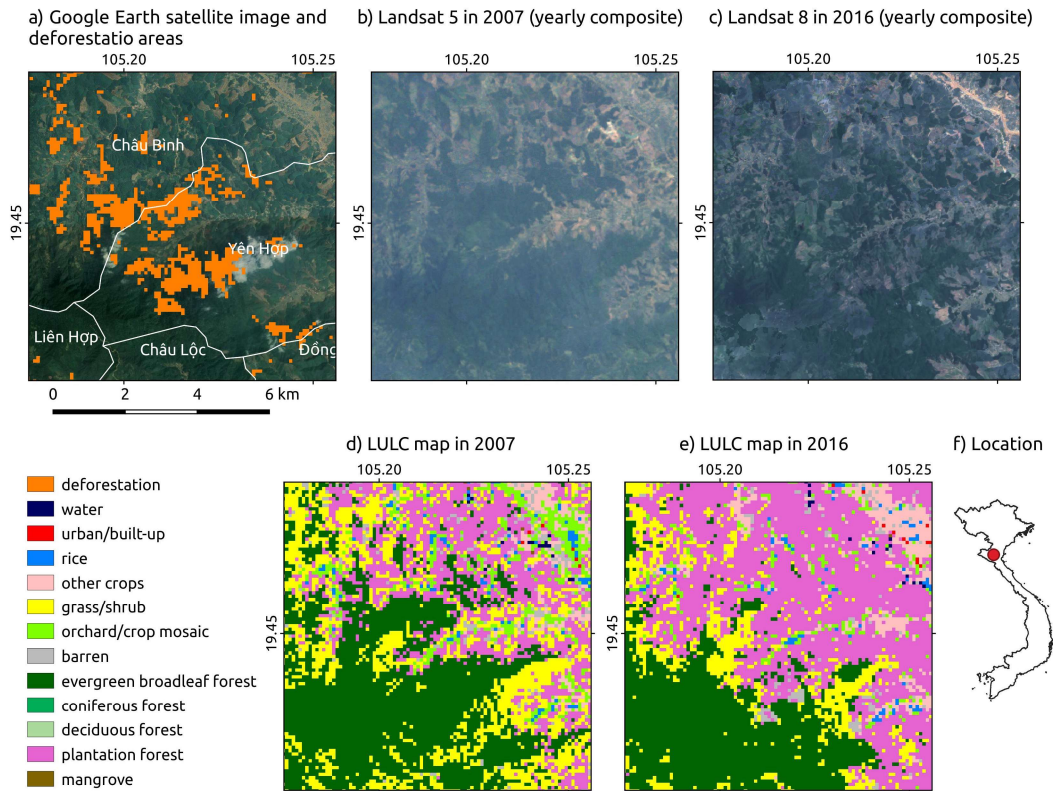
Appendix Figure A4. Deforestation between 2007–2016 identified by this study’s land use/land cover (LULC) maps in Muong Nhe district, Dien Bien province, Vietnam. (a) Google Earth satellite and the deforestation areas; (b) Landsat 5 image in 2007; (c) Landsat 8 image in 2016; (d) The LULC map in 2007; (e) The LULC map in 2016; (f) The location of Muong Nhe district, Dien Bien province, Vietnam.

Baotainguyenmoitruong.vn (2016) informed that Muong Nhe district in Dien Bien province was considered a small-scale deforestation hot spot. The deforestation situation was mainly attributed to the demand for cultivation land of immigrants from other provinces. Between 2011–2016, there were approximately 2000 immigrants settled down in Muong Nhe district. The information on deforestation in Muong Nhe was in agreement with the results of this study’s maps which showed the conversion from natural forests to croplands, orchards, and plantation forests (Appendix Figure A4d,e).



Appendix Figure A5. Deforestation between 2007–2016 identified by this study’s land use/land cover (LULC) maps in Son Dong district, Bac Giang province, Vietnam. (a) Google Earth satellite and the deforestation areas; (b) Landsat 5 image in 2007; (c) Landsat 8 image in 2016; (d) The LULC map in 2007; (e) The LULC map in 2016; (f) The location of Son Dong district, Bac Giang province, Vietnam.

Thiennhien.net (2008) informed a conversion from natural forests to acacia plantation by local residents circa 2008 in Son Dong district, Bac Giang province. The cause of this change was due to the high economic value of acacia plantation which overweighed the benefit from natural forests which had been allocated to each local household. The conversion was continued until 2017, reported by kinhtenongthon.vn (2017). The conversion was also reflected in this study’s maps by the change from natural forests to plantation forests in Appendix Figure A5d,e.



Appendix Figure A6. Deforestation between 2007–2016 identified by this study’s land use/land cover (LULC) maps in Yen Hop commune, Quy Hop district, Nghe An province, Vietnam. (a) Google Earth satellite and the deforestation areas; (b) Landsat 5 image in 2007; (c) Landsat 8 image in 2016; (d) The LULC map in 2007; (e) The LULC map in 2016; (f) The location of Yen Hop commune, Quy Hop district, Nghe An province, Vietnam.

Nongnghiep.vn (2015) informed the deforestation case in Yen Hop commune, Quy Hop district, Nghe An province circa 2015 which was due to natural forest logging and then growing acacia plantation by local people. The underlying cause of this change was also due to the high benefit of acacia plantation. This deforestation case was indicated in this study’s maps by the conversion from natural forests to plantation forests in Appendix Figure A6d,e.



Appendix List A1. PALSAR-2/ScanSAR image list

- |                        |                         |                         |
|------------------------|-------------------------|-------------------------|
| 1. N09E104_W02DC042DR  | 53. N11E104_W02DC053DR  | 105. N12E106_W02DC062DR |
| 2. N09E104_W02DC045DR  | 54. N11E104_W02DC056DR  | 106. N12E107_W02DC042DR |
| 3. N09E104_W02DC048DR  | 55. N11E104_W02DC059DR  | 107. N12E107_W02DC045DR |
| 4. N09E104_W02DC051DR  | 56. N11E104_W02DC062DR  | 108. N12E107_W02DC048DR |
| 5. N09E104_W02DC053DR  | 57. N11E105_W02DC042DR  | 109. N12E107_W02DC051DR |
| 6. N09E104_W02DC056DR  | 58. N11E105_W02DC045DR  | 110. N12E107_W02DC053DR |
| 7. N09E104_W02DC059DR  | 59. N11E105_W02DC048DR  | 111. N12E107_W02DC056DR |
| 8. N09E104_W02DC062DR  | 60. N11E105_W02DC051DR  | 112. N12E107_W02DC059DR |
| 9. N09E105_W02DC042DR  | 61. N11E105_W02DC053DR  | 113. N12E107_W02DC062DR |
| 10. N09E105_W02DC045DR | 62. N11E105_W02DC056DR  | 114. N12E108_W02DC039DR |
| 11. N09E105_W02DC048DR | 63. N11E105_W02DC059DR  | 115. N12E108_W02DC042DR |
| 12. N09E105_W02DC051DR | 64. N11E105_W02DC062DR  | 116. N12E108_W02DC045DR |
| 13. N09E105_W02DC053DR | 65. N11E106_W02DC042DR  | 117. N12E108_W02DC048DR |
| 14. N09E105_W02DC056DR | 66. N11E106_W02DC045DR  | 118. N12E108_W02DC051DR |
| 15. N09E105_W02DC059DR | 67. N11E106_W02DC048DR  | 119. N12E108_W02DC053DR |
| 16. N09E105_W02DC062DR | 68. N11E106_W02DC051DR  | 120. N12E108_W02DC056DR |
| 17. N10E104_W02DC042DR | 69. N11E106_W02DC053DR  | 121. N12E108_W02DC059DR |
| 18. N10E104_W02DC045DR | 70. N11E106_W02DC056DR  | 122. N12E108_W02DC062DR |
| 19. N10E104_W02DC048DR | 71. N11E106_W02DC059DR  | 123. N12E109_W02DC039DR |
| 20. N10E104_W02DC051DR | 72. N11E106_W02DC062DR  | 124. N12E109_W02DC042DR |
| 21. N10E104_W02DC053DR | 73. N11E107_W02DC042DR  | 125. N12E109_W02DC045DR |
| 22. N10E104_W02DC056DR | 74. N11E107_W02DC045DR  | 126. N12E109_W02DC048DR |
| 23. N10E104_W02DC059DR | 75. N11E107_W02DC048DR  | 127. N12E109_W02DC051DR |
| 24. N10E104_W02DC062DR | 76. N11E107_W02DC051DR  | 128. N12E109_W02DC053DR |
| 25. N10E105_W02DC042DR | 77. N11E107_W02DC053DR  | 129. N12E109_W02DC056DR |
| 26. N10E105_W02DC045DR | 78. N11E107_W02DC056DR  | 130. N12E109_W02DC059DR |
| 27. N10E105_W02DC048DR | 79. N11E107_W02DC059DR  | 131. N12E109_W02DC062DR |
| 28. N10E105_W02DC051DR | 80. N11E107_W02DC062DR  | 132. N13E106_W02DC042DR |
| 29. N10E105_W02DC053DR | 81. N11E108_W02DC039DR  | 133. N13E106_W02DC045DR |
| 30. N10E105_W02DC056DR | 82. N11E108_W02DC042DR  | 134. N13E106_W02DC048DR |
| 31. N10E105_W02DC059DR | 83. N11E108_W02DC045DR  | 135. N13E106_W02DC051DR |
| 32. N10E105_W02DC062DR | 84. N11E108_W02DC048DR  | 136. N13E106_W02DC053DR |
| 33. N10E106_W02DC042DR | 85. N11E108_W02DC051DR  | 137. N13E106_W02DC056DR |
| 34. N10E106_W02DC045DR | 86. N11E108_W02DC053DR  | 138. N13E106_W02DC059DR |
| 35. N10E106_W02DC048DR | 87. N11E108_W02DC056DR  | 139. N13E106_W02DC062DR |
| 36. N10E106_W02DC051DR | 88. N11E108_W02DC059DR  | 140. N13E107_W02DC042DR |
| 37. N10E106_W02DC053DR | 89. N11E108_W02DC062DR  | 141. N13E107_W02DC045DR |
| 38. N10E106_W02DC056DR | 90. N12E105_W02DC042DR  | 142. N13E107_W02DC048DR |
| 39. N10E106_W02DC059DR | 91. N12E105_W02DC045DR  | 143. N13E107_W02DC051DR |
| 40. N10E106_W02DC062DR | 92. N12E105_W02DC048DR  | 144. N13E107_W02DC053DR |
| 41. N11E103_W02DC042DR | 93. N12E105_W02DC051DR  | 145. N13E107_W02DC056DR |
| 42. N11E103_W02DC045DR | 94. N12E105_W02DC053DR  | 146. N13E107_W02DC059DR |
| 43. N11E103_W02DC048DR | 95. N12E105_W02DC056DR  | 147. N13E107_W02DC062DR |
| 44. N11E103_W02DC051DR | 96. N12E105_W02DC059DR  | 148. N13E108_W02DC042DR |
| 45. N11E103_W02DC053DR | 97. N12E105_W02DC062DR  | 149. N13E108_W02DC045DR |
| 46. N11E103_W02DC056DR | 98. N12E106_W02DC042DR  | 150. N13E108_W02DC048DR |
| 47. N11E103_W02DC059DR | 99. N12E106_W02DC045DR  | 151. N13E108_W02DC051DR |
| 48. N11E103_W02DC062DR | 100. N12E106_W02DC048DR | 152. N13E108_W02DC053DR |
| 49. N11E104_W02DC042DR | 101. N12E106_W02DC051DR | 153. N13E108_W02DC056DR |
| 50. N11E104_W02DC045DR | 102. N12E106_W02DC053DR | 154. N13E108_W02DC059DR |
| 51. N11E104_W02DC048DR | 103. N12E106_W02DC056DR | 155. N13E108_W02DC062DR |
| 52. N11E104_W02DC051DR | 104. N12E106_W02DC059DR | 156. N13E109_W02DC039DR |

157. N13E109\_W02DC042DR 212. N15E109\_W02DC056DR 267. N18E106\_W02DC053DR  
158. N13E109\_W02DC045DR 213. N15E109\_W02DC059DR 268. N18E106\_W02DC056DR  
159. N13E109\_W02DC048DR 214. N15E109\_W02DC062DR 269. N18E106\_W02DC059DR  
160. N13E109\_W02DC051DR 215. N16E107\_W02DC042DR 270. N18E106\_W02DC062DR  
161. N13E109\_W02DC053DR 216. N16E107\_W02DC045DR 271. N18E107\_W02DC042DR  
162. N13E109\_W02DC056DR 217. N16E107\_W02DC048DR 272. N18E107\_W02DC045DR  
163. N13E109\_W02DC059DR 218. N16E107\_W02DC051DR 273. N18E107\_W02DC048DR  
164. N13E109\_W02DC062DR 219. N16E107\_W02DC053DR 274. N18E107\_W02DC051DR  
165. N14E107\_W02DC042DR 220. N16E107\_W02DC056DR 275. N18E107\_W02DC053DR  
166. N14E107\_W02DC045DR 221. N16E107\_W02DC059DR 276. N18E107\_W02DC056DR  
167. N14E107\_W02DC048DR 222. N16E107\_W02DC062DR 277. N18E107\_W02DC059DR  
168. N14E107\_W02DC051DR 223. N16E108\_W02DC042DR 278. N18E107\_W02DC062DR  
169. N14E107\_W02DC053DR 224. N16E108\_W02DC045DR 279. N19E104\_W02DC042DR  
170. N14E107\_W02DC056DR 225. N16E108\_W02DC048DR 280. N19E104\_W02DC045DR  
171. N14E107\_W02DC059DR 226. N16E108\_W02DC051DR 281. N19E104\_W02DC048DR  
172. N14E107\_W02DC062DR 227. N16E108\_W02DC053DR 282. N19E104\_W02DC051DR  
173. N14E108\_W02DC042DR 228. N16E108\_W02DC056DR 283. N19E104\_W02DC053DR  
174. N14E108\_W02DC045DR 229. N16E108\_W02DC059DR 284. N19E104\_W02DC056DR  
175. N14E108\_W02DC048DR 230. N16E108\_W02DC062DR 285. N19E104\_W02DC059DR  
176. N14E108\_W02DC051DR 231. N17E106\_W02DC042DR 286. N19E104\_W02DC062DR  
177. N14E108\_W02DC053DR 232. N17E106\_W02DC045DR 287. N19E105\_W02DC042DR  
178. N14E108\_W02DC056DR 233. N17E106\_W02DC048DR 288. N19E105\_W02DC045DR  
179. N14E108\_W02DC059DR 234. N17E106\_W02DC051DR 289. N19E105\_W02DC048DR  
180. N14E108\_W02DC062DR 235. N17E106\_W02DC053DR 290. N19E105\_W02DC051DR  
181. N14E109\_W02DC039DR 236. N17E106\_W02DC056DR 291. N19E105\_W02DC053DR  
182. N14E109\_W02DC042DR 237. N17E106\_W02DC059DR 292. N19E105\_W02DC056DR  
183. N14E109\_W02DC045DR 238. N17E106\_W02DC062DR 293. N19E105\_W02DC059DR  
184. N14E109\_W02DC048DR 239. N17E107\_W02DC042DR 294. N19E105\_W02DC062DR  
185. N14E109\_W02DC051DR 240. N17E107\_W02DC045DR 295. N19E106\_W02DC042DR  
186. N14E109\_W02DC053DR 241. N17E107\_W02DC048DR 296. N19E106\_W02DC045DR  
187. N14E109\_W02DC056DR 242. N17E107\_W02DC051DR 297. N19E106\_W02DC048DR  
188. N14E109\_W02DC059DR 243. N17E107\_W02DC053DR 298. N19E106\_W02DC051DR  
189. N14E109\_W02DC062DR 244. N17E107\_W02DC056DR 299. N19E106\_W02DC053DR  
190. N15E107\_W02DC042DR 245. N17E107\_W02DC059DR 300. N19E106\_W02DC056DR  
191. N15E107\_W02DC045DR 246. N17E107\_W02DC062DR 301. N19E106\_W02DC059DR  
192. N15E107\_W02DC048DR 247. N17E108\_W02DC042DR 302. N19E106\_W02DC062DR  
193. N15E107\_W02DC051DR 248. N17E108\_W02DC045DR 303. N20E103\_W02DC042DR  
194. N15E107\_W02DC053DR 249. N17E108\_W02DC048DR 304. N20E103\_W02DC045DR  
195. N15E107\_W02DC056DR 250. N17E108\_W02DC051DR 305. N20E103\_W02DC048DR  
196. N15E107\_W02DC059DR 251. N17E108\_W02DC053DR 306. N20E103\_W02DC051DR  
197. N15E107\_W02DC062DR 252. N17E108\_W02DC056DR 307. N20E103\_W02DC053DR  
198. N15E108\_W02DC042DR 253. N17E108\_W02DC059DR 308. N20E103\_W02DC056DR  
199. N15E108\_W02DC045DR 254. N17E108\_W02DC062DR 309. N20E103\_W02DC059DR  
200. N15E108\_W02DC048DR 255. N18E105\_W02DC042DR 310. N20E103\_W02DC062DR  
201. N15E108\_W02DC051DR 256. N18E105\_W02DC045DR 311. N20E104\_W02DC042DR  
202. N15E108\_W02DC053DR 257. N18E105\_W02DC048DR 312. N20E104\_W02DC045DR  
203. N15E108\_W02DC056DR 258. N18E105\_W02DC051DR 313. N20E104\_W02DC048DR  
204. N15E108\_W02DC059DR 259. N18E105\_W02DC053DR 314. N20E104\_W02DC051DR  
205. N15E108\_W02DC062DR 260. N18E105\_W02DC056DR 315. N20E104\_W02DC053DR  
206. N15E109\_W02DC039DR 261. N18E105\_W02DC059DR 316. N20E104\_W02DC056DR  
207. N15E109\_W02DC042DR 262. N18E105\_W02DC062DR 317. N20E104\_W02DC059DR  
208. N15E109\_W02DC045DR 263. N18E106\_W02DC042DR 318. N20E104\_W02DC062DR  
209. N15E109\_W02DC048DR 264. N18E106\_W02DC045DR 319. N20E105\_W02DC042DR  
210. N15E109\_W02DC051DR 265. N18E106\_W02DC048DR 320. N20E105\_W02DC045DR  
211. N15E109\_W02DC053DR 266. N18E106\_W02DC051DR 321. N20E105\_W02DC048DR

322. N20E105\_W02DC051DR 372. N22E102\_W02DC048DR 422. N23E102\_W02DC053DR  
323. N20E105\_W02DC053DR 373. N22E102\_W02DC051DR 423. N23E102\_W02DC056DR  
324. N20E105\_W02DC056DR 374. N22E102\_W02DC053DR 424. N23E102\_W02DC059DR  
325. N20E105\_W02DC059DR 375. N22E102\_W02DC056DR 425. N23E102\_W02DC062DR  
326. N20E105\_W02DC062DR 376. N22E102\_W02DC059DR 426. N23E103\_W02DC042DR  
327. N20E106\_W02DC042DR 377. N22E102\_W02DC062DR 427. N23E103\_W02DC045DR  
328. N20E106\_W02DC045DR 378. N22E103\_W02DC042DR 428. N23E103\_W02DC048DR  
329. N20E106\_W02DC048DR 379. N22E103\_W02DC045DR 429. N23E103\_W02DC051DR  
330. N20E106\_W02DC051DR 380. N22E103\_W02DC048DR 430. N23E103\_W02DC053DR  
331. N20E106\_W02DC053DR 381. N22E103\_W02DC051DR 431. N23E103\_W02DC056DR  
332. N20E106\_W02DC056DR 382. N22E103\_W02DC053DR 432. N23E103\_W02DC059DR  
333. N20E106\_W02DC059DR 383. N22E103\_W02DC056DR 433. N23E103\_W02DC062DR  
334. N20E106\_W02DC062DR 384. N22E103\_W02DC059DR 434. N23E104\_W02DC042DR  
335. N21E103\_W02DC042DR 385. N22E103\_W02DC062DR 435. N23E104\_W02DC045DR  
336. N21E103\_W02DC045DR 386. N22E104\_W02DC042DR 436. N23E104\_W02DC048DR  
337. N21E103\_W02DC048DR 387. N22E104\_W02DC045DR 437. N23E104\_W02DC051DR  
338. N21E103\_W02DC051DR 388. N22E104\_W02DC048DR 438. N23E104\_W02DC053DR  
339. N21E103\_W02DC053DR 389. N22E104\_W02DC051DR 439. N23E104\_W02DC056DR  
340. N21E103\_W02DC056DR 390. N22E104\_W02DC053DR 440. N23E104\_W02DC059DR  
341. N21E103\_W02DC059DR 391. N22E104\_W02DC056DR 441. N23E104\_W02DC062DR  
342. N21E103\_W02DC062DR 392. N22E104\_W02DC059DR 442. N23E105\_W02DC042DR  
343. N21E104\_W02DC042DR 393. N22E104\_W02DC062DR 443. N23E105\_W02DC045DR  
344. N21E104\_W02DC045DR 394. N22E105\_W02DC042DR 444. N23E105\_W02DC048DR  
345. N21E104\_W02DC048DR 395. N22E105\_W02DC045DR 445. N23E105\_W02DC051DR  
346. N21E104\_W02DC051DR 396. N22E105\_W02DC048DR 446. N23E105\_W02DC053DR  
347. N21E104\_W02DC053DR 397. N22E105\_W02DC051DR 447. N23E105\_W02DC056DR  
348. N21E104\_W02DC056DR 398. N22E105\_W02DC053DR 448. N23E105\_W02DC059DR  
349. N21E104\_W02DC059DR 399. N22E105\_W02DC056DR 449. N23E106\_W02DC042DR  
350. N21E104\_W02DC062DR 400. N22E105\_W02DC059DR 450. N23E106\_W02DC045DR  
351. N21E105\_W02DC042DR 401. N22E106\_W02DC042DR 451. N23E106\_W02DC048DR  
352. N21E105\_W02DC045DR 402. N22E106\_W02DC045DR 452. N23E106\_W02DC051DR  
353. N21E105\_W02DC048DR 403. N22E106\_W02DC048DR 453. N23E106\_W02DC053DR  
354. N21E105\_W02DC051DR 404. N22E106\_W02DC051DR 454. N23E106\_W02DC059DR  
355. N21E105\_W02DC053DR 405. N22E106\_W02DC053DR 455. N24E104\_W02DC042DR  
356. N21E105\_W02DC056DR 406. N22E106\_W02DC059DR 456. N24E104\_W02DC045DR  
357. N21E105\_W02DC059DR 407. N22E107\_W02DC042DR 457. N24E104\_W02DC048DR  
358. N21E106\_W02DC042DR 408. N22E107\_W02DC045DR 458. N24E104\_W02DC051DR  
359. N21E106\_W02DC045DR 409. N22E107\_W02DC048DR 459. N24E104\_W02DC053DR  
360. N21E106\_W02DC048DR 410. N22E107\_W02DC051DR 460. N24E104\_W02DC056DR  
361. N21E106\_W02DC051DR 411. N22E107\_W02DC053DR 461. N24E104\_W02DC059DR  
362. N21E106\_W02DC053DR 412. N22E107\_W02DC059DR 462. N24E104\_W02DC062DR  
363. N21E106\_W02DC059DR 413. N22E108\_W02DC042DR 463. N24E105\_W02DC042DR  
364. N21E107\_W02DC042DR 414. N22E108\_W02DC045DR 464. N24E105\_W02DC045DR  
365. N21E107\_W02DC045DR 415. N22E108\_W02DC048DR 465. N24E105\_W02DC048DR  
366. N21E107\_W02DC048DR 416. N22E108\_W02DC051DR 466. N24E105\_W02DC051DR  
367. N21E107\_W02DC051DR 417. N22E108\_W02DC059DR 467. N24E105\_W02DC053DR  
368. N21E107\_W02DC053DR 418. N23E102\_W02DC042DR 468. N24E105\_W02DC056DR  
369. N21E107\_W02DC059DR 419. N23E102\_W02DC045DR 469. N24E105\_W02DC059DR  
370. N22E102\_W02DC042DR 420. N23E102\_W02DC048DR  
371. N22E102\_W02DC045DR 421. N23E102\_W02DC051DR

Appendix List A2. ALOS/AVNIR-2 ORI image list

1. ALAV2A050483220
2. ALAV2A050773300
3. ALAV2A050773310
4. ALAV2A050773320
5. ALAV2A052523350
6. ALAV2A052523360
7. ALAV2A052523370
8. ALAV2A052523380
9. ALAV2A052523390
10. ALAV2A053983140
11. ALAV2A053983150
12. ALAV2A053983160
13. ALAV2A053983170
14. ALAV2A053983180
15. ALAV2A055003270
16. ALAV2A055003310
17. ALAV2A055003320
18. ALAV2A055003330
19. ALAV2A055003340
20. ALAV2A055003350
21. ALAV2A055003360
22. ALAV2A055003370
23. ALAV2A055003380
24. ALAV2A055003390
25. ALAV2A055003400
26. ALAV2A055003410
27. ALAV2A055003420
28. ALAV2A055733240
29. ALAV2A055733260
30. ALAV2A055733270
31. ALAV2A055733380
32. ALAV2A055733390
33. ALAV2A055733400
34. ALAV2A056173140
35. ALAV2A056173150
36. ALAV2A058943140
37. ALAV2A058943150
38. ALAV2A058943160
39. ALAV2A058943180
40. ALAV2A058943190
41. ALAV2A059963370
42. ALAV2A059963380
43. ALAV2A059963390
44. ALAV2A059963400
45. ALAV2A059963410
46. ALAV2A059963420
47. ALAV2A059963430
48. ALAV2A063173390
49. ALAV2A065943350
50. ALAV2A065943360
51. ALAV2A065943370
52. ALAV2A065943380
53. ALAV2A065943390
54. ALAV2A065943420
55. ALAV2A065943430
56. ALAV2A070903400
57. ALAV2A070903410
58. ALAV2A070903420
59. ALAV2A073383250
60. ALAV2A073383360
61. ALAV2A073383370
62. ALAV2A073383380
63. ALAV2A073383390
64. ALAV2A073383400
65. ALAV2A073383410
66. ALAV2A073383420
67. ALAV2A073383430
68. ALAV2A073823140
69. ALAV2A074113390
70. ALAV2A074113400
71. ALAV2A074843160
72. ALAV2A074843170
73. ALAV2A074843180
74. ALAV2A074843190
75. ALAV2A074843200
76. ALAV2A074843210
77. ALAV2A074843220
78. ALAV2A075133270
79. ALAV2A075133280
80. ALAV2A075133290
81. ALAV2A075133300
82. ALAV2A075133310
83. ALAV2A075133320
84. ALAV2A075133330
85. ALAV2A075133340
86. ALAV2A075133350
87. ALAV2A075573140
88. ALAV2A077323180
89. ALAV2A077323190
90. ALAV2A077323200
91. ALAV2A077613260
92. ALAV2A077613270
93. ALAV2A077613280
94. ALAV2A078343190
95. ALAV2A078343200
96. ALAV2A078343230
97. ALAV2A078343240
98. ALAV2A078633330
99. ALAV2A078633340
100. ALAV2A078633350
101. ALAV2A078633360
102. ALAV2A078633370
103. ALAV2A080093250
104. ALAV2A080093260
105. ALAV2A080093270
106. ALAV2A080093280
107. ALAV2A080093370
108. ALAV2A080093380
109. ALAV2A082573240
110. ALAV2A082573380
111. ALAV2A082573400
112. ALAV2A083303210
113. ALAV2A083303220
114. ALAV2A083303230
115. ALAV2A083303240
116. ALAV2A085053160
117. ALAV2A085053230
118. ALAV2A085053240
119. ALAV2A086073290
120. ALAV2A086073300
121. ALAV2A086073310
122. ALAV2A086073330
123. ALAV2A086073340
124. ALAV2A086073350
125. ALAV2A086073390
126. ALAV2A086073420
127. ALAV2A086073430
128. ALAV2A086803360
129. ALAV2A086803370
130. ALAV2A086803380
131. ALAV2A087533140
132. ALAV2A087533150
133. ALAV2A087533160
134. ALAV2A087533170
135. ALAV2A087533180
136. ALAV2A089283160
137. ALAV2A089283170
138. ALAV2A089283180
139. ALAV2A091033360
140. ALAV2A091033370
141. ALAV2A091033380
142. ALAV2A091033390
143. ALAV2A091033400
144. ALAV2A091033410

145. ALAV2A091033420  
146. ALAV2A092493140  
147. ALAV2A092493150  
148. ALAV2A092493160  
149. ALAV2A092493170  
150. ALAV2A092493180  
151. ALAV2A092783380  
152. ALAV2A092783390  
153. ALAV2A093513180  
154. ALAV2A093513430  
155. ALAV2A098473160  
156. ALAV2A098473170  
157. ALAV2A098473180  
158. ALAV2A098473190  
159. ALAV2A098473200  
160. ALAV2A100223250  
161. ALAV2A100223260  
162. ALAV2A100223270  
163. ALAV2A100223280  
164. ALAV2A100223380  
165. ALAV2A100223390  
166. ALAV2A100223400  
167. ALAV2A100223410  
168. ALAV2A100223420  
169. ALAV2A100223430  
170. ALAV2A100663140  
171. ALAV2A100663150  
172. ALAV2A100663160  
173. ALAV2A101243360  
174. ALAV2A101683190  
175. ALAV2A101683200  
176. ALAV2A101683210  
177. ALAV2A101683220

Appendix List A3. ALOS/PALSAR RTC image list

1. ALPSRP099860460
2. ALPSRP099860450
3. ALPSRP099860440
4. ALPSRP099860430
5. ALPSRP099860420
6. ALPSRP099860410
7. ALPSRP099860400
8. ALPSRP099860390
9. ALPSRP099860380
10. ALPSRP099860370
11. ALPSRP099860360
12. ALPSRP099860350
13. ALPSRP099860340
14. ALPSRP099860330
15. ALPSRP099860320
16. ALPSRP099860240
17. ALPSRP099860230
18. ALPSRP099860220
19. ALPSRP099860210
20. ALPSRP099860200
21. ALPSRP096360440
22. ALPSRP096360430
23. ALPSRP096360420
24. ALPSRP096360410
25. ALPSRP096360400
26. ALPSRP096360370
27. ALPSRP096360360
28. ALPSRP096360200
29. ALPSRP096360190
30. ALPSRP096360180
31. ALPSRP096360170
32. ALPSRP096360160
33. ALPSRP096360150
34. ALPSRP095630450
35. ALPSRP095630440
36. ALPSRP095630430
37. ALPSRP095630420
38. ALPSRP095630410
39. ALPSRP095630400
40. ALPSRP095630390
41. ALPSRP095630380
42. ALPSRP095630370
43. ALPSRP095630360
44. ALPSRP095630350
45. ALPSRP095630340
46. ALPSRP095630330
47. ALPSRP095630320
48. ALPSRP095630230
49. ALPSRP095630220
50. ALPSRP095630210
51. ALPSRP095630200
52. ALPSRP095630190
53. ALPSRP095630180
54. ALPSRP095630170
55. ALPSRP094610200
56. ALPSRP094610190
57. ALPSRP093880450
58. ALPSRP093880440
59. ALPSRP093880430
60. ALPSRP093880420
61. ALPSRP093880410
62. ALPSRP093880400
63. ALPSRP093880390
64. ALPSRP093880380
65. ALPSRP093880370
66. ALPSRP093880360
67. ALPSRP093880220
68. ALPSRP093880210
69. ALPSRP093880200
70. ALPSRP093880190
71. ALPSRP093880180
72. ALPSRP093880170
73. ALPSRP093880160
74. ALPSRP092130420
75. ALPSRP092130410
76. ALPSRP092130400
77. ALPSRP092130200
78. ALPSRP092130190
79. ALPSRP092130180
80. ALPSRP091690430
81. ALPSRP091690420
82. ALPSRP091690410
83. ALPSRP091690300
84. ALPSRP091690290
85. ALPSRP091690280
86. ALPSRP091690270
87. ALPSRP091690260
88. ALPSRP091690250
89. ALPSRP091690240
90. ALPSRP091690230
91. ALPSRP091690220
92. ALPSRP091400450
93. ALPSRP091400440
94. ALPSRP091400430
95. ALPSRP091400420
96. ALPSRP091400410
97. ALPSRP091400400
98. ALPSRP091400390
99. ALPSRP091400380
100. ALPSRP091400370
101. ALPSRP091400360
102. ALPSRP091400350
103. ALPSRP091400340
104. ALPSRP091400220
105. ALPSRP091400210
106. ALPSRP091400200
107. ALPSRP091400190
108. ALPSRP091400180
109. ALPSRP091400170
110. ALPSRP090960430
111. ALPSRP090960420
112. ALPSRP090960410
113. ALPSRP089940470
114. ALPSRP089940460
115. ALPSRP089940450
116. ALPSRP089940440
117. ALPSRP089940430
118. ALPSRP089940420
119. ALPSRP089940410
120. ALPSRP089940400
121. ALPSRP089940390
122. ALPSRP089940320
123. ALPSRP089940310
124. ALPSRP089940300
125. ALPSRP089940290
126. ALPSRP089940280
127. ALPSRP089940270
128. ALPSRP089940260
129. ALPSRP089940250
130. ALPSRP089940240
131. ALPSRP089940230
132. ALPSRP089940220

133. ALPSRP089940210 179. ALPSRP088190390 225. ALPSRP086440400  
134. ALPSRP089940200 180. ALPSRP088190380 226. ALPSRP086440390  
135. ALPSRP089650440 181. ALPSRP088190370 227. ALPSRP086440380  
136. ALPSRP089650430 182. ALPSRP088190360 228. ALPSRP086440370  
137. ALPSRP089650420 183. ALPSRP088190350 229. ALPSRP086440360  
138. ALPSRP089650410 184. ALPSRP088190340 230. ALPSRP086440350  
139. ALPSRP089650400 185. ALPSRP088190330 231. ALPSRP086440340  
140. ALPSRP089650370 186. ALPSRP088190320 232. ALPSRP086440330  
141. ALPSRP089650360 187. ALPSRP088190310 233. ALPSRP086440320  
142. ALPSRP089650200 188. ALPSRP088190300 234. ALPSRP086440240  
143. ALPSRP089650190 189. ALPSRP088190290 235. ALPSRP086440230  
144. ALPSRP089650180 190. ALPSRP088190280 236. ALPSRP086440220  
145. ALPSRP089650170 191. ALPSRP088190270 237. ALPSRP086440210  
146. ALPSRP089650160 192. ALPSRP088190260 238. ALPSRP086440200  
147. ALPSRP089650150 193. ALPSRP088190250 239. ALPSRP086440190  
148. ALPSRP089210430 194. ALPSRP088190240 240. ALPSRP086440180  
149. ALPSRP089210420 195. ALPSRP088190230 241. ALPSRP085710470  
150. ALPSRP088920450 196. ALPSRP088190220 242. ALPSRP085710460  
151. ALPSRP088920440 197. ALPSRP088190210 243. ALPSRP085710450  
152. ALPSRP088920430 198. ALPSRP088190200 244. ALPSRP085710440  
153. ALPSRP088920420 199. ALPSRP088190190 245. ALPSRP085710430  
154. ALPSRP088920410 200. ALPSRP087900200 246. ALPSRP085710420  
155. ALPSRP088920400 201. ALPSRP087900190 247. ALPSRP085710410  
156. ALPSRP088920390 202. ALPSRP087460450 248. ALPSRP085710400  
157. ALPSRP088920380 203. ALPSRP087460440 249. ALPSRP085710390  
158. ALPSRP088920370 204. ALPSRP087460430 250. ALPSRP085710380  
159. ALPSRP088920360 205. ALPSRP087460420 251. ALPSRP085710350  
160. ALPSRP088920350 206. ALPSRP087460410 252. ALPSRP085710340  
161. ALPSRP088920340 207. ALPSRP087460400 253. ALPSRP085710330  
162. ALPSRP088920330 208. ALPSRP087460310 254. ALPSRP085710320  
163. ALPSRP088920320 209. ALPSRP087460300 255. ALPSRP085710310  
164. ALPSRP088920230 210. ALPSRP087460290 256. ALPSRP085710300  
165. ALPSRP088920220 211. ALPSRP087460280 257. ALPSRP085710290  
166. ALPSRP088920210 212. ALPSRP087460270 258. ALPSRP085710280  
167. ALPSRP088920200 213. ALPSRP087460260 259. ALPSRP085710270  
168. ALPSRP088920190 214. ALPSRP087460250 260. ALPSRP085710260  
169. ALPSRP088920180 215. ALPSRP087460240 261. ALPSRP085710250  
170. ALPSRP088920170 216. ALPSRP087460230 262. ALPSRP085710240  
171. ALPSRP088190470 217. ALPSRP087460220 263. ALPSRP085710230  
172. ALPSRP088190460 218. ALPSRP087460210 264. ALPSRP085710220  
173. ALPSRP088190450 219. ALPSRP086440460 265. ALPSRP085710210  
174. ALPSRP088190440 220. ALPSRP086440450 266. ALPSRP085710200  
175. ALPSRP088190430 221. ALPSRP086440440 267. ALPSRP085420420  
176. ALPSRP088190420 222. ALPSRP086440430 268. ALPSRP085420410  
177. ALPSRP088190410 223. ALPSRP086440420 269. ALPSRP085420400  
178. ALPSRP088190400 224. ALPSRP086440410 270. ALPSRP085420200

271. ALPSRP085420190 317. ALPSRP083960330 363. ALPSRP082210440  
272. ALPSRP085420180 318. ALPSRP083960320 364. ALPSRP082210430  
273. ALPSRP084980430 319. ALPSRP083960310 365. ALPSRP082210420  
274. ALPSRP084980420 320. ALPSRP083960300 366. ALPSRP082210410  
275. ALPSRP084980410 321. ALPSRP083960240 367. ALPSRP082210400  
276. ALPSRP084980300 322. ALPSRP083960230 368. ALPSRP082210390  
277. ALPSRP084980290 323. ALPSRP083960220 369. ALPSRP082210380  
278. ALPSRP084980280 324. ALPSRP083960210 370. ALPSRP082210370  
279. ALPSRP084980270 325. ALPSRP083960200 371. ALPSRP082210360  
280. ALPSRP084980260 326. ALPSRP083960190 372. ALPSRP082210350  
281. ALPSRP084980250 327. ALPSRP083230470 373. ALPSRP082210340  
282. ALPSRP084980240 328. ALPSRP083230460 374. ALPSRP082210330  
283. ALPSRP084980230 329. ALPSRP083230450 375. ALPSRP082210320  
284. ALPSRP084980220 330. ALPSRP083230440 376. ALPSRP082210230  
285. ALPSRP084690450 331. ALPSRP083230430 377. ALPSRP082210220  
286. ALPSRP084690440 332. ALPSRP083230420 378. ALPSRP082210210  
287. ALPSRP084690430 333. ALPSRP083230410 379. ALPSRP082210200  
288. ALPSRP084690420 334. ALPSRP083230400 380. ALPSRP082210190  
289. ALPSRP084690410 335. ALPSRP083230390 381. ALPSRP082210180  
290. ALPSRP084690400 336. ALPSRP083230320 382. ALPSRP082210170  
291. ALPSRP084690390 337. ALPSRP083230310 383. ALPSRP081480470  
292. ALPSRP084690380 338. ALPSRP083230300 384. ALPSRP081480460  
293. ALPSRP084690370 339. ALPSRP083230290 385. ALPSRP081480450  
294. ALPSRP084690360 340. ALPSRP083230280 386. ALPSRP081480440  
295. ALPSRP084690350 341. ALPSRP083230270 387. ALPSRP081480430  
296. ALPSRP084690340 342. ALPSRP083230260 388. ALPSRP081480420  
297. ALPSRP084690220 343. ALPSRP083230250 389. ALPSRP081480410  
298. ALPSRP084690210 344. ALPSRP083230240 390. ALPSRP081480400  
299. ALPSRP084690200 345. ALPSRP083230230 391. ALPSRP081480390  
300. ALPSRP084690190 346. ALPSRP083230220 392. ALPSRP081480380  
301. ALPSRP084690180 347. ALPSRP083230210 393. ALPSRP081480370  
302. ALPSRP084690170 348. ALPSRP083230200 394. ALPSRP081480360  
303. ALPSRP083960470 349. ALPSRP082940440 395. ALPSRP081480350  
304. ALPSRP083960460 350. ALPSRP082940430 396. ALPSRP081480340  
305. ALPSRP083960450 351. ALPSRP082940420 397. ALPSRP081480330  
306. ALPSRP083960440 352. ALPSRP082940410 398. ALPSRP081480320  
307. ALPSRP083960430 353. ALPSRP082940400 399. ALPSRP081480310  
308. ALPSRP083960420 354. ALPSRP082940370 400. ALPSRP081480300  
309. ALPSRP083960410 355. ALPSRP082940360 401. ALPSRP081480290  
310. ALPSRP083960400 356. ALPSRP082940200 402. ALPSRP081480280  
311. ALPSRP083960390 357. ALPSRP082940190 403. ALPSRP081480270  
312. ALPSRP083960380 358. ALPSRP082940180 404. ALPSRP081480260  
313. ALPSRP083960370 359. ALPSRP082940170 405. ALPSRP081480250  
314. ALPSRP083960360 360. ALPSRP082940160 406. ALPSRP081480240  
315. ALPSRP083960350 361. ALPSRP082940150 407. ALPSRP081480230  
316. ALPSRP083960340 362. ALPSRP082210450 408. ALPSRP081480220



409. ALPSRP081480210 455. ALPSRP079000230 501. ALPSRP077250440  
410. ALPSRP081480200 456. ALPSRP079000220 502. ALPSRP077250430  
411. ALPSRP081480190 457. ALPSRP079000210 503. ALPSRP077250420  
412. ALPSRP081190200 458. ALPSRP079000200 504. ALPSRP077250410  
413. ALPSRP081190190 459. ALPSRP078710420 505. ALPSRP077250400  
414. ALPSRP080460450 460. ALPSRP078710410 506. ALPSRP077250390  
415. ALPSRP080460440 461. ALPSRP078710400 507. ALPSRP077250380  
416. ALPSRP080460430 462. ALPSRP078710200 508. ALPSRP077250370  
417. ALPSRP080460420 463. ALPSRP078710190 509. ALPSRP077250360  
418. ALPSRP080460410 464. ALPSRP078710180 510. ALPSRP077250350  
419. ALPSRP080460400 465. ALPSRP078270430 511. ALPSRP077250340  
420. ALPSRP080460390 466. ALPSRP078270420 512. ALPSRP077250330  
421. ALPSRP080460380 467. ALPSRP078270410 513. ALPSRP077250320  
422. ALPSRP080460370 468. ALPSRP078270300 514. ALPSRP077250310  
423. ALPSRP080460360 469. ALPSRP078270290 515. ALPSRP077250300  
424. ALPSRP080460220 470. ALPSRP078270280 516. ALPSRP077250240  
425. ALPSRP080460210 471. ALPSRP078270270 517. ALPSRP077250230  
426. ALPSRP080460200 472. ALPSRP078270260 518. ALPSRP077250220  
427. ALPSRP080460190 473. ALPSRP078270250 519. ALPSRP077250210  
428. ALPSRP080460180 474. ALPSRP078270240 520. ALPSRP077250200  
429. ALPSRP080460170 475. ALPSRP078270230 521. ALPSRP077250190  
430. ALPSRP080460160 476. ALPSRP078270220 522. ALPSRP076520470  
431. ALPSRP080020430 477. ALPSRP077980450 523. ALPSRP076520460  
432. ALPSRP080020420 478. ALPSRP077980440 524. ALPSRP076520450  
433. ALPSRP079000470 479. ALPSRP077980430 525. ALPSRP076520440  
434. ALPSRP079000460 480. ALPSRP077980420 526. ALPSRP076520430  
435. ALPSRP079000450 481. ALPSRP077980410 527. ALPSRP076520420  
436. ALPSRP079000440 482. ALPSRP077980400 528. ALPSRP076520410  
437. ALPSRP079000430 483. ALPSRP077980390 529. ALPSRP076520400  
438. ALPSRP079000420 484. ALPSRP077980380 530. ALPSRP076520390  
439. ALPSRP079000410 485. ALPSRP077980370 531. ALPSRP076520320  
440. ALPSRP079000400 486. ALPSRP077980360 532. ALPSRP076520310  
441. ALPSRP079000390 487. ALPSRP077980350 533. ALPSRP076520300  
442. ALPSRP079000380 488. ALPSRP077980340 534. ALPSRP076520290  
443. ALPSRP079000350 489. ALPSRP077980220 535. ALPSRP076520280  
444. ALPSRP079000340 490. ALPSRP077980210 536. ALPSRP076520270  
445. ALPSRP079000330 491. ALPSRP077980200 537. ALPSRP076520260  
446. ALPSRP079000320 492. ALPSRP077980190 538. ALPSRP076520250  
447. ALPSRP079000310 493. ALPSRP077980180 539. ALPSRP076520240  
448. ALPSRP079000300 494. ALPSRP077980170 540. ALPSRP076520230  
449. ALPSRP079000290 495. ALPSRP077540430 541. ALPSRP076520220  
450. ALPSRP079000280 496. ALPSRP077540420 542. ALPSRP076520210  
451. ALPSRP079000270 497. ALPSRP077540410 543. ALPSRP076520200  
452. ALPSRP079000260 498. ALPSRP077250470 544. ALPSRP076230440  
453. ALPSRP079000250 499. ALPSRP077250460 545. ALPSRP076230430  
454. ALPSRP079000240 500. ALPSRP077250450 546. ALPSRP076230420

547. ALPSRP076230410 593. ALPSRP073750400  
548. ALPSRP076230400 594. ALPSRP073750390  
549. ALPSRP076230370 595. ALPSRP073750380  
550. ALPSRP076230360 596. ALPSRP073750370  
551. ALPSRP076230200 597. ALPSRP073750360  
552. ALPSRP076230190 598. ALPSRP073750220  
553. ALPSRP076230180 599. ALPSRP073750210  
554. ALPSRP076230170 600. ALPSRP073750200  
555. ALPSRP076230160 601. ALPSRP073750190  
556. ALPSRP076230150 602. ALPSRP073750180  
557. ALPSRP074770470 603. ALPSRP073750170  
558. ALPSRP074770460 604. ALPSRP073750160  
559. ALPSRP074770450 605. ALPSRP073020460  
560. ALPSRP074770440 606. ALPSRP073020450  
561. ALPSRP074770430 607. ALPSRP073020440  
562. ALPSRP074770420 608. ALPSRP073020430  
563. ALPSRP074770410 609. ALPSRP073020420  
564. ALPSRP074770400 610. ALPSRP073020410  
565. ALPSRP074770390 611. ALPSRP073020400  
566. ALPSRP074770380 612. ALPSRP073020390  
567. ALPSRP074770370 613. ALPSRP073020380  
568. ALPSRP074770360 614. ALPSRP073020370  
569. ALPSRP074770350 615. ALPSRP073020360  
570. ALPSRP074770340 616. ALPSRP073020350  
571. ALPSRP074770330 617. ALPSRP073020340  
572. ALPSRP074770320 618. ALPSRP073020330  
573. ALPSRP074770310 619. ALPSRP073020320  
574. ALPSRP074770300 620. ALPSRP073020240  
575. ALPSRP074770290 621. ALPSRP073020230  
576. ALPSRP074770280 622. ALPSRP073020220  
577. ALPSRP074770270 623. ALPSRP073020210  
578. ALPSRP074770260 624. ALPSRP073020200  
579. ALPSRP074770250 625. ALPSRP073020190  
580. ALPSRP074770240 626. ALPSRP073020180  
581. ALPSRP074770230  
582. ALPSRP074770220  
583. ALPSRP074770210  
584. ALPSRP074770200  
585. ALPSRP074770190  
586. ALPSRP074480200  
587. ALPSRP074480190  
588. ALPSRP073750450  
589. ALPSRP073750440  
590. ALPSRP073750430  
591. ALPSRP073750420  
592. ALPSRP073750410

Appendix Table A5. Number of image of data collected from Google Earth Engine

Name	Number of Time steps*	Year	Number of 1° × 1° tiles	Total number of images
Sentinel-1	8	2016	60	480
Sentinel-2	8	2016	60	480
Landsat 8	8	2016	60	480
Landsat 5	8	2007	60	480
Landsat 7	8	2007	60	480

\* Each time step is equal to 1.5 month.